ADDIS ABABA UNIVERSITY
SCHOOL OF GRADUATE STUDIES
DEPARMENT OF CHEMISTRYGRADUATE

PROJECT (Chem.774)

SYNTHESIS AND PARTIAL CHARACTERIZATION OF LADDER AND QUINOXALINE-BASED CO-FLUORENE LOW BANDGAP POLYMERS

By

Fiseha Bogale

Advisor: Wendimagegn Mammo (Professor)

A Graduate Project Submitted to the School of Graduate Studies of Addis Ababa University in Partial Fulfillment of the Requirements for the Degree of Master of Science in Chemistry

July, 2009

Acknowlegement

I am highly indebted to Prof. Wendimagegn Mammo for his guidance, moral and professional support, affection and being role model. I am also grateful for Mekelle University and the school of Graduate Studies of Addis Ababa University for financing my study. It is my pleasure to extend my gratitude to my laboratory mates for the golden time I spent with them. Finally, I would like to thank my family, friends, and relatives for their helping hand and kindness and therefore I have dedicated this project work for them.

List of Abbrevation

DMF: N,N-dimethylformamide

DMSO: dimethyl sulfoxide

NBS: N-bromosuccinimide

NMR: Nuclear Magnetic Resonance

HOMO: Highest Occupied Molecular Orbital

J: coupling constant

LUMO: Lowest Unoccupied Molecular Orbital

PPV: poly(phenylenevinylene)

THF: tetrahydrofuran

m: multiplet

dd: doublets of doublets

δ: chemical shift

s: singlet

t: triplet

°C: degree Celsius

%: percentage

TABLE OF CONTENTS PAGE No.

LIST OF SCHEMES PAGE No.

LIST OF FIGURES

LIST OF TABLES

Synthesis and Partial Characterization of Ladder and Quinoxaline-Based Co-Fluorene Low Bandgap Polymers

By: Fiseha Bogale

Advisor: Wendimagegn Mammo (Professor)

Abstract

Thiophene-phenylene-thiophene fused heteroarene ladder-type monomeric unit which hinders "chain folding" and allows extended conjugation was synthesized along with two variants of quinoxaline-based donor-acceptor monomeric units. Subsequently the copolymerization between these monomeric units and previously synthesized 2,2'-(9,9-dioctyl-9H-fluorene-2,7-diyl)bis(4,4,5,5-tetramethyl-1,3,2-dioxaborolane) was effected by a modified Suzuki polymerization methodology. The copolymers were partially characterized using UV-vis absorption spectroscopy in both thin film and as chloroform solution, cyclic voltammetry and fluorescence spectroscopy, for their bandgap and quantum yield. The results from the electrochemical and spectroscopic analysis revealed a bandgap of 2.4, 2.1, and 1.9 eV for polymers ***53****,* ***54*** *and* ***55****, respectively.*

1. INTRODUCTION

Polymers have emerged as one of the most important materials in the twentieth century. The twenty-first century will undoubtedly see the use of polymers move from primarily passive materials such as coatings and containers to active materials with useful optical, electronic, energy storage and mechanical properties. Indeed, this development has already begun with the discovery and study of conducting polymers. Electronically conducting polymers possess a variety of properties related to their electrochemical behavior and are therefore active materials whose properties can be altered as a function of their electrochemical potential.

The importance and potential impact of this new class of materials was recognized by the world scientific community when Hideki Shirakawa, Alan J. Heeger and Alan G. MacDiarmid were awarded the Nobel Prize in Chemistry in 2000 for their research in this field [1–5]. Although these materials are known as new materials in terms of their properties, the first work describing the synthesis of a conducting polymer was published in the nineteenth century [6]. At that time 'aniline black' was obtained as the product of oxidation of aniline, however, its electronic properties were not established. It has been known for more than 40 years that the electronic conductivity of conjugated organic polymer chains is orders of magnitude higher than that of other polymeric materials [7–9]. Although they are not metallic, however, the possibility of producing polymers with conductivities approaching those of metals was not recognized.

A key discovery that changed the outlook for producing highly conducting polymers was the finding in 1973 that the inorganic polymer poly sulfur nitride $(SN)_x$ is highly conducting [10]. The room-temperature conductivity of $(SN)_x$ is of the order of 103 S/cm, approaching the conductivity of copper, 105 S/cm.

Below a critical temperature of about 0.3 K, $(SN)_x$ becomes a superconductor [11]. These discoveries were of particular importance because they proved the possibility of generating highly conducting polymers, and stimulated the enormous amount of focus and activity necessary for the discovery of other polymeric conductors. In the period of 1976 and 1977, it was observed that the room-temperature conductivity of $(SN)_x$ could be enhanced by an order of magnitude following exposure to bromine or other similar oxidizing agents [12], suggesting that it was possible to increase the number of charge carriers in the material *via* doping. In 1958, polyacetylene was first synthesized by Natta *et al.* as a black powder and found to be a semiconductor with conductivity in the range of 10^{-11} to 10^{-3} S/cm, depending upon how the polymer was processed and manipulated [13]. This polymer remained a scientific curiosity until 1967, when a coworker of Hideki Shirakawa at the Tokyo Institute of Technology was attempting to synthesize polyacetylene, and a silvery thin film was produced as a result of a mistake. It was found that the amount of Ziegler–Natta catalyst, $Ti(O\text{-}n\text{-}But)_4\text{-}Et_3Al$, was three orders of magnitude higher than required. When this film was investigated it was found to possess a higher conductivity than previously observed, approaching that of the best carbon black (graphite) powders.

In the years between 1971 and 1975, Shirakawa and coworkers prepared crystalline polyacetylene films using refinements of the technique in the presence of Ziegler catalyst; however, the nature of conductivity was not pursued. The real breakthrough in the development of conjugated organic conducting polymers was only reached after the discovery of metallic conductivity in crystalline polyacetylene films with p-type dopants such as halogens during collaborative research involving Shirakawa, MacDiarmid and Heeger in 1977 [1, 2]. A year later, it was discovered that analogous effects could be induced by electron donors (n-type dopant). Following this work there has been an explosion of activity around the characterization, synthesis and

use of conducting polymers in a wide range of fields from electronics to medicine.

An organic polymer that possesses the electrical and optical properties of a metal while retaining its mechanical properties and processability, is termed an 'intrinsically conducting polymer' (ICP). These properties are intrinsic to the 'doped' form of the polymer. The conductivity of ICPs lies above that of insulators and extends well into the region of common metals; therefore, they are often referred to as 'synthetic metals.' The common feature of most ICPs is the presence of alternating single and double bonds along the polymer chain, which enable the delocalization or mobility of charge along the polymer backbone. The conductivity is thus assigned to the delocalization of π-bonded electrons over the polymeric backbone, exhibiting unusual electronic properties, such as low energy optical transitions, low ionization potentials and high electron affinities [14].

Most conducting organic molecules are π-conjugated compounds, i.e., materials in which single and double or single and triple bonds alternate throughout the molecule or polymer backbone. The second and third bonds of a double or triple bond are π bonds, i.e., if the backbone of the molecule or polymer is along the x axis, then the orbitals which define these π bonds are formed from overlapping atomic pz or py orbitals. Since the energy of electrons in π orbitals is usually higher than in the σ orbitals (which are generated from $sp3$, $sp2$, or sp hybridized atomic orbitals), the gap between the highest occupied molecular π orbital (HOMO) and the lowest unoccupied molecular π orbital (LUMO) is typically in the 1.5–3 eV range, i.e., the materials are semiconductors [15]. Due to the overlap of π orbital wave functions of adjacent carbon atoms, the electrons occupying such orbitals are relatively delocalized. The π electron clouds in PPV for example, are generated from electrons in the overlapping atomic pz orbitals. Since these pz orbitals have lobes above and

below the *x*-*y* plane of the σ bonds of poly(phenylenevinylene) (PPV), the π electrons lie above and below this plane. The distance between two C atoms is shorter and the π electron cloud between them is denser in the double C-C than in the single C–C bond. The difference between these distances, or, equivalently, between the densities of the π electrons in the double *vs.* the single bond, is a measure of the "alternation parameter," and it may strongly impact the electronic structure of the molecule or polymer [16, 17]. Due to the π conjugation, in the perfect isolated polymer chain the delocalized π electron cloud extends along the whole length of the chain. However, in the J. Shinar and V. Savvateev real chain various defects, such as external impurities (e.g., H, O, Cl, or F atoms which eliminate the double bond, etc.) or intrinsic defects (e.g., kinks, torsional conformations, a cross-link with a neighboring chain, etc.) break the conjugation. In the typical polymer film, the length of a conjugated segment typically varies from 5 repeat units to 15 repeat units. The HOMO-LUMO gap decreases with increasing conjugation length to an asymptotic value usually reached at 10 repeat units [16].

2. REVIEW OF RELATED LITRATURE

2.1. Intrinsic *versus* extrinsic electrical conduction of conjugated polymers

Conjugated polymers are organic semiconductors that with respect to electronic energy levels hardly differ from inorganic semiconductors. Both have their electrons organized in bands rather than in discrete levels and both have their ground state energy bands either completely filled or completely empty [18, 19]. The band structure of a conjugated polymer originates from the interaction of the π-orbital of the repeating units throughout the chain.

2.1.1. Extrinsic conduction

Since a conjugated polymer is a semiconductor with a finite bandgap, conversion into a conductor necessitates introduction of charges onto the polymer chain which can be accomplished by various methods. The first method concerns the introduction of charges either by electron-removal (oxidation or p-doping) or -injection (reduction or n-doping) [13, 14]. The major part of conjugated polymers known today is built up of electron-releasing units, making them p-type semiconductors which can be doped with oxidants like I_2, $FeCl_3$, etc. The removal of one electron through oxidation produces a mobile charge in the form of a radical cation, also called a polaron. The positive charge tends to induce local atomic displacements (``clothing phonons"), leading to the polaronic behavior. Further oxidation can either convert the polaron into a spinless bipolaron or introduce another polaron. In either case, introduction of each positive charge also means introduction of a negatively charged counterion (Ox^-).

The second method consists of acid doping of conjugated polymers bearing a site prone to protonation, which introduces charges in the main chain. The

best known example is polyaniline. The neutral leucoemeraldine form **1a** can be oxidized to the emeraldine base **1b** without introduction of counterions. However, the emeraldine base **1b** only becomes conductive after treatment with a sufficiently strong acid (HX) which protonates the imine nitrogens and, at the same time, introduces a counterion (X^-). The conducting emeraldine **1c** can also be represented by the mesomeric structure **1d**, in which all phenyl rings are aromatic and radical cations are present on every second nitrogen atom. This degenerate mesomerism is thought to account for a high charge carrier mobility, and thus high conductivity, but conformational factors like the crystallinity of polyaniline films also play a crucial role.

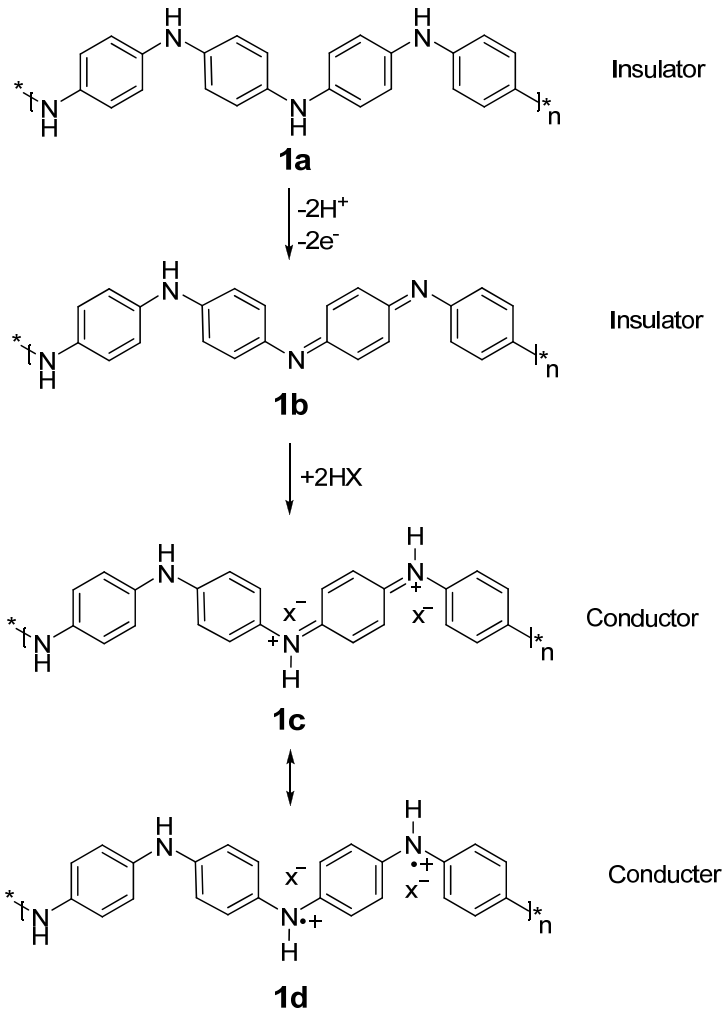

Scheme 1. Acid doping in polyaniline

In the above two examples, introduction of charge carriers is inevitably accompanied by the introduction of counter-ions. It is defined here that extrinsically conducting polymers are π-conjugated polymers that become conductive after doping, i.e., after the introduction of charged species that are delocalized along the conjugated main chain (charge carriers), accompanied by the introduction of counter-charged species that are not delocalized along the conjugated main chain. It is analogous to interstitial doping in inorganic semiconductors, in which case the counter-charge is also more or less localized on the interstitial species. The definition covers all π-conjugated polymers that are made conductive either by means of doping with an oxidizing or reducing agent, or by means of acid doping. Furthermore, "self-doping" polymers like poly(carboxyethylpyrrole) [20] and sulfonated polyaniline are not considered intrinsically conducting polymers since the negative charge is not delocalized along the main chain.

2.1.2. Intrinsically conducting polymers

Intrinsically conducting polymers are conducting π-conjugated polymers which do not need additional doping and are characterized by electrically neutral conjugated systems in which some π-electron bands are only partially filled. The character of their conductivity may range from "hopping" to metallic, depending on the degree of overlap of the π-orbitals of neighboring molecules. These intrinsic conductors owe their conductivity to the partial filling of the valence band up to the Fermi-level. To imitate such a partially filled band with a semiconductor, its bandgap should be zero or close to zero.

2.2. Ladder-type monomeric units

Environmental issues such as fossil fuel shortage and global warming have gained a worldwide acknowledgement and there is a great demand for green and renewable energy option. Among all the renewable energy sources, solar

energy, which is clean, abundant and virtually limitless, is gaining a lot of attention in the scientific community.

The major issue that is threatening the sun-driven energy alternative is the low power conversion efficiency of the currently existing organic polymer solar cells, which could not exceed 5%. In theory the efficiency can be further improved through careful engineering of both polymeric conducting materials and the device. The key issue for material engineering includes ease of processability, effective light harvesting (such as low bandgap semiconducting material with broad absorption and high absorptivity) and high carrier mobility property. However, it is more challenging to improve the charge mobility of the conjugated polymer in comparison with improving the absorption property [21].

To increase the hole mobility of the polymers, other than increasing molecular weight and decreasing the polydispersity of polymers, enhancing π-π stacking of the polymer backbone and to produce highly organized morphology by either side chain self assembly or introduction of a more rigid planar monomer to form a liquid-crystalline phase structure have been proven to be an effective approach. Another way is canceling the bond-length, which is reducing or eliminating the structural deformations that lead to the localization of alternating double and single bonds along the conjugated main-chain. This would mean the construction of ladder polymers [7, 22-25] of which the best-known example is polyacene (**2**). This polymer can be regarded as two fused *trans*-polyacetylene chains.

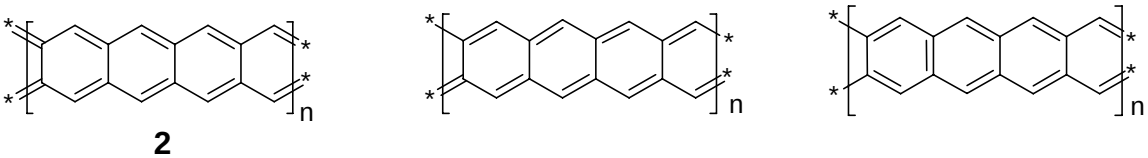

2

Figure 1. Polyacene

Indeed, calculations have shown that polyacene would be a metallic conductor [26]. However, due to their difficult synthesis [27], no well-defined examples of these systems are known. Not all ladder polymers are necessarily zero bandgap materials, i.e., polyphenanthrene (**3**), which can be regarded as two fused *cis*-polyacetylene chains, has a calculated gap of 4-5 eV due to the large difference in energy between the aromatic and quinoid structures [17, 28, 29].

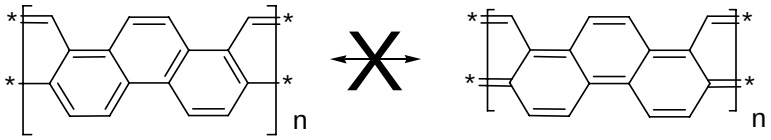

3

Figure 2. Polyphenanthrene.

Furthermore, conjugated ladder polymers like the poly-*p*-phenylene derivative **4** [30-32] exist, which are partially linked with saturated bonds with the purpose of planarization of the consecutive units. Although these polymers show a reduced bandgap compared to their non-planar counterparts such as poly-*p*-phenylene, it is evident that these systems suffer from bond length alternation as well, and should, therefore, not be classified in the group of ``fully'' conjugated ladder polymers of type **2** and **3**.

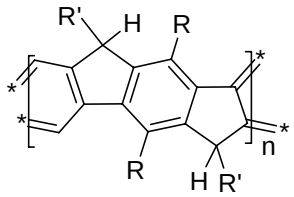

4

Figure 3. Poly-*p*-phenylene derivative.

Thiophene-thiadiazole copolymers (PBTTT) and benzodithiophene copolymers have been reported that, by incorporating fused aromatic units in to the polymer backbone, can achieve high field effect carrier mobility up to 0.1-0.8 $cm^2(Vs)$[33].

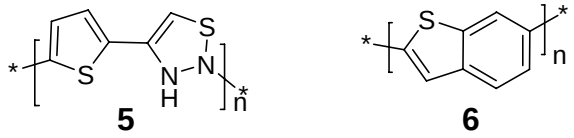

5 **6**

Figure 4. Thiophene-thiadazole (**5**) and benzothiophene (**6**) copolymers

The presence of a rigid fused ring is expected to enhance the degree of conjugation, and also benefit to avoid possible "chain folding" which may limit the charge carrier mobility of the semiconducting polymer at higher molecular weight [34].

2.2.1. Synthesis of Thiophene-phenylene-thiophene (TPT) monomeric unit

Recently, Wong *et al.*, have designed and synthesized a noble thiophene-phenylene-thiophene (TPT) fused chromophore. The molecular configuration of the π-conjugated backbone was confirmed by XRD, and the heteroarene fused molecular framework of the TPT unit exhibits nearly planar conformation [35].
The acid-mediated intramolecular ring closure between a tertiary hydroxyl group and adjacent arene(s) is a useful reaction for establishing the coplanarity of the conjugated backbone. This versatile synthetic strategy provides the flexibility to introduce various heteroarenes as constituent of the conjugated backbone and so as to effectively manipulate the energy levels, as well as the electronic behavior, of the resulting coplanar molecules. Along this line, Pd-catalyzed Negishi cross coupling reaction of diethyl-2,5-dibromoterephthalate (**8**) with 2-thienyl zinc chloride, which was generated *in situ* through transmetallation of a corresponding 2-thienyl Grignard reagent (**7**) with $ZnCl_2$, afforded the doubly coupled product **9** in 73% yield [25] (Scheme 2). After the double addition and acid-promoted intramolecular cyclization reaction sequence, the desired product **11** was isolated in 65% yield.

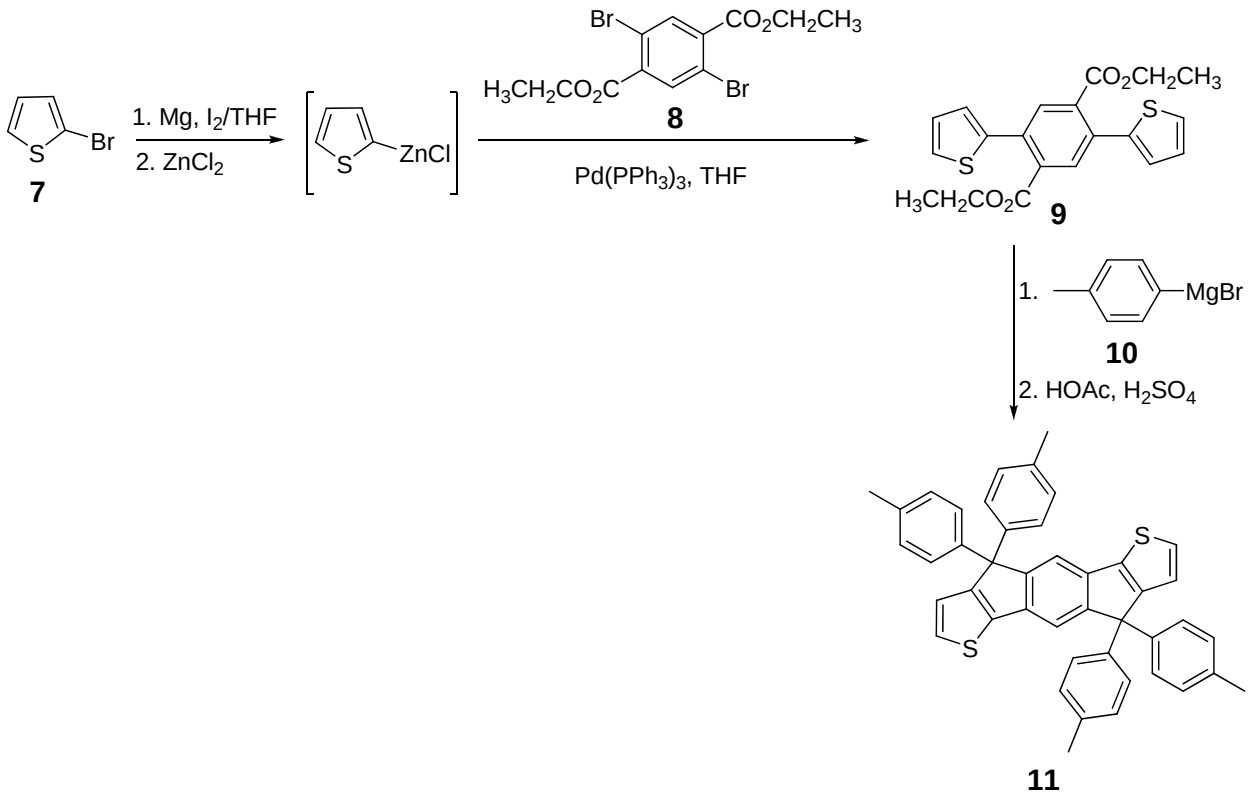

Scheme 2. Synthesis of thiophene-phenylene-thiophene ladder-type monomeric unit.

2.3. Donor-Acceptor monomers

The other general approach towards reduction of bandgap in conducting conjugated polymers is alternation of electron-donors and acceptors in the main polymer chain. Figure 5 shows the structure of some donor acceptor momomers. The interaction between donor **(D)** and acceptor **(A)** may give rise to an increased double bond character between the donor and acceptor units. Since, the donor-acceptor units can accommodate charges that are associated with the canonical forms of the particular donor-acceptor monomeric structure. Hence, a conjugated polymer with an alternating sequence of the appropriate

donor and acceptor units in the main polymer chain shows a decreased bandgap [7].

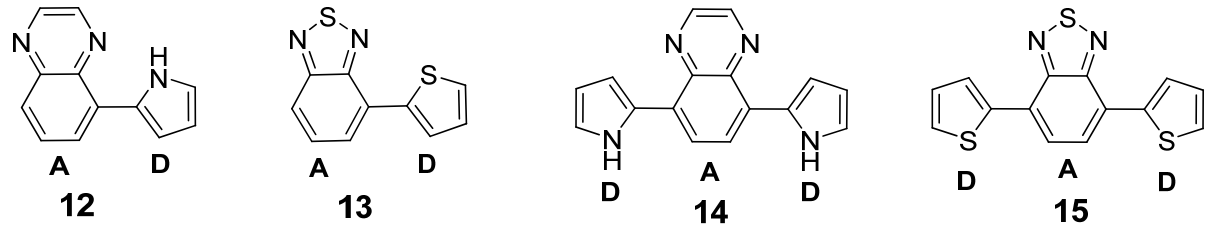

Figure 5. Some examples of Donor-Acceptor monomeric units

It was shown with PITN5 that reduction of bond-length alternation by increasing the double bond character between the repeating units of a conjugated polymer, results in a decreased bandgap. The driving force for such a process in PITN is the gain in aromaticity of the fused benzene ring. The interaction between a strong electron-donor (D) and a strong electron-acceptor (A) may also give rise to an increased double bond character between these units, since they can accommodate the charges that are associated with such a mesomerism ($D\text{-}A \leftrightarrow D^{+}=A^{-}$). Hence, a conjugated polymer with an alternating sequence of the appropriate donor- and acceptor-units in the main-chain may show a decreased bandgap. The donor-acceptor (D-A) repeating unit strategy was introduced with polymers 16-20 [36, 37] (Figure 6). Gel permeation chromatography (GPC) of copolymer **19** with R, heptyl or dodecyl shows molecular weights up to 15 kDa (*versus* polystyrene). The copolymer **20** (R = Me) shows a bandgap of 0.45 eV (absorption edge) and an absorption maximum energy of 0.9 eV. The conductivity measured with the usual four probe method on virgin samples was 10^{-5} S cm^{-1}, in agreement with calculation.

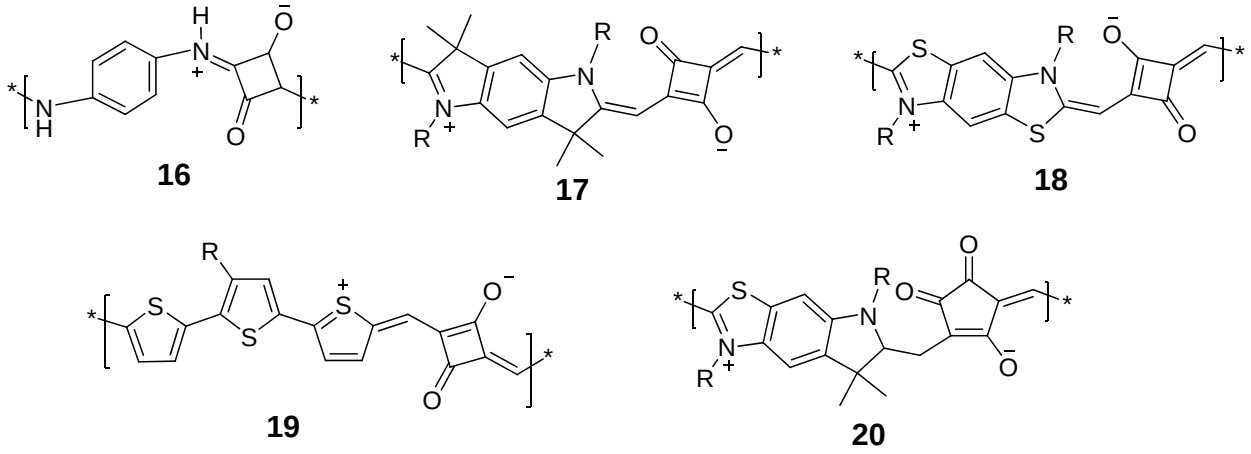

Figure 6. Polysquarines

The low values were initially explained by the fact that the conjugated main chain of these polymers, with their alternation of electron-withdrawing and -releasing units, represents the one dimensional analogue of a so-called n-i-p-i semiconductor structure. In these semiconductors, the valence- and conduction-band are curved by space-charge effect, which leads to a diminished bandgap energy when the spatial alternation of the levels is taken into account. However, calculations have shown that the hybridization of the energy levels of the donor and the acceptor, particularly the high-lying HOMO of the donor fragment and the low-lying LUMO of the acceptor fragment, yield a D-A monomer with an unusually small HOMO-LUMO separation [38, 39]. Further hybridization upon chain extension then converges to the small bandgaps. For this reason, bandgap reduction by means of an alternating donor-acceptor repeating unit strategy is primarily concerned with the combination of very strong donor and acceptor units, of which various attempts will be discussed here. In the following part, the various narrow bandgap donor-acceptor conjugated polymers are subdivided by the nature of their electron-accepting unit. For the electron-donating part, thiophene or pyrrole with various substitution patterns often represent the best choice since these are very electron-rich subunits that allow numerous chemical

transformations. The most obvious choice for the design of an electron-withdrawing subunit would be an aryl unit substituted with a cyano- or a nitro-group, since the latter two are among the most widespread electron withdrawing groups in organic chemistry. Examples of these polymer **21a-c** was claimed to feature a bandgap of 0.6 eV versus 1.5 and 1.4 eV for polymers **21a** and **21b**, respectively. However, the electronic absorption spectrum from which this small bandgap was derived shows a shoulder at high wavelength which may indicate residual doping and, therefore, obscures the accurate determination of the bandgap [40] (Figure 7).

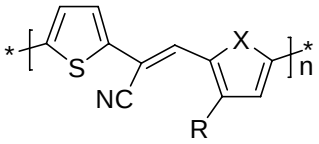

21

a X = S, R = H
b X = S, R = Me
c X = O, R = H

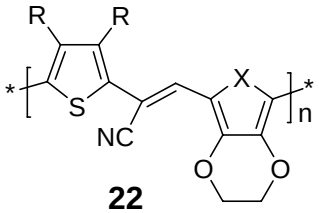

22

a R = H
b R = OCH_2CH_2O

Figure 7. Some examples of polymers withelectron rich subunits as donors and cyano group as acceptor

Electrochemical determination of the bandgap on polymers **22 a-b** resulted in values of 1.3 for 39a and 1.0 eV for **22b**. Since the 3,4-ethylenedioxythiophene unit is among the strongest thiophene-based electron-donors, and the acceptor-unit in **22a-b** is unchanged compared to **21a-c**, the reported bandgap value of 0.6 eV for **21c** is doubtful.

Conjugated polymers in which the electron-donating group is pyrrole and/or thiophene, and the electron-accepting group is a cyano-substituted aryl unit, are depicted in Figure 8 [**23-25**]. The polymers were prepared by electrochemical oxidation (acetonitrile/NBu_4ClO_4) of their corresponding monomers. The bandgaps of polymers **23-25**were estimated at 2.2, 2.7, 1.6, and 2.0 eV, respectively. Although these values are much lower compared to the identical polymers without a cyano-group-except for polymer **24**, which

suffers from steric hindrance along the pyrrole-phenyl bond-the bandgaps are still quite high.

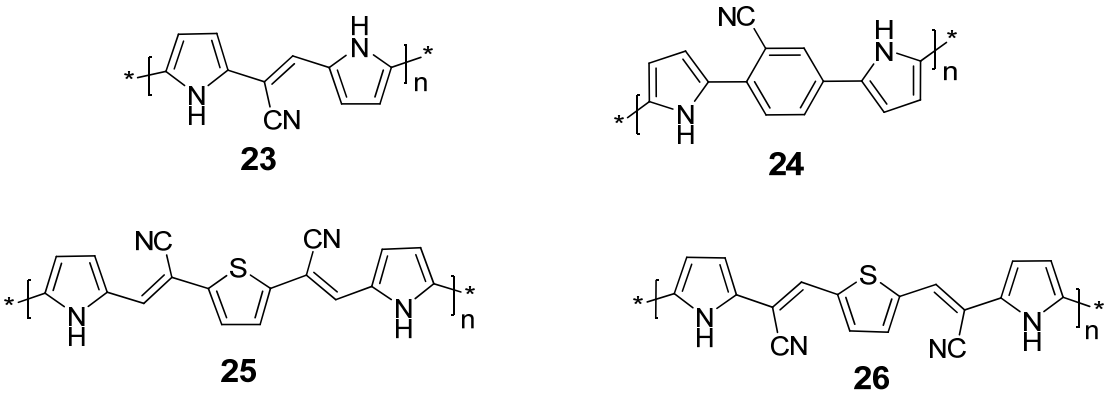

Figure 8. Conjugated polymers with pyrrole and/or thiophene as electron-donating group and cyano-substituted aryl group as electron-accepting unit.

An example of a conjugated polymer containing an electron-accepting group differing from a cyano-substituted aryl unit is depicted in Scheme 3 [42-46].
The solution and solid state optical bandgaps for **27** are 1.4 and 1.1 eV, respectively. It is suggested that this diminished bandgap originates from rigidification of the conjugated backbone due to the occurrence of mesomeric structures. When the bandgaps that have been found for the donor-acceptor conjugated polymers (in which a cyano- or nitro-substituted aryl unit is the acceptor) presented above are reviewed, only the value measured for polymer 21c is below 1 eV, a value which is probably due to residual doping. Since, particularly in the case of Scheme 3, very strong electron-donor and -acceptor units are applied, these bandgap values falls short of expectations.

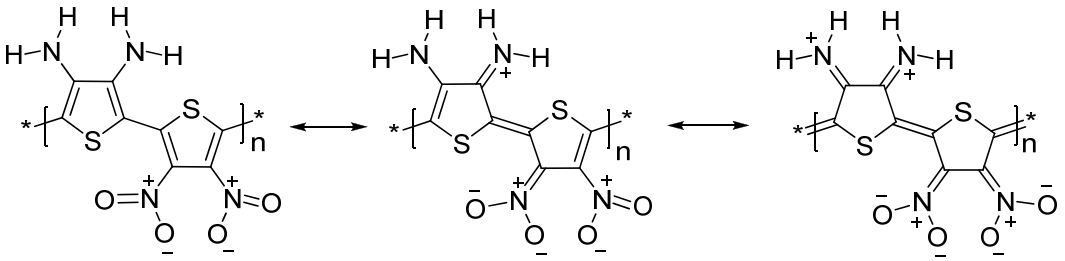

27

Scheme 3. Conjugated polymer with an electron-accepting group different from a cyano-substituted aryl unit.

2.3.1. Synthesis of qunoxaline monomeric unit

The synthesis of the quinoxaline monomeric unit was achieved starting with 2,1,3-benzothiadiazole as depicted in Scheme 2. Bromination of 2,1,3-benzothiadiazole (2**8**) (prepared from *o*-phenylenediamine and $SOCl_2$) gives 4,7-dibromo-2,1,3-benzothiadiazole (**29**) [47], which can be reduced to dibromo-*o*-phenylenediamine (**30**) [48] by the action of a reducing agent like Zn or $SnCl_2$ in HCl. Reaction of this diamine with a suitable diketone yields dibromoquinoxaline (**32**). This building block serves as the starting-point to construct donor-acceptor co-timers by means of organometallic aryl-aryl coupling reactions like the Grignard or Stille coupling [49]. Bromination of the co-timer **33** with NBS gives a dibrominated product (**34**).

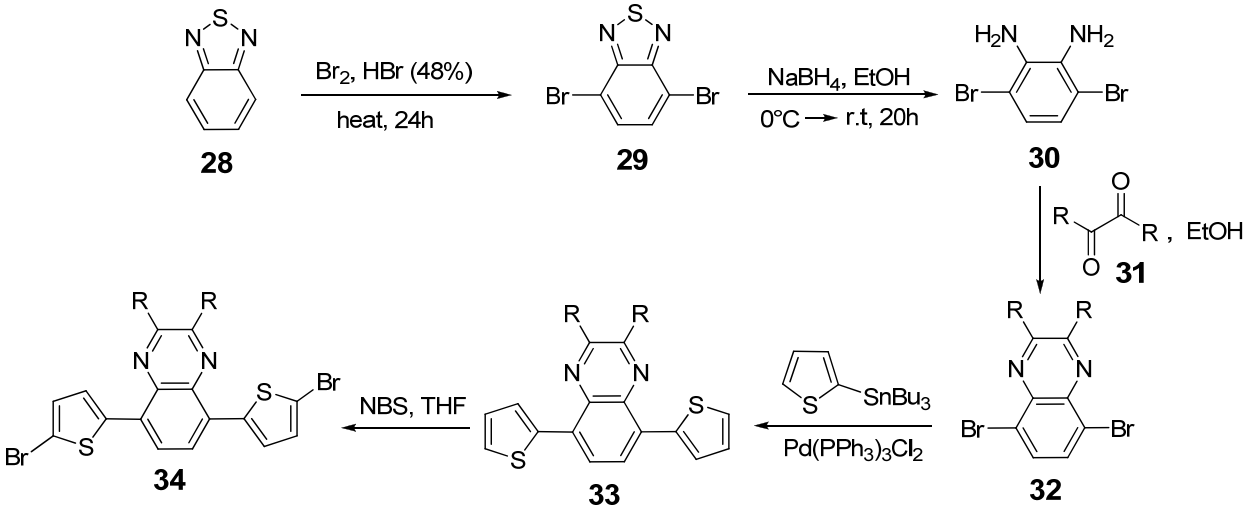

Scheme 4. Synthesis of donor-acceptor quinoxaline monomeric unit.

3. OBJECTIVE OF THE PROJECT WORK

The issue we will be addressing while conducting this research work is synthesis of low bandgap monomeric units such as diethyl-2,5-*bis*(5-bromothiophen-2-yl)terephthalate monomeric unit, thiophene-phenylene-thiophene ladder-type monomeric unit, and two varieties of quinoxaline-based monmomeric units and subsequent polymerization of these monomers with previously synthesized 2,2'-(9,9-dioctyl-9H-fluorene-2,7-diyl)bis(4,4,5,5-tetramethyl-1,3,2-dioxaborolane) unit. The resulting polymers will also be partially characterized using cyclic voltammetry, Uv-Vis spectroscopy and fluorescence spectroscopy for their bandgap and quantum yield.

4. RESULTS AND DISCUSSION

In the course of this project, attempt was first made to prepare a ladder-type monomer and to subsequently prepare polymers out of it. The synthesis of this monomer was achieved starting from *p*-xylene as shown in Schemes 5 and 6. The discussions that follow describe the synthesis of the ladder-type monomer and its subsequent reactions.

4.1. Synthesis of diethyl-2,5-*bis*(5-bromothiophen-2-yl)-terephthalate monomeric unit

The synthesis of diethyl-2,5-bis(5-bromothiophen-2-yl)terephthalate is depicted in Scheme 4. Thus, 1,4-dibromo-2,5-dimethylbenzene (**36**) was first prepared by $FeCl_3.3H_2O$-catalyzed bromination of *p*-xylene. The mixture of the monobromo *p*-xylene and **36** formed from the bromination protocol were separated by reduced pressure distillation technique to give a white solid product in 66.1% yield.

The structure of compound **36** was confirmed by its NMR data. The ^1H NMR spectrum showed (Table 1, Appendix 1) two singlets at δ7.41 and δ2.35. The peak at δ7.41, which integrated for two protons, is accounted for the two aromatic hydrogens on C-2 and C-5. The other peak at δ 2.35, which integrated for three protons, is due to the benzylic hydrogens on the methyl substituents at C-3 and C-6.

The ^{13}C NMR spectrum of **36** (Table 2, Appendix 2) showed a total of four peaks at δ137.0, 134.0, 123.4, and 22.1. The DEPT-135 spectrum confirmed that the peaks at δ137.0 and 123.4, which are both in the aromatic region are for the quaternary carbon atoms and are assigned to equivalent pairs of carbons C-1 and C-4 and C-2 and C-5, respectively. The other ^{13}C peak at δ134.0 is

attributable to the equivalent pair of methine carbons (C-3 and C-6). The peak at δ22.1 is due to the methyl carbons at C-2 and C-5.

1,4-Dibromo-2,5-dimethylbenzene (**36**) was subsequently transformed in to 2,5-dibromoterephtalic acid (**37**). Initially, oxidation of 1,4-dibromo-2,5-dimethylbenzene(**36**) was attempted by refluxing it with a basic aqueous solution of $KMnO_4$. Unfortunately, the reaction was inefficient in producing the compound in good percentage yield and much of the starting material was collected unreacted after long reaction time. Following this failed effort, a modified oxidation methodology, which involved a two-step cascade oxidation using an aqueous solution of potassium permanganate gave 2,5-dibromoterephtalic acid (**37**) in 71.7% yield.

The ^{1}H NMR spectrum of compound **37** (Table 1, Appendix 4) shows a broad peak at about δ14 which integrated for two protons. This peak can be assigned to the two acidic hydrogen atoms on the carboxyl groups. The sharp singlet centered at δ8.02 that integrated for two protons is attributed to the two equivalent hydrogen atoms on C-3 and C-6.

The ^{13}C NMR spectrum of compound **37** (Table 2, Appendix 5) showed four peaks, all above δ100. Three of the four signals appearing at δ137.5, 135.4, and 119.3 are for the aromatic carbon atoms. The fourth peak at δ166.0 is typical for carbonyl carbon of a carboxyl group. The peak at δ135.4 is assignable to the two equivalent methine carbons C-3 and C-6, while the peak at δ137.5 is due to the two equivalent quaternary carbons C-1 and C-4, down-field shifted by the strong electron withdrawing effect of the carboxyl group. The relatively up-field peak at δ119.3 is assignable to equivalent carbons C-2 and C-6, up-field shifted by the strong deshielding van der Waals effect of the large bromine atoms. In agreement with the above assignment the DEPT-135 spectrum showed that all the peaks, except the peak at δ135.4, disappeared proving that these are due to quaternary carbon atoms.

2,5-Dibromoterephtalic acid (**37**) was transformed to the corresponding diethyl ester (**38**) by acid catalyzed esterification reaction to give a white solid product in 66.5% yield. The identity of compound **38** was confirmed by its NMR spectra as discussed below.

Table 1. ^{1}H NMR (400.13 MHz, $CDCl_3$) data (δ ppm) of compounds **36**, **37** and **38**.

36	**37***	**38**
7.41	14.00	8.04
(s, 2H, H-2, H-5)	(s, 2H, H-1')	(s, 2H, H-2, H-5)
2.35	8.02	4.43
(s, 6H, H-1')	(s, 2H, H-3, H-6)	(q, *J* = 7.2 Hz, 4H, H-2')
		1.43
		(t, *J* = 7.2Hz, 6H, H-3')

***** Solvent DMSO-d_6

Table 2. ^{13}C NMR (100.6 MHz, $CDCl_3$) data (δ ppm) for compounds **36**, **37** and **38**

C	**36**	**37***	**38**
1	137.0	137.5	135.7
2	123.4	135.4	136.5
3	134.0	119.3	120.1
4	137.0	137.5	135.7
5	123.4	135.4	136.5
6	134.0	119.3	120.1
1'	22.1	166.0	164.3
2'	_	_	62.4
3'	_	_	14.2

***** Solvent DMSO-d_6

Three peaks are evident from the ^{1}H NMR spectrum of compound **38** (Table 1, Appendix 6). They appeared at δ8.04, 4.43, and 1.43, integrating for 2, 4, and 6 protons, respectively. The singlet peak at δ8.04 is due to the two equivalent aromatic protons on C-3 and C-6. The quartet peak centered at δ4.43 (J = 7.2 Hz) is assigned to two equivalent methylene protons at C-2', down-field shifted by the electron withdrawing effect of the neighboring oxygen. The remaining triplet peak centered at δ1.43 (J = 7.2 Hz), which integrated for six protons, is attributed to methyl protons at C-3'.

The ^{13}C NMR spectrum of compound **38** (Table 2, Appendix 8) showed a total of five peaks at δ164.3, 136.5, 135.7, 120.1, 62.4 and 14.2. The peak at δ164.3 is assignable to the ester carbonyl carbons, C-1'. The other three aromatic signals at δ136.5, 135.7, and 120.1 are assignable to the equivalent pairs of carbons C-2 and C-5, C-1 and C-4 and C-3 and C-6, respectively. The peak at δ 62.4 is assignable to the methylene carbons, C-2'. The final peak at δ14.2 is for the remaining two equivalent methyl carbons, C-3'. In agreement with the expected structure for the product, the DEPT-135 spectrum further confirmed that the peaks at δ164.3, 135.7, and 120.1 are all quaternary carbons. In addition, the peak at δ62.4 is due to a methylene carbon and the peak at δ14.2 is attributed to the methyl carbon.

The transformation of diethyl-2,5-dibromoterephthalate (**38**) to diethyl-2,5-di(thiophen-2-yl)terephthalate (**39**) was effected by Pd(II)-catalyzed Stille reaction between diethyl-2,5-dibromoterephthalate and tributyl(thiophen-2-yl)stannane. Compound **39** was obtained as a white crystalline product in 59.1% yield and was characterized by its NMR spectra as described below.

The ^{1}H NMR spectrum of compound **39** (Table 3, Appendix 10) consists of five peaks in total. The singlet peak at δ7.85 is meant for pairs of equivalent aromatic hydrogen atoms at C-3 and C-6. The doublet of doublets peak centered at δ7.42 (J = 1.2, 5 Hz), that is integrated for two protons is

assignable to the pair of aromatic protons on C-5' of the thiophene rings. The complex overlapping multiplet between δ7.09 and 7.13 is assignable to two pairs of equivalent aromatic protons on C-3' and C-4'. A down-field-shifted quartet centered at δ4.25 (J = 7.2 Hz) is due a pair of equivalent methylene protons next to the ester oxygen. The remaining triplet centered at δ1.18, that integrated for three protons (J = 7.2 Hz) is attributable to pair of equivalent methyl groups neighbored by the methylene groups.

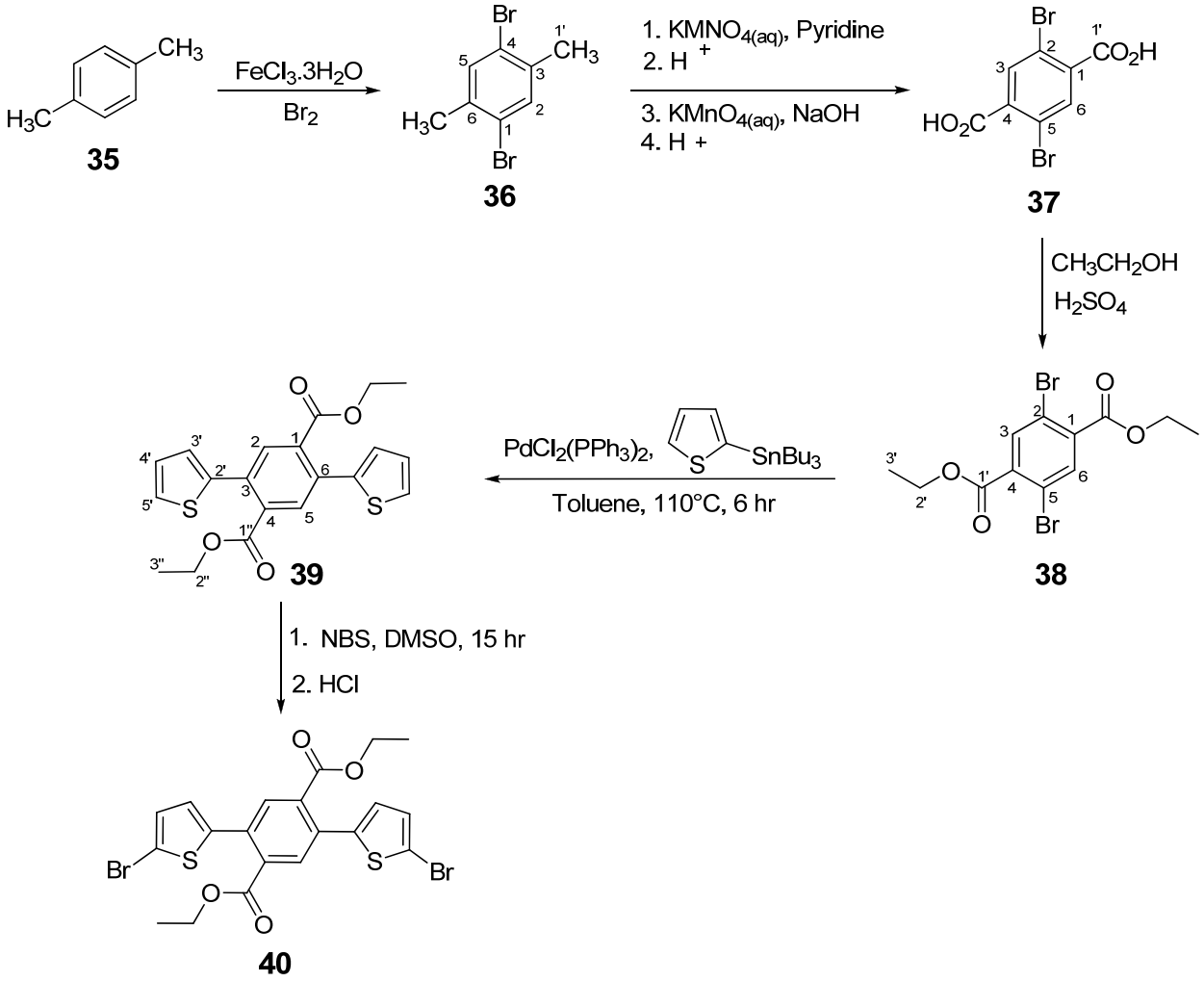

Scheme 5. Synthesis of diethyl-2,5-bis(5-bromothiophen-2-yl)terephthalate monomeric unit.

The ^{13}C NMR spectrum of compound **39** (Table 4, Appendix 11) showed a total of ten signals. The peak at δ167.7 is assignable to two equivalent carbonyl

carbons (C-1"). The peak at δ 140.5 is due to the two equivalent carbons, C-2', down-field-shifted by both the electron withdrawing effect of the nearby sulfur atom and the deshielding of the benzene ring in the same plane as the thiophene units. The peak at δ134.1 can be accounted for C-3 and C-6, two equivalent carbons on the benzene ring core, directly attached to the thiophene rings. The signal at δ133.5 is due to C-1 and C-4. The down-field position of this signal is due to the electron withdrawing effect of the nearby carbonyl carbons. The peak at δ 131.9 is for the methine carbons of the benzene ring. The other three peaks at δ127.4, 127.0, 126.5 are accounted for the equivalent pairs C-4', C-3', and C-5', respectively. The peak at about δ61.9 is due to the equivalent carbons, C-2", experiencing the electron withdrawing effect of the neighboring ester oxygen atoms. The remaining peak in the aliphatic region is attributed to the methyl carbons C-3". The DEPT-135 spectrum also supports the above assignment. Thus, peaks at 167.7, 140.5, 134.1, and 133.5, which disappeared in the DEPT-135 spectrum, are due to quaternary carbons, while the peaks at 131.9, 127.4, 127.0, and 126.2 are pointing upward and are due to methine carbons. The peak at δ61.7 pointed downwards and is attributed to the methylene carbon and the final peak at δ13.8 pointing upward is assigned to the methyl carbon.

Diethyl-2,5-di(thiophen-2-yl)terephthalate (**39**) was reacted with N-bromosuccinimide in DMF to give diethyl-2,5-bis(5-bromothiophen-2-yl)terephthalate (**40**) as pale-yellow product in 85.3% yield.

The ^{1}H NMR of compound **40** (Table 3, Appendix 13) displayed five proton resonances. The singlet at δ7.80, which integrated for two protons, can be ascribed to the pair of equivalent protons at C-2 and C-5 on the benzene ring. The doublet centered at δ7.06 is due to the two equivalent protons at C-4' on the thiophene rings. This signal appears at a relatively up-field position due to the electron withdrawing resonance effect of the benzene ring and is close to the bromine to experience its strong deshielding van der Waals effect. The other

doublet centered at δ6.87 (J = 4 Hz) is assignable to pairs of equivalent protons at C-3' on the thiophene ring. They are down-field shifted relative to the former pair, because they are far away from the heavy bromine atoms and are in the less deshielding region of the benzene ring through resonance. The quartet at about δ4.28 (J = 7.2) is assigned to the four methylene protons on C-2". The down-field appearance of this signal is because of the electron withdrawing effect of the nearby ester oxygen and the splitting pattern is accounted by the presence of the neighboring methyl protons, which signal is a triplet centered at δ1.23.

Table 4 (Appendix 14) shows the ^{13}C spectrum of compound **40**. The peak at δ167.0 is due to carbonyl carbons. The ^{13}C NMR spectrum further depicts a total of six peaks in the aromatic region. The peak at δ140.2 is due to C-2' on the thiophene rings. The down-field appearance of this signal is the consequence of the combined effect of the deshielding van der Waals effect of the large bromine atom and the electron withdrawing effect of the benzene ring by resonance. The peak at δ133.9 is due to C-3 and C-6 on the benzene ring. They are deshielded relative to the other benzene carbons because they are directly attached to the thiophene rings, which are electron withdrawing. The other peak at δ133.0 is attributed to C-1 and C-4 on the benzene core, directly attached to the electron withdrawing carbonyl carbons. The peak at δ132.1 is due to the pair of equivalent carbons, C-2 and C-5. The two aromatic at carbon signals at δ130.1 and 127.4 are for two equivalent pairs of carbons C-4' and C-3' on the thiophene ring, respectively. The signal at δ113.3 is attributed to C-5' on the thiophene ring containing the bromine substituents. Two signals appeared in the aliphatic region at δ61.9 and 13.9. The peak at δ61.9 is due to methylene carbons, C-2" next to the ester oxygen. The signal at δ13.9 is attributed to the methyl carbons, C-3". The DEPT-135 spectrum further confirmed that the carbon signals at δ132.1, 130.2, and 127.4 are due to methine carbons, the peak at δ13.9 is assigned to methyl carbons, and the peak at 61.9 is due to methylene carbons. In addition, those carbon signals

that prevailed in the ^{13}C NMR spectrum, but not in the DEPT-135 spectrum are attributable to quaternary carbon atoms.

Table 3. ^{1}H NMR (400.13 MHz, $CDCl_3$) data (δ ppm) of compounds **39** and **40**.

39	**40**
7.85	7.80
(s, 2H, H-2, H-5)	(s, 2H, H-3, H-6),
7.41	7.06
(dd, *J* = 1.2, 5 Hz, 2H, H-5')	(d, *J* = 3.6, H-4')
7.09-7.13	6.87
(m, 4H, H-3', H-4')	(d, *J* = 4Hz, H-3')
4.24	4.28
(q, *J* = 7.2 Hz, 2H, H-2")	(q, *J* = 7.2, 4H, H-2")
1.18	1.42
(t, *J* = 7.2, 6H, H-3")	(t, *J* = 2, 6H, H-3")

Table 4. ^{13}C NMR (100.6 MHz, $CDCl_3$) data (δ ppm) for compounds **39** and **40**.

C	**39**	**40**
1	133.5	133.0
2	134.1	133.9
3	131.9	132.1
4	133.5	133.0
5	134.1	133.9
6	131.9	132.1
2'	140.5	140.2
3'	127.0	127.4
4'	127.0	130.1
5'	126.5	113.3
1"	167.7	167.0
2"	66.9	61.9
3"	13.8	13.8

4.2. Synthesis of the ladder type thiophene-phenylene-thiophene (TPT) monomeric unit.

Scheme 6 shows the synthesis of the ladder-type thiophene-phenylene-thiophene (TPT) monomeric unit **44** staring from compound **39**. Thus, compound **39** was first transformed to **42** by reaction of an organolithium compound derived from 1-bromo-4-heptyloxybenzene and *n*-butyllithium. The nucleophile underwent a nucleophilic addition-elimination reaction at the ester carbonyl carbon followed by a nucleophilic addition to the intermediate ketone to form the lithium salt of a tertiary alcohol, which was subsequently converted to the tertiary alcohol, **42**, upon acid treatment in 93.3% yield.

The ^{1}H NMR spectrum of compound **42** (Table 5, Appendix 16) showed a singlet centered at δ7.28 attributable to the equivalent protons at C-3 and C-5. The doublet centered at δ7.21, which integrated for two protons, is assignable to H-5' and H-5" on the thiophene rings. The other doublet centering at δ7.12 is due to the eight equivalent protons at C-2"' and C-6"' on the benzene rings. The doublet of doublets at δ6.85 is assignable to the pair of equivalent protons H-4' and H-4" and the doublet at δ6.79 is attributed to the pair of equivalent protons H-3' and H-3" on the thiophene rings. The peak at δ6.26 is due to the H-3"" and H-5"". The triplet at δ3.99 is due to methylene protons on the heptyloxy side chain next to the ether oxygen, while the very prominent singlet at δ3.47 is due to the hydroxyl proton on the aliphatic quaternary carbon atom. The pentate centering at δ1.82 (J = 6.8 Hz) is due to the methylene protons on the heptyloxy side chain, two bonds away from the ether oxygen. The remaining methylene protons resonances appeared as a complex multiplet between δ1.30-1.0. The final triplet centering at δ0.93 is attributed to terminal methyl protons on the heptyloxy side chains.

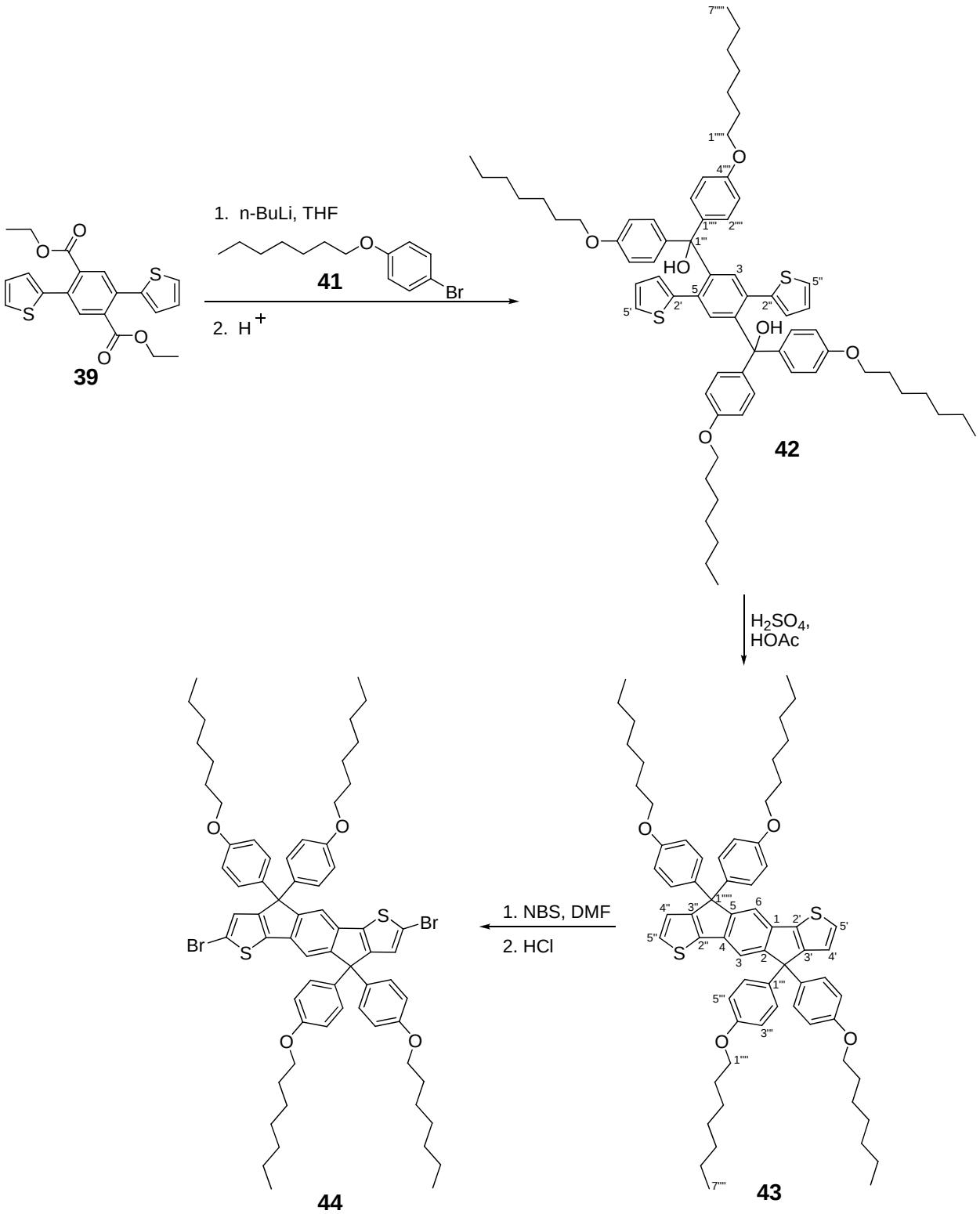

Scheme 6. Synthesis of the thiophene-phenylene-thiophene (TPT) ladder-type monomeric unit

The ^{13}C NMR spectrum of compound **42** (Table 6, Appendix 17) showed a total of 19 peaks of which 11 signals appeared in the aromatic region and the remaining eight appeared in the aliphatic region. The relatively highly down-field shifted peak at δ158.3 is due to C-4". The other peak at δ145.2 can be assigned to C-2 and C-5. There appeared also a peak at δ142.5 that is assignable to carbons C-2' and C-2". The signal at δ139.8 is due to C-1"', and, the peak at δ136.1 is attributable to the equivalent pair, C-1 and C-4. The methine carbon peak at δ131.9 is assigned to C-3 and C-6 while the peak at δ129.2 is attributed to C-3"'. The peaks centering at δ127.9, 127.0, and 126.8 are for the equivalent pairs of methine carbons on the thiophene rings. The last signal in the aromatic region at δ133.8 is due to C-2"' and C-6"'. The signal at δ82.5 is due to the quaternary aliphatic carbon that is bonded to the hydroxyl group. Another peak at δ68.0 is due to the methylene carbon adjacent to the ether oxygen on the heptyloxy side chain. Five peaks at δ31.8, 29.3, 29.1, and 22.7 are due to internal methylene carbons on the heptyloxy side chain and the final peak at δ14.2 is accountable to the terminal methyl carbon.

The HMBC spectrum of **42** gave a very valuable connectivity between the hydroxyl proton and carbons, C-1"', C-4, and C-1"", which justified that the hydroxyl group is part of the giant structural architecture.

Compound **42** was allowed to undergo intramolecular annulation reaction by refluxing it in acetic acid with few drops of concentrated sulfuric acid as a catalyst, as shown in Scheme 6. The cyclized product **43**, which was impure, gave a 50% yield after chromatographic purification on silica gel. Compound **43** was characterized based on its NMR spectra as discussed below.

The ^{1}H NMR spectrum of compound **43** (Table 5, Appendix 19) showed a singlet peak centered at δ7.48 that is assignable to the two equivalent protons on C-3, and C-6. The two-proton doublet at δ7.29 (J = 4.8) is due to H-5' and H-5". The other doublet centered at δ7.23 (J = 7.6 Hz) which integrated for eight

protons is due to H-2''' and H-6''' on the substituted benzene rings. The two-proton doublet at δ7.03 (*J* = 5.2 Hz) is attributed to H-4', H-4''. The final doublet peak in the aromatic region at δ6.83 (*J* = 8.8 Hz) is attributed to H-3''' and H-5''' and is due to eight equivalent hydrogens. The triplet centered at δ3.95 (*J* = 6.4 Hz) is for eight hydrogens of the methylene groups on the heptyloxy side chains next to the ether oxygen atom. The pentate centered at δ1.81 is due to the methylene protons on the heptyloxy substituent two bonds away from the electronegative oxygen atom. The complex multiplet between δ1.36-1.56 is due to the twenty four remaining methylene protons. The final triplet at δ0.95 (*J* = 6.4 Hz) is due to the twelve methyl protons on the heptyloxy substituent.

The ^{13}C NMR spectrum of compound **43** (Table 6, Appendix 20) displayed eleven signals in the aromatic region, and eight peaks in the alipahtic region. The spectrum resembled that of compound **42** except for the signal due to the SP^3 hybridized quaternary carbon atom C-1''''. The resonance due to this carbon atom was upfield shifted from δ82.5 in **42** to δ62.0 in **43**. This clearly shows that C-1'''' is no more oxygenated and that cyclization reaction has taken place to afford the ladder-type structure in **43**.

The final stage in the synthesis of the thiophene-phenylene-thiophene (TPT) ladder type monomeric unit was the dibromination of compound **43** as depicted in Scheme 6. The bromination reaction was achieved using NBS as a brominating agent, and DMF as a solvent. The reaction mixture was then quenched with 1M HCl solution to give compound **44** as a dark brown-colored solid in 86.2% yield.

The ^{1}H NMR spectrum of compound **44** (Table 5, Appendix 22) showed a singlet peak at δ7.38 which is due to the equivalent pair of aromatic protons on C-3 and C-6, and C-3''' and C-5''', respectively. The thiophene ring protons on C-4' and C-4'' displayed a singlet in agreement with bromination at C-5'and C-

5”. The remaining proton resonances are in agreement with structure **43** as depicted in Table 5.

The ^{13}C NMR spectrum of compound **44** (Table 6, Appendix 23) showed eleven signals in the aromatic region, and eight peaks in the aliphatic region. The fact that the bromine atoms are incorporated at C-5’ and C-5” of the thiophene rings is evident from the carbon resonance at δ117.1, which is upfield-shifted compared to the corresponding carbon signal in **43**. In addition the DEPT-135 spectrum showed that the signal at δ117.1 is due to a quaternary carbon atom in agreement with the incorporation of the bromine atoms at C-5’ and C-5”. The remaining carbon resonances are in agreement with structure **44**, as shown in Table 6.

Table 5. ^{1}H NMR (400.13 MHz, $CDCl_3$) data (δ ppm) of compounds **42**, **43**, and **44**.

42	**43**	**44**
7.30 (m, 2H,H-3, H-5) 7.21 (d, *J* = 5.2, 8H, H-3”’, H-5”’) 6.79 (dd, *J* = 3.6, 5.6 Hz, 2H, H-4’, H-4”) 6.26 (d, *J* = 2.8, 2H, H-2’, H-2”), 3.99 (t, *J* = 6.4 Hz, 8H), 3.47 (s, 2H, H-*) 1.82 (p, *J* = 6.8, 2H) 1.30-1.51 (m, 24H) 0.93 (t, *J* = 6.8, 12H)	7.48 (s, 2H,H-3, H-6) 7.29 (d, *J* = 4.8 Hz, 2H, H-5’, H-5”) 7.23 (d, *J* = 8.8 Hz, 8H, H-2”’, H-6”’) 7.03 (d, *J* = 5.2 Hz, 2H, H-4’, H-4”) 6.83 (d, J = 8.8 Hz, 8H, H-3”’, H-5”’) 3.95 (t, *J* = 6.4 Hz, 8H) 1.81 (p, *J* = ??, 8H, 2””) 1.36-1.56 (m, 24H) 0.95 (t, *J* = 6.4 Hz, 12H, 7””)	7.38 (s, 2H,H-3, H-6) 7.19 (d, *J* = 8.8, 8H, H-2”’, H-6”’) 7.04 (s, 2H, H-4’, H-4”) 6.85 (d, *J* = 8.8, 8H, H-3”’, H-5”’) 3.96 (t, *J* = 7.2 Hz, 8H) 1.81 (p, *J* =6.4 , 8H) 1.37-1.49 (m, 24H) 0.95 (t, *J* = 6.4, 12H)

Table 6. ^{13}C NMR (100.6 MHz, $CDCl_3$) data (δ ppm) for compound **42**, **43** and **44**.

C	**42**	**43**	**44**
1	136.1	141.1	141.2
2	145.2	153.8	155.2
3	131.9	129.4	129.0
4	136.1	141.1	141.2
5	145.2	153.8	155.2
6	131.9	129.4	129.0
2’	142.5	135.1	135.0
3’	127.0	136.8	135.9
4’	127.9	120.5	114.4
5’	126.8	123.0	117.1
2”	142.5	135.1	135.0
3”	127.0	136.8	135.9
4”	127.9	120.5	114.4
5”	126.8	123.0	117.1
1”’	139.8	153.8	153.0
2”’	129.2	114.6	113.6
3”’	133.8	127.6	126.0
4”’	158.3	158.0	158.3
5”’	133.8	127.6	126.0
6”’	129.2	114.6	113.6
1””	68.0	68.0	68.0
2””	31.8	31.8	31.9
3””	29.3	29.4	29.4
4””	29.1	29.1	29.1
5””	26.1	26.1	26.1
6””	22.7	22.7	22.7
7””	14.2	14.16	14.2
1”””	82.5	62.0	62.0

4.3. Synthesis of quinoxaline-based monomeric moieties

As the part of the project work, two quinoxaline-based monomers were synthesized and characterized. Such quinoxaline-based materials have been used in synthesizing copolymers with appropriate diboronate esters with the aim of preparing a low bandgap conducting material.

The synthetic strategies adopted for the synthesis of the quinoxaline-based monomers are depicted in Schemes 7 and 8. 2,3-Bis(4-octyloxyphenyl)-5,8-bis(tributylstannyl)thiophen-2-yl)quinoxaline (**49**) was synthesized from 4,7-di(thiophen-2-yl)benzo[c][1,2,3]thiadiazole (**45**). Thus, reduction of compound **45** using activated zinc dust in acetic acid, and condensation of the resulting diamine (**46**) with 1,2-bis(4-(heptyloxy)phenyl)ethane-1,2-dione, gave compound **47**, which was subsequently brominated to compound **48**. Distannylation of the dibromide **48** was achieved by metal halogen exchange followed by treatment with tributylstannyl chloride.

The ^{1}H NMR spectrum of compound **47** (Table 7, Appendix 25) revealed a singlet at δ8.11 integrating for two protons due to the two equivalent protons, H-6 and H-7 on the benzene ring core of the quinoxaline moiety. The doublet peak centered at δ7.87 (J = 3.6 Hz) integrating for two protons is assignable to the pair of equivalent protons H-5' on the thiophene ring. The other doublet centered at δ7.75 is due to the two pairs of equivalent protons H-2" and H-6" on the *para*-substituted aromatic rings. There exists also a doublet centering at δ7.53 which is assigned to the equivalent pairs of hydrogen H-3' on the thiophene ring. The doublet of doublets peak appearing at δ7.20 is accounted to H-4' and the peak at δ6.93 is due to the equivalent pairs H-3" and H-5". The triplet centering at δ4.02 is attributed to the methylene protons on the heptyloxy side chain next to the oxygen atom. A pentate centered at δ1.84 is assigned to the methylene hydrogens two bonds away from the ether oxygen.

The complex multiplet between δ1.34-1.54 is due to the sixteen internal methylene protons. The final triplet centering at δ0.93 is due to the six methyl hydrogens on the terminal methyl groups.

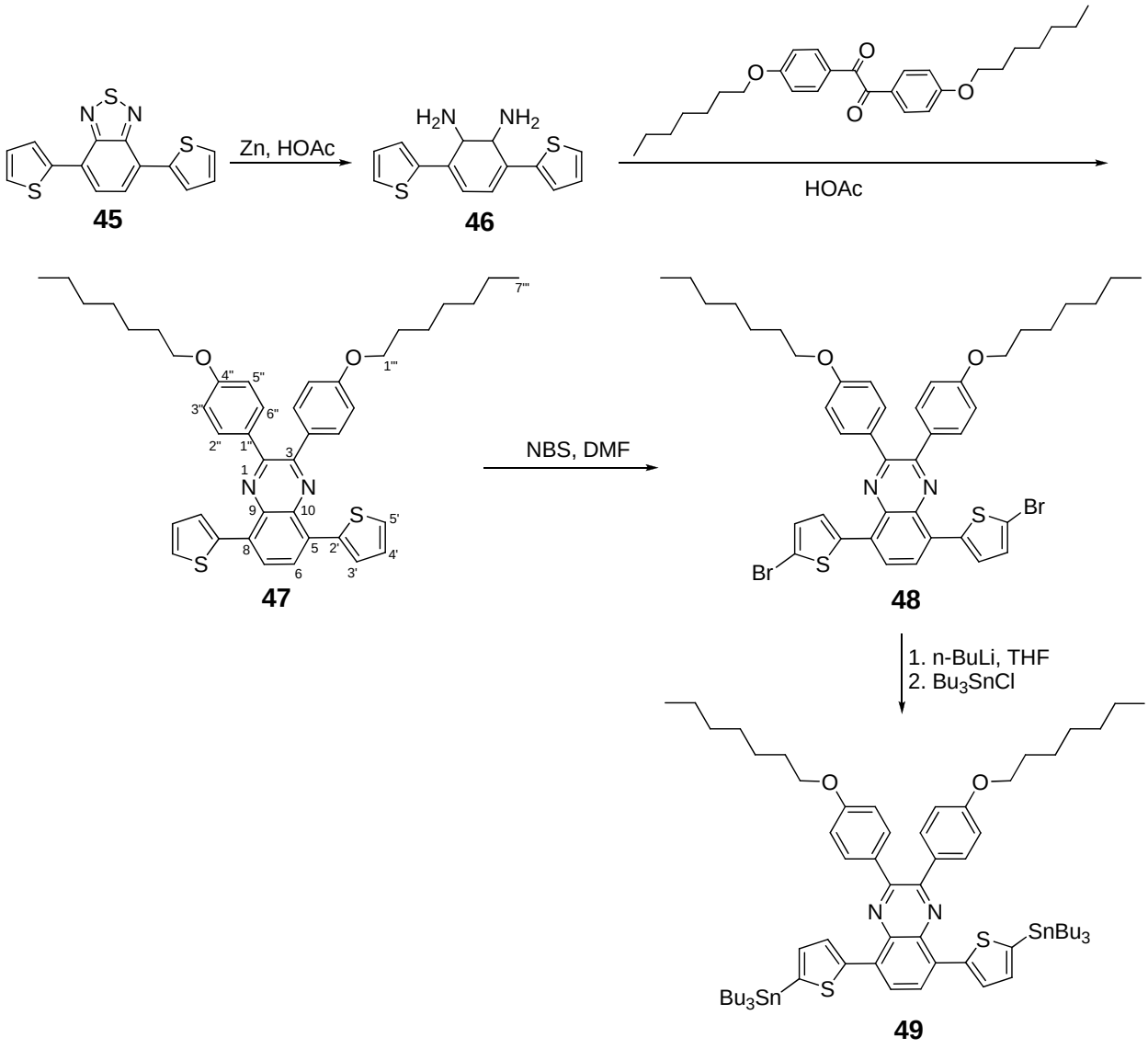

Scheme 7. Synthesis 2,3-bis(4-octyloxyphenyl)-5,8-bis(tributylstannyl)thiophen-2-yl)quinoxaline-based monomeric unit.

The ^{13}C NMR spectrum of compound **47** (Table 8, Appendix 26) showed a total of 11 peaks in the aromatic region. The peak at δ160.0 is assigned to C-4". The quaternary carbon peak at δ151.3 is attributed to C-2 and C-3. There appears also a peak at δ139.0 which is probably due to the quaternary carbons C-9 and C-10. The peak at δ137.0 is due to another equivalent quaternary carbon pair

C-2' on the thiophene rings. The quaternary carbon peak at δ131.9 is assignable to C-5 and C-8. The signals due C-4' appeared at δ131.8, while the peak at δ131.0 is due to C-2" and C-6". The other peaks in the aromatic region are assignable to the three methine carbons on the thiophene rings. The peaks in the aliphatic region at δ68.1, 31.9, 29.4, 29.3, 26.1, 22.7, and 14.1 are due to the carbons on the heptyloxy side chain.

Compound **47** was brominated by slow addition of a solution of NBS in DMF in to a solution of **47** in DMF, in the dark, to give a greenish yellow precipitate that was collected and purified by washing with MeOH to afford compound **48** in 89.8% yield.

Table 7. ^{1}H NMR (400.13 MHz, $CDCl_3$) data (δ ppm) of compound **47** and **48**.

47	**48**
8.11	7.85
(s, 2H, H-4, H-6, H-7)	(s, 2H, H-4, H-5)
7.87	7.63
(d, *J* = 3.6 Hz, 2H, H-5')	(d, *J* = 8.8 Hz, 4H, H-2", H-6")
7.75	7.43
(d, *J* = 8.4 Hz, 4H, H-2", H-6")	(d, *J* = 4.4 Hz, 2H, H-4')
7.53	7.06
(dd, J = 1.2, 5.2 Hz , 2H, H-3')	(d, *J* = 4 Hz, 2H, H-3')
7.20	4.20
(dd, *J* = 4 Hz, 5Hz, 2H, H-4')	(t, *J* = 6.4 Hz, 4H)
6.93	1.83
(d, *J* = 8.8 Hz, 4H, H-3", H-5"')	(p, *J* = 6.4 Hz, 4H)
1.34-1.54	1.25-1.53
(m, 12H)	(m, 12H)
0.93	0.92
(t, *J* = 6.4 Hz, 6H).	(t, *J* = 7.2 Hz, 6H).

Table 8. ^{13}C NMR (100.6 MHz, $CDCl_3$) data (δ ppm) for compound **47** and **48**.

C	**47**	**48**
2	151.3	151.7
3	151.3	151.7
5	131.9	131.7
6	128.7	125.0
7	128.7	125.0
8	131.9	131.7
9	139.0	136.2
10	139.0	136.2
2’	137.0	132.4
3’	131.2	129.0
4’	131.8	130.1
5’	114.2	114.7
1”	126.5	116.9
2”	131.0	125.2
3”	126.2	114.2
4”	160.0	160.2
5”	126.2	114.2
6”	131.0	125.5
1”’	68.1	68.1
2”’	31.9	31.9
3”’	29.4	29.4
4”’	29.3	29.3
5”’	26.1	26.1
6”’	22.7	22.7
7”’	14.13	14.2

The ^{1}H NMR spectrum of compound **48** (Table 7, Appendix 28) showed a singlet peak at δ 7.85 due to the pair of equivalent protons on C-6 and C-7. The doublet centering at δ7.63 is due to the methine protons H-2" and H-6" on the benzene rings. The other doublet centering at δ7.43 is assignable to H-4'. This signal is down-field shifted by the van der Waals effect of the adjacent big bromine atoms. The doublet appearing at δ7.06 integrating for two protons is due to the other pair of equivalent protons H-3' on the thiophene ring. The final group of aromatic protons, H-3" and H-5", have their resonance appearing at δ6.91. The triplet at δ4.02 is assignable to the pair of methylene protons on the heptyloxy side chain which experience the electron withdrawing inductive effect of the electronegative oxygen atom. The peak at δ1.83 attributed to the methylene protons two bonds away from the ether oxygen on the heptyloxy side chain. The complex multiplet signal between δ1.25-1.53 is due to the internal methylene protons and the final peak at δ0.93 is due to the terminal methyl protons.

The ^{13}C NMR spectrum of compound **48** (Table 8, Appendix 29) showed a total of twelve signals in the aromatic region. The peak at δ160.2 is assigned for C-4", whereas, the peak at δ151.7 is due to C-2 and C-3, on the core quinoxaline unit. The peak at δ136.2 is attributable to another equivalent carbon pairs, C-9 and C-10. The signals at δ132.4 and 131.7 are, respectively, due to C-2' and C-5 and C-8 equivalent pairs, while, the peaks at δ130.1 and 129.0, are assigned to the equivalent pairs C-4' and C-3', respectively of the thiophene rings. The peak at 125.2 is due to C-2" and C-6". The peak appearing at 116.9 is due to C-1", and the peak appearing at δ114.7 and 114.2 are, respectively, for C-5' and C-3" and C-5". There are also peaks in the aliphatic region at δ68.1, 31.9, 29.3, 26.1, 22.7, 21.0, and 14.2, which are assignable to for the seven aliphatic carbons on the heptyloxy side chain.

The last step in the synthesis of compound **52** involved the distannylation of **51**. Thus, **51** was dissolved in anhydrous THF and was subjected to a metal-

halogen exchange reaction by treatment with *n*-butyllithium and was then reacted with tributylstannylchloride to afford **49** as a brownish oil. The ^{1}H and ^{13}C spectra of the product clearly showed the incorporation of the tributylstannyl group. However, there were also some impurity signals in the spectra. An attempt was then made to purify the compound by passing it through a column of silica gel using ethyl acetate:hexane as eluent. However, this led to the decomposition of compound **49**. The identified decomposition product was found to be **47** which presumably arose due to protolysis via silica gel-mediated destannylation of **49**.

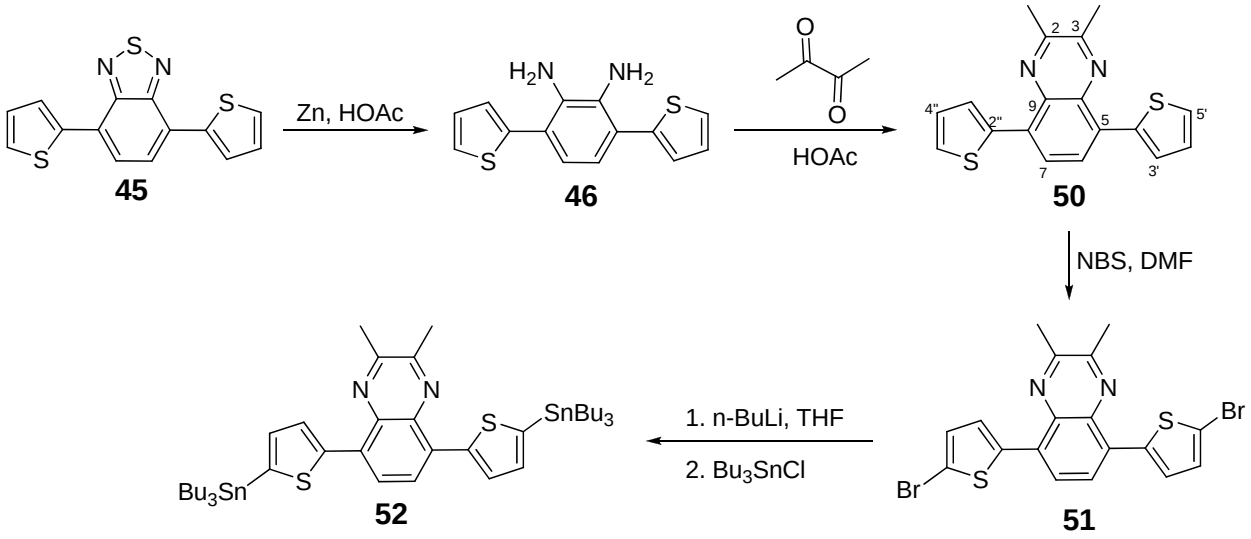

Scheme 8. Synthesis of 2,3-dimethyl-5,8-bis(5-(tributylstannyl)thiophen-2-yl)quinoxaline

Another attempt was made to synthesize the distannylated quinoxaline **52** following a similar sequence of reactions as described above for compound **49**. Thus, the diamine **46**, which was obtained from **45** by reduction with zinc and acetic acid, was condensed with 2,3-butanedione and the resulting quinoxaline (**52**) was brominated with NBS and stannylated with *n*-butyllithium and tributylstannylchloride as depicted in Scheme 8. Compounds **50**, **51** and **52** were characterized based on their ^{1}H and ^{13}C NMR spectra. Table 9 shows the ^{1}H NMR data of these compounds. In the ^{1}H NMR spectrum of compound **50**, the singlet peak at δ8.03 is due to the two equivalent protons, H-6 and H-7 on

the benzene ring of the quinoxaline unit. The doublet of doublets centering at δ7.86 (*J* = 1.2, 3.8 Hz) is assigned to, H-5' and H-5" on the thiophene rings. While the other doublet of doublets centering at δ7.51 (J = 0.8, 5.2 Hz) is due to the pair of equivalent protons on C-3' and C-3" of the thiophene ring, the doublet of doublet at δ 7.51 is attributed to the other pair of equivalent protons on C-4' and C-4" of the same thiophene ring. The final peak at δ2.82 is assignable to the benzylic methyl groups on the quinoxaline core structure.

The ^{13}C NMR spectrum of **50** (Table 10, Appendix 32) displayed a peak at δ152.2 which is assigned to C-2 and C-3. The quaternary carbon peaks at δ139.2 and 137.6 are attributed to the equivalent pairs C-9 and C-10 and C-2' and C-2", respectively. The remaining quaternary carbon peak at δ130.9 is assigned to C-5 and C-8; whereas, the peak at δ128.3 is due to the equivalent methine carbon pair C-6 and C-7 on the benzene ring of the quinoxaline core unit. The remaining three methine carbon peaks at δ126.6, 126.4 and 126.1 are attributed to the methine carbons C-4' and C-4", C-3' and C-3" and C-5' and C-5", respectively, on the thiophene rings. There is also another signal in the aliphatic region that appeared at δ22.7 which can be assigned to the methyl carbons directly attached to the quinoxaline core.

The ^{1}H NMR spectrum of compound **51** (Table 9, Appendix 34) is in good agreement with the incorporation of the bromine atoms at positions 5' and 5" of the thiophene moieties. Thus, the singlet peak at δ7.99 is attributed to the two equivalent hydrogens H-6 and H-7, on the benzene ring of the quinoxaline core. The doublets at δ7.53 and 7.12 (*J* = 4 Hz) are assignable to the other equivalent pairs of hydrogens, H-3' and H-3" and H-4' and H-4" on the thiophene rings. There exists also a peak at δ2.84 that is attributed to the methyl protons on the quinoxaline core.

Table 9. ^{1}H NMR (400.13 MHz, CDCl3) data (δ ppm) of compounds **50** and **51**.

50	**51**
8.03	7.99
(s, 2H, H-4, H-5),	(s, 2H, H-4, H-5)
7.86	7.53
(dd, *J* = 1.2 ,3.6 Hz, 2H, H-5', H-5")	(d, *J* = 4 Hz, 2H, H-3', H-3")
7.51	7.12
(dd, *J* = 0.8, 5.2 Hz, 2H, H-3', H-3")	(d, *J* = 4 Hz, 2H, H-4', H-4")
7.19	2.84
(dd, *J* = 3.6, 4.4 Hz, 2H, H-4', H-4")	(s, 6H, H-1"')
2.82	
(s, 6H, H-1"')	

Table 10. ^{13}C NMR (100.6 MHz, $CDCl_3$) data (δ ppm) for compound **50**.

C	**50**
2	155.2
3	155.2
5	130.9
6	128.3
7	128.3
8	130.9
9	139.2
10	139.9
2'	137.6
3'	126.4
4'	126.6
5'	126.1
1"	22.7

4.4. SYNTHESIS OF COPOLYMERS

As the primary objective of this project work was the synthesis of conjugated polymers, the monomers **40**, **44**, and **51** synthesized following the routes described in Scheme 5, 6 and 8 were subsequently polymerized with a previously synthesized fullorene-based monomeric unit. The polymerizations were achieved using the modified Suzuki coupling methodology, with freshly prepared tetrakis(triphenylphosphine)palladium(0) as the catalyst and tetraethylammonium hydroxide as a base instead of K_2CO_3 or $NaHCO_3$, which are usually used for the standard Suzuki polymerization as shown in Scheme 9. The reaction is believed to be considerably faster and supposedly gives a higher molecular weight polymer. Thus, the Suzuki polymerization technique resulted in polymers **53** (light yellow), **54** (deep red) and **55** (pale red) as solid products.

Cyclic voltammetry

Cyclic voltammetry is the simplest experimental tool to estimate the values of the highest occupied molecular orbital (HOMO), the lowest unoccupied molecular orbital (LUMO) and bandgaps. The most commonly used method is based on the detailed quantum chemical studies of Bredas [50], which can be expressed as:

$$I_p \text{ (HOMO)} = -(E^{ox} + 4.4 \text{ eV})$$

$$E_a \text{ (LUMO)} = -(E^{red} + 4.4 \text{ eV})$$

Where, E^{ox} and E^{red} are the onset potential values in volts for oxidation and reduction processes against Ag/AgCl reference electrode. From the cyclic voltammetry results shown in Figures 9, 10 and 11, the HOMO and LUMO levels of the polymers were estimated. Thus, the HOMO and LUMO positions of polymer **53** were found to be 5.6 and 3.2 eV, respectively. The HOMO value for polymer **54** was determined to be 5.2 eV. The value for the LUMO could not be

determined directly as the voltammogram could not clearly show the anodic peak. But, the value could be predicted from the UV-vis absorption spectrum and was found to be 2.9 eV. The LUMO and HOMO levels of polymer **55** were determined by the cyclic voltammetry (Figure 11) to be 5.7 and 3.8 eV, respectively. Thus, the band-gaps were estimated to be 2.4, 2.1, and 1.9 eV, respectively, for polymers **53**, **54** and **55**.

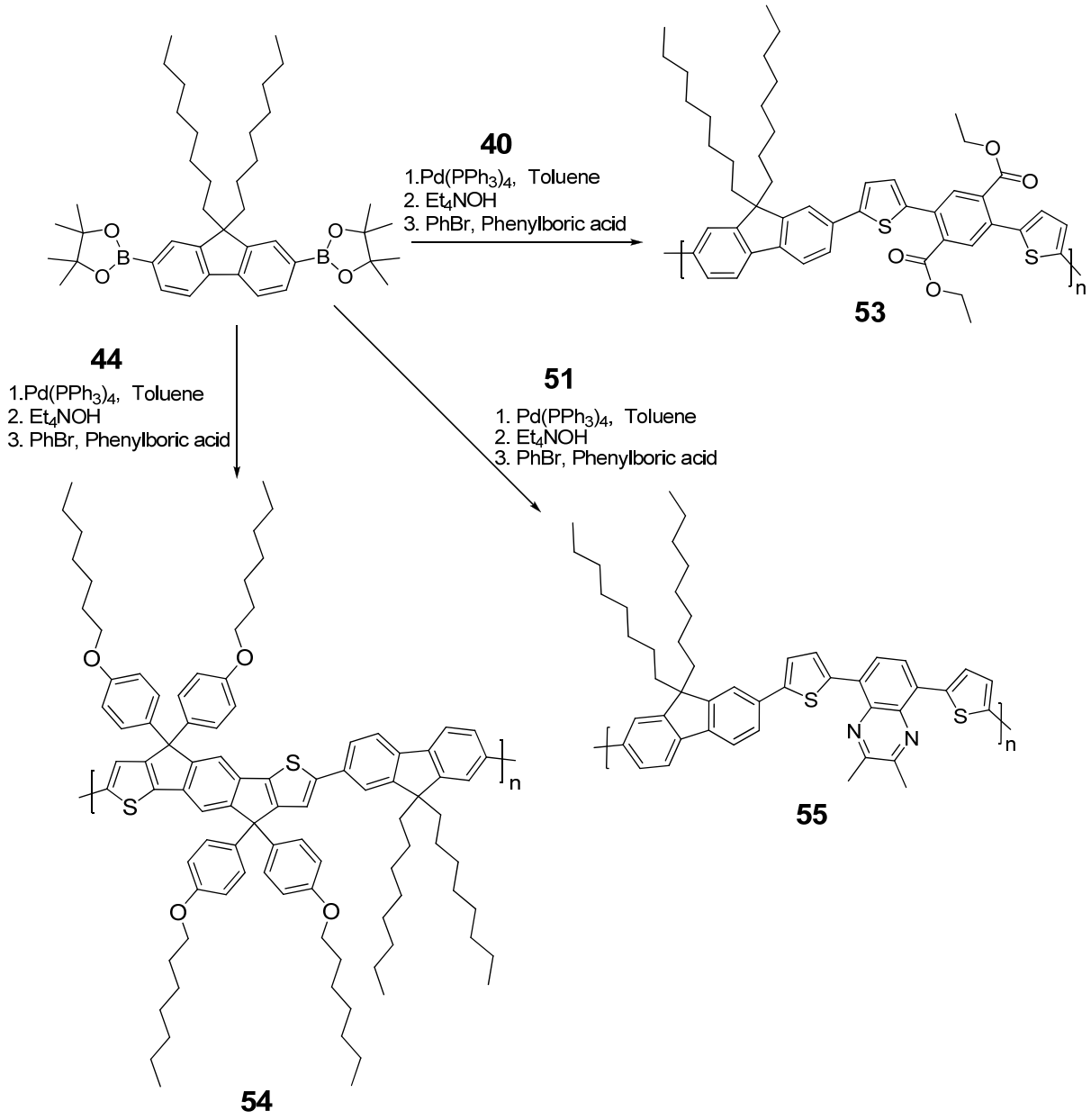

Scheme 9. Synthesis of polymers, **53**, **54** and **55**.

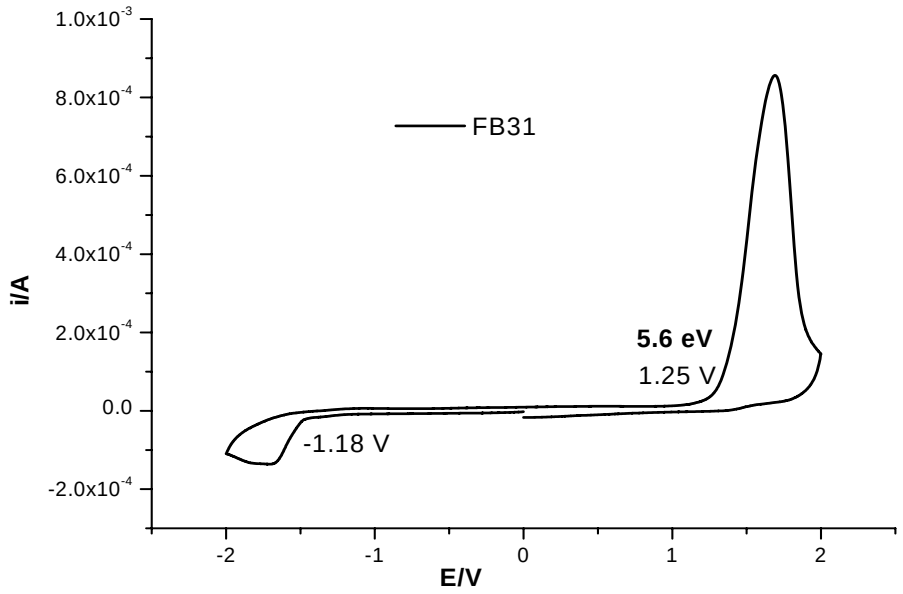

Figure 9. The cyclic voltammogram of polymer **53**.

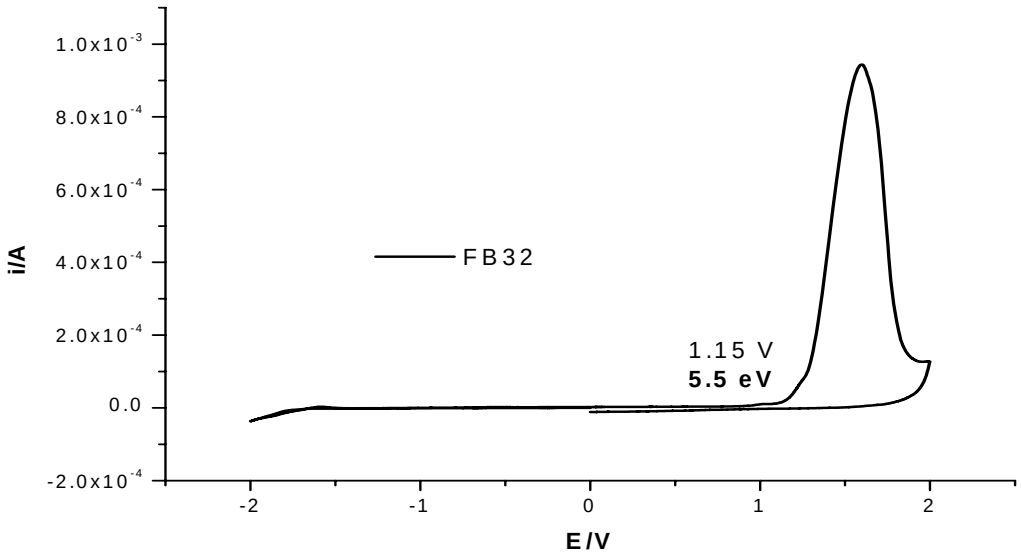

Figure 10. The cyclic voltammogram of polymer **54**.

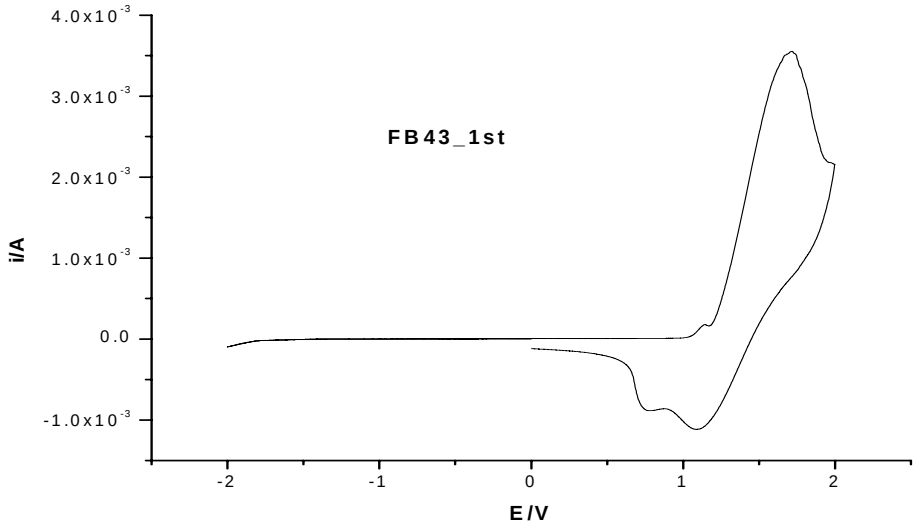

Figure 11. The cyclic voltammogram of polymer **55**.

UV-vis spectroscopy

Figures 12, 13 and 14 show the UV-Vis spectra for polymers **53**, **54** and **55**, respectively. The absorption spectra of the polymers spin-coated on glass slides showed red shifts compared to the spectra recorded from dilute solutions of the polymers in $CHCl_3$. In addition, the absorption maxima for polymers **53** and **54** were at 501 and 408 nm, respectively, for the film. And, two absorption maxima were observed for polymer **55**, at about 370 and 515 nm. The fact that the absorption maximum for polymer **53** is red-shifted relative to polymers **54** and **55** is informative of the extended conjugation as a result of the incorporation of the ladder-type monomeric unit. The absorption maximum at about 515 nm for polymer **55** is accounted to charge transfer excitation and is an indication for the incorporation of the donor-acceptor monomeric unit. The optical bandgaps were estimated from the onset of absorption and were found to be 2.1, 2.4, and 1.9 eV, respectively, for polymers **53**, **54**, and **55**. These values are close to the bandgaps estimated from the cyclic volatmmograms of the polymers.

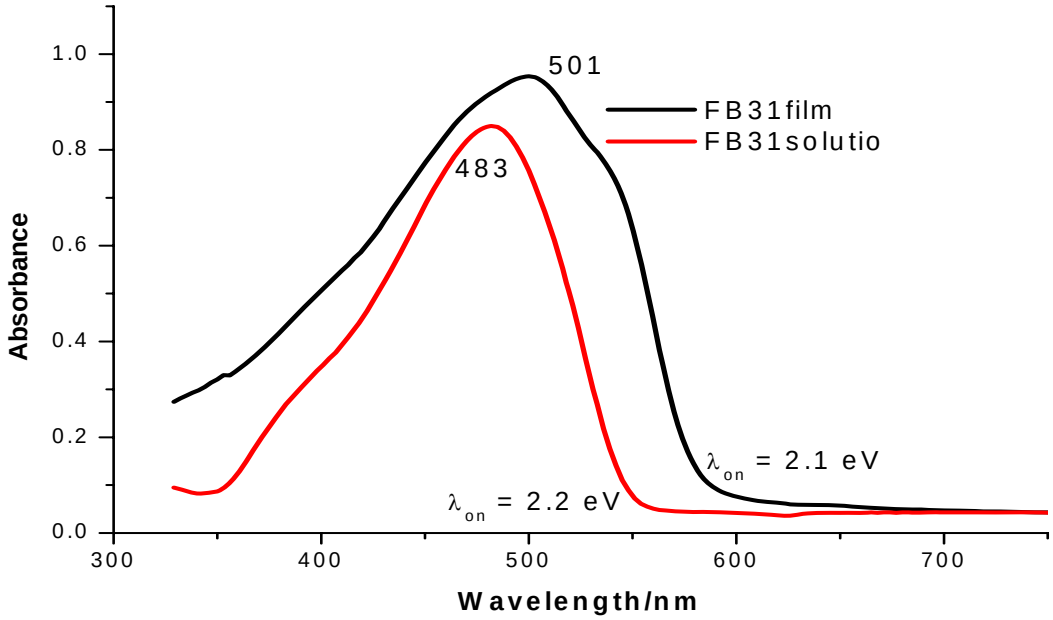

Figure 12. The UV-vis absorption spectrum of polymer **53** in film and solution.

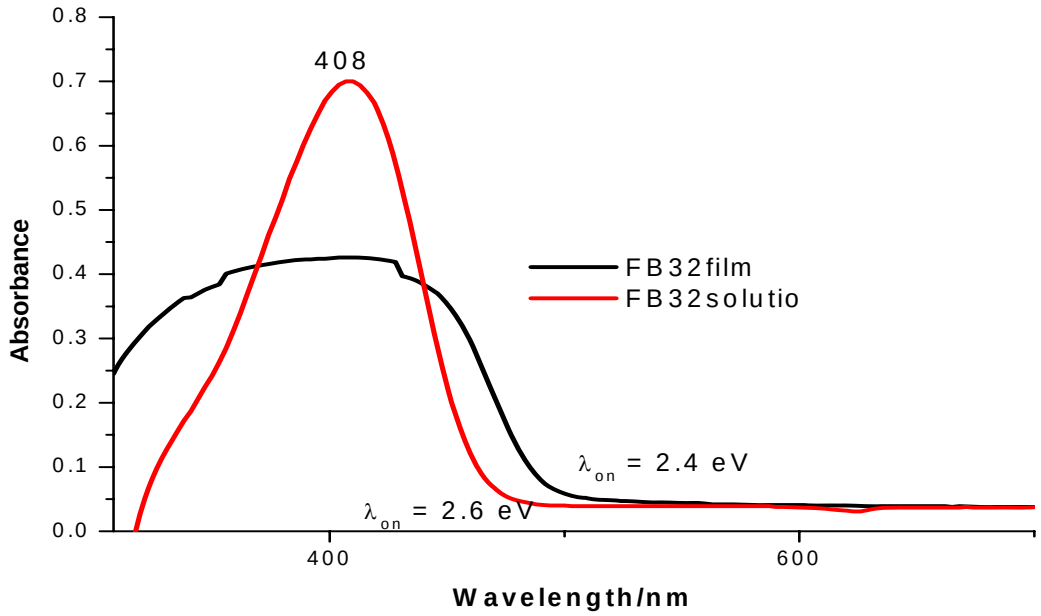

Figure 13. The UV-vis absorption spectrum of polymer 54 in film and solution.

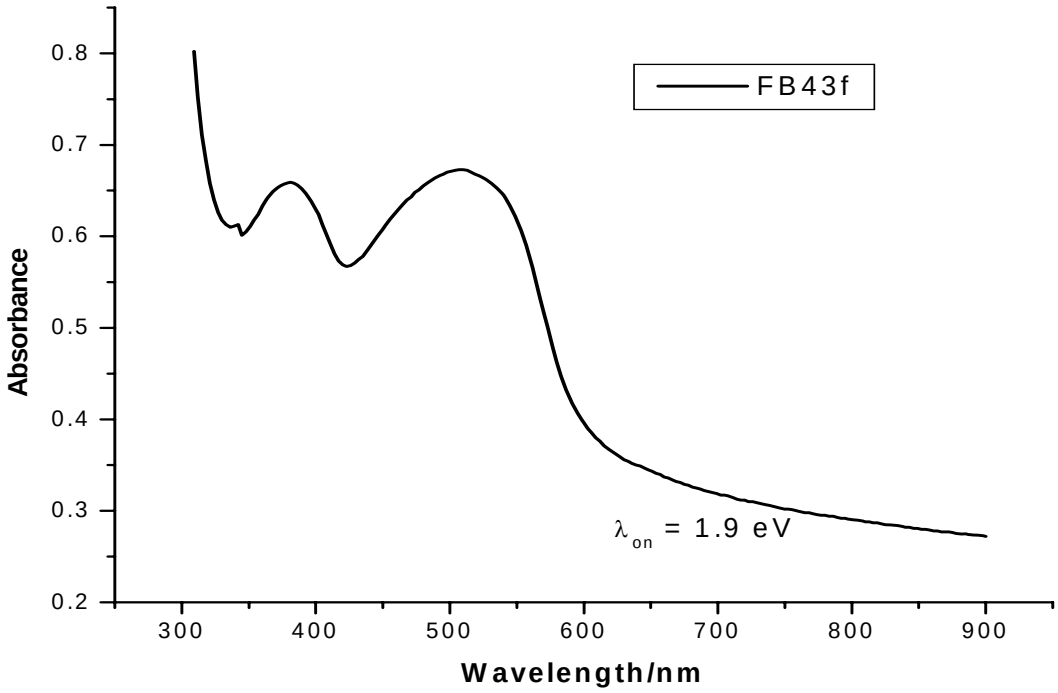

Figure 14. The UV-vis absorption spectrum of polymer 55.

5. CONCLUSION

In this project work, a thiophene-phenylene-thiophene bridged ladder-type monomer, diethyl-2,5-bis(5-bromothiophen-2-yl)terephthalate monomeric unit, and two types of quinoxaline-based donor-acceptor-donor monomeric units were prepared. Subsequently, alternating copolymers of these monomers were synthesized by reaction of these monomers with a previously prepared 2,2'-(9,9-dioctyl-9H-fluorene-2,7-diyl)bis(4,4,5,5-tetramethyl-1,3,2-dioxaborolane) using the Pd(0)-catalyzed Suzuki protocol. The polymers so synthesized were also partially characterized by cyclic voltammetry and Uv-vis spetrometery. The studies we have conducted revealed that the polymers may be promising candidates for solar cell and photodiode application.

6. EXPERIMENTAL

6.1. Materials and Methods

The ^{1}H NMR and ^{13}C NMR spectra were recorded on Bruker Avance 400 instrument at 400.13 and 100.6 MHz, respectively, in $CDCl_3$ and DMSO-d_6. UV-Vis spectra were run for the polymers in both thin film and as $CHCl_3$ solution using SPECTRONIC GENESYS 2PC spectrophotometer with 1cm cell at room temperature. Melting points of compounds synthesized in the project work were determined using Mettler FP85HT hot stage with FP90 processor melting point apparatus.

6.2. Reagents

Diethyl ether (Riedel haën), hexane (Riedel haén), bromine (BDH), hydrochloric acid (Riedel haën), hydrobromic acid (Fisher), dichloromethane (Aldrich), $PdCl_2$ (BDH), N-bromosuccinimide (NBS) (Aldrich), $CHCl_3$ (BDH), Methanol (BDH), ethyl acetate (Aldrich), NaOH (Aldrich), toluene (BDH), 2-(tributylstannyl) thiophene (Aldrich), ethanol (BDH), Acetic acid (Riedel haën), zinc dust (BDH), p-xylene (Riedel haén), $KMnO_4$(BDH), sulfuric acid (BDH), n-BuLi (Aldrich), hydrazine hydrate (Aldrich), phenyl boric acid (Aldrich), bromobenzene (Riedel haën), tetraethyl ammonium hydroxide (Aldrich), triethyl amine (Aldrich), $FeCl_3$ (Aldrich), $Na_2S_2O_3$ (BDH), NaCl (Oxford), 3-benzyl-5-(2-hydroxyethyl)-4-methylthiazoilumchoride (Aldrich), N,N-dimethylformamide (DMF) (Sigma Aldrich), PPh_3 (Aldrich), $PdCl_2(PPh_3)_2$ (Aldrich). All reagents were used as received, while solvents were distilled before use. Tetrahydrofuran (THF) was dried over sodium metal/benzophenone in an atmosphere of nitrogen prior to use. Silica gel 60 (43-63 μm) was used as stationary phase during all column chromatography based purification works. 0.25 mm silica gel pre-coated plates (Fluka) were used for thin layer chromatography and a UV lamp (at 254 and

365 nm) was used for all visualization purposes in column and thin layer chromatography.

6.3. Procedures

1,4-Dibromo-2,5-dimethylbenzene (36)

p-Xylene (16.5 mL, d=0.861 g/mL, 0.139 mmol), anh. ferric chloride (0.29 g, 0.0018 mmol) , deionized water (0.1 mL) were mixed in 250 mL two-necked round bottom flask, fitted with a condenser and a pressure equalizing funnel. To this mixture was added bromine (8.71 mL, d = 3.11 g/mL, 0.169 mmol) drop wise from a pressure equalizing dropping funnel while stirring the reaction mixture and keeping the temperature of the reaction between 10-15°C, until 15% of the bromine addition was completed, followed by a temperature drop to 0-5°C until all the bromine addition was completed. Stirring was continued at room temperature till the hydrogen bromide gas evolution ceased and distilled water was added and the mixture was washed with sodium thiosulfate ($Na_2S_2O_{3)}$ to remove the color of excess bromine. The solution was extracted with dichloromethane (2x), and the organic solution was washed with brine. The organic layer was subsequently dried over anhydrous sodium sulfate, the solvent was removed by rotary evaporator, to give a crude product consisting of mainly a mono and dibromo *p*-xylene. The desired dibromo *p*-xylene product was separated from the monobromo *p*-xylene, by reduced pressure distillation at 0.78 torr, where the boiling point of the monobromo *p*-xylene product was about 36°C and the dibromo *p*-xylene boiled at 50°C. The 1,4-dibromo-2,5-dimethylbenzene crystallized to give a white solid (23.4 g, 66.13%) upon standing.

^{1}H-NMR (400.13 MHz, $CDCl_3$) δ: 7.41(s, 2H, H-2, H-5), 2.35 (s, 6H, H-1'); ^{13}C-NMR (100.6 MHz, $CDCl_3$) δ: 137.0 (C-1, C-4), 134.0 (C-3, C-6), 123.35 (C-2, C-5), 22.11(C-1').

2,5-Dibromoterephtalic acid (37)

To 1,4-dibromo-2,5-dimethylbenzene (17.5 g, 66.29 mmol) in pyridine (195 mL) under reflux was added $KMnO_4$ (41.12 g, 260 mmol) in boiling water (130 mL) over a period of three hours. After the addition of $KMnO_4$ was complete, stirring was continued until the purple color of $KMnO_4$ was completely changed to brown. The reaction mixture was allowed to come to room temperature, and filtered. The residue was washed with hot water and ethyl acetate. The aqueous layer was extracted (2x) with ethyl acetate. The combined organic layer was dried to afford a white solid. The aqueous layer was acidified with 3N HCl to P^H~1 and the resulting white solid was filtered and the mother liquor was extracted with ethyl acetate. Removing the ethyl acetate with rotary evaporator afforded a white solid which was combined with the solid obtained above. The combined white solid was then suspended in water (100 mL) and NaOH (5 g, 125 mmol) of was added, and the reaction mixture was heated under reflux. To the refluxing mixture, a hot solution of potassium permanganate (22 g, 139.2 mmol) in water was added over about 2 hours. After addition was complete, the mixture was refluxed for about 1 more hour and cooled to room temperature, and a few milliliters of methanol was added to destroy the excess $KMnO_4$. The brown precipitate was separated by filtration and was washed with hot water and ethyl acetate. The filtrate was subsequently acidified with 3N HCl to P^H~1, in which case a white solid precipitated which was collected by suction filtration, washed with water and dried to afford **37** (15.84 g, 73.65% yield with respect to the reacted 1,4-dibromo-2,5-dimethylbenzene acid). Mp: 265.4-267.9°C;
^{1}H-NMR (400.13 MHz, DMSO-d_6): δ14 (s, 2H, H-1'), 8.02 (s, 2H, H-3, H-6). ^{13}C-NMR (100.6 MHz, DMSO-d_6): 166.0 (C-1'), δ137.59 (C-1,C-4), δ119.3 (C-3, C-6), C-135.40 (C-2, C-5);

Diethyl-2,5-dibromoterephthalate (38)

2,5-Dibromoterephthalic acid (15.48 g, 48.6 mmol) was mixed with absolute ethanol (165 mL, 2.75 mmol) and conc. H_2SO_4 (6.6 mL) and was refluxed for about 24 hours. The mixture was cooled to room temperature, to give a white precipitate which was then filtered, washed with water, and dried to give diethyl-2,5-dibromoterephtalic acid (12.34 g, 66.5%).

^{1}H-NMR (400.13 MHz, $CDCl_3$) δ: 8.04 (s, 2H, H-2, H-5), 4.43 (q, *J* = 7.2 Hz, 4H, H-2'), 1.43 (t, *J* = 7.2Hz, 6H, H-3', H-3"); ^{13}C-NMR (100.6 MHz, $CDCl_3$)δ: 164.3 (C-1'), 136.5 (C-2, C-5), 135.7 (C-1, C-4), 120.1(C-3, C-6), 62.4 (C-2'), 14.2 (C-3').

Diethyl-2,5-di(thiophen-2-yl)terephthalate (39)

2,5-dibromoterephthalate (5 g, 13.16 mmol), $PdCl_2(PPh_3)_2$ (0.28 g, 0.024 mmol), tributylstannylthiophene (10.34 g, 26.32 mmol) were mixed with toluene (165 mL), and refluxed for about 6 hours over argon atmosphere. At the end of the 6th hour, the mixture was allowed to cool to room temperature and washed with a saturated NH_4Cl solution. The organic solution was dried and the solvent was removed by rotary evaporator. The crude product was mixed with methanol (15 mL) which induced precipitation. The resulting white solid was suction filtered, washed with methanol and collected to give compound **39** (3.2 g, 64.3%).

^{1}H-NMR (400.13 MHz, $CDCl_3$) δ: 7.85 (s, 2H, H-3, H-6), 7.41 (dd, *J* = 1.2, 5 Hz, 2H, H-5'), 7.09-7.13 (m, 4H, H-3', H-4'), 4.25 (q, *J* = 7.2 Hz, 2H, H-2"), 1.18 (t, *J* = 7.2, 6H, H-3"); ^{13}C-NMR (100.6 MHz, $CDCl_3$) δ: 167.7 (C-1"), 140.5 (C-2'), 134.1 (C-3, C-6), 133.5 (C-1, C,4), 131.9 (C-2, C-5), 127.4 (C-4'), 127.0 (C-3'), 126.5 (C-5'), 61.9 (C-2"), 13.8 (C-3").

Diethyl-2,5-di(bromothiophen-2-yl)terephthalate (**40**)

In 100 mL round bottom flask, equipped with a pressure equalizing funnel, flask diethyl-2,5-di(thiophen-2-yl)terephthalate (1.45 g, 3.77 mmol) was dissolved in DMF (50 mL). NBS (1.34 g, 7.54 mmol) was dissolved in DMF (20 mL) and placed in the pressure equalizing dropping funnel. The flask was covered with aluminum foil, and while stirring the reaction mixture at room temperature, the NBS in DMF was added drop by drop into the reaction flask over a period of 2 hours. The mixture was stirred for about 15 hours while monitoring the reaction progress by TLC using hexane:dichloromethane (3:2) as an eluent. At the end of the 15th hour, stirring was stopped and to the flask was added a few milliliters of 1M HCl. The addition of the HCl resulted in precipitating out a yellow solid. The yellow solid was suction filtered, washed (3x) with methanol and dried to afford compound **40** (1.75 g, 85.3%). Mp: 136.5-138.5°C;

^{1}H-NMR (400.13 MHz, $CDCl_3$) δ: 7.80 (s, 2H, H-2, H-5), 7.06 (d, *J* = , H-4'), 6.87 (d, *J* = 4Hz, H-3'), 4.28 (q, *J* = 7.2, 4H, H-2"), 1.42 (t, *J* = 2, 6H, H-3"); ^{13}C-NMR (100.6 MHz, $CDCl_3$) δ: 167.0 (C-1"), 140.2 (C-2'), 133.9 (C-2, C-5), 133.0 (C-1, C-4), 132.1 (C-3, C-6), 130.1 (C-4'), δ127.4 (C-3'), 113.3 (C-2, C-5), 61.9 (C-2"), 13.9 (C-3").

Compound 41

1-Bromo-4-heptyloxybenzene (4 g, 16.27 mmol) was dissolved in dried THF (30 mL) at -78°C. While stirring, to this solution was added n-BuLi (6.6 mL, 16.5 mmol) and the mixture was stirred for about 15 minutes. A solution of diethyl-3,5-di(thiophen-2-yl)terephthalate (1.5 g, 3.89 mmol) in THF (15 mL) was then added and the mixture was stirred overnight. The reaction was quenched with saturated NH_4Cl solution, extracted with ethyl acetate (3x) and the combined

organic layer was then dried and the solvent was removed using rotary evaporator to give compound **22** (4.02 g, 97.3%). Mp: 133-136°C;
^{1}H-NMR (400.13 MHz, $CDCl_3$) δ: 7.30 (m, 2H,H-3, H-6), 7.21 (d, *J* = 5.2, 8H, H-3"', H-5'"), 6.79 (dd, *J* = 3.6, 5.6 Hz, 2H, H-4', H-4"), 6.26 (d, *J* = 2.8, 2H, H-2', H-2"), 3.99 (t, *J* = 6.4 Hz, 8H), 3.47 (s, 2H, H-1'''') 1.82 (p, *J* =6.8, 2H), 1.30-1.51 (m, 24H), 0.93 (t, *J* = 6.8, 12H) ; ^{13}C-NMR (100.6 MHz, $CDCl_3$) δ: 158.3 (C-4"), 145.2 (C-3, C-5), 142.5 (C-2',C-2"), 139.8 (C-1"'), 136.1 (C-1, C-4), 131 (C-3, C-6), δ129.2 (C-3"'), 127.9 (C-5', C-5"), 127.0 (C-3', C-3"), 126.8 (C-4', C-4"), 133.8 (C-3"', C-5"'), 62.0 31.8, 29.4, 29.1, 26.1, 22.7, and 14.2 (C-1''''-C-7''''), 82.5 (C-1'''').

Compound 43

Compound **41** (3.5 g, 3.29 mmol) was dissolved in acetic acid (100 mL), to the solution was added conc. H_2SO_4 (seven drops). The mixture was refluxed for about four hours while checking the reaction progress by TLC using CH_2Cl_2:hexane (3:5) as an eluent. At the end of the fourth hour the reaction was allowed to cool down to room temperature, and was extracted with ethyl acetate (2x). The combined organic layer was dried over anhydrous Na_2SO_4, the solvent was removed by rotary evaporator, to give Compound **43** (3.41 g, 97.4%) as greenish sticky matter.
^{1}H-NMR (400.13 MHz, $CDCl_3$) δ: 7.48 (s, 2H,H-3, H-6), δ7.29 (d, *J* = 4.8 Hz, 2H, H-5', H-5"), 7.23 (d, *J* = 8.8 Hz, 8H, H-2"',H-6"'), δ7.03 (d, *J* = 5.2 Hz, 2H, H-4', H-4"), 6.83 (d, J = 8.8 Hz, 8H, H-3"', H-5'"), 3.95 (t, *J* = 6.4 Hz, 8H, H-1''''), 1.81 (p, 8H, H-2''''), 1.36-1.56 (m, 24H), 0.95 (t, *J* = 6.4 Hz, 12H, H-7'''') ; ^{13}C-NMR (100.6 MHz, $CDCl_3$) δ: 158.0 (C-), 155.2 (C-2, C-5), 153.8 (C-), 141.1(C-2, C-4), 136.8 (C-3',C-3"), 135.1 (C-2', C-2"), 129.4 (C-3, C-6), 127.6 (C-3"', C-5'"), 123.0 (C-5', C-5"), 120.5 (C-4', C-4"), 114.6 (C-2"', C-6"'), 31.8, 29.4, 29.1, 26.1, 22.7, and 14.2 (C-2'''' – C-7''''), 68.0 (C-1''''), 62.0 (C-1'''').

Compound 44

Compound **43** (3.4 g, 3.31 mmol) was suspended in DMF (20 mL) and to this solution was added NBS (11.8 mL, 0.56M in DMF, 6.62mmols) drop-wise over 40 minutes in the dark. The reaction mixture was then stirred for about 15 hours at room temperature. At the end of the 15th hour, a few milliliters of 1M HCl was added, which resulted in the precipitating out of a solid product. The resulting precipitate was suction filtered, washed thoroughly with methanol and dried to give compound **44** (2.9 g, 74.4%) as a reddish brown colored solid. Mp: 110-112°C; ^{1}H-NMR (400.13 MHz, $CDCl_3$) δ: 7.38 (s, 2H,H-3, H-6), 7.19 (d, *J* = 8.8, 8H, H-2"', H-6"'), 7.04 (s, 2H, H-4', H-4"), 6.85 (d, *J* = 8.8, 8H, H-3"', H-5"'), 3.96 (t, *J* = 7.2 Hz, 8H), 1.81 (p, *J* =6.4 , 8H), 1.37-1.49 (m, 24H), 0.95 (t, *J* = 6.4, 12H) ; ^{13}C-NMR (100.6 MHz, $CDCl_3$) δ: 158.3 (C-), 155.2 (C-2, C-5), 153.0 (C-), 141.2 (C-2, C-4), 135.9 (C-3',C-3"), 135.0 (C-2', C-2"), 129.0 (C-3, C-6), 126.0 (C-3"', C-5"'), 117.1 (C-5', C-5"), 114.4 (C-4', C-4"), 113.9 (C-2"', H-6"'), 31.9, 29.4, 29.1, 26.1, 22.7, and 14.2 (C-2""-C-7""), δ68.0 (C-1""), 62.8 (C-1""').

Tetrakis(triphenylphosphine)Palladium(0), $Pd(PPh_3)_3$

$PdCl_2$ (0.3 g, 1.70 mmol), triphenylphosphine (2.22 g, 8.47 mmol) were mixed with DMSO (20 mL) and the mixture was heated at 140°C under nitrogen atmosphere for about one hour until a clear solution was observed. When the mixture became clear, hydrazine hydrate (0.36 mL) was added portion-wise over one minute. The heating was discontinued and Stirring was continued until the solution became dark. At that stage, the solution was cooled in an ice bath while it was under nitrogen atmosphere. The resulting yellow solid was collected by suction filtration under an atmosphere nitrogen, washed with ethyl alcohol and dried to give tetrakis(triphenylphosphine)Pd(0) (1.67 g, 85%).

Compound 47

4,7-Di(thiophen-2-yl)benzo[c][1,2,5]thiadiazole (600 mg, 1.0 mmol) was suspended of acetic acid (30 mL) and to it was added zinc dust (2.64 g, 40.6 mmol). The mixture was then stirred at 80°C, while controlling the reaction progress by TLC using hexane:ethyl acetate (9:1) as an eluent. At the end of the third hour, the solution was suction filtered and the zinc dust was washed several times with acetic acid. To the filtrate was added, 1,2-bis(4-(heptyloxy)phenyl)ethane-1,2-dione (500 mg, 1.5 mmol) and the mixture was stirred at 60°C while controlling the reaction progress by TLC using ethyl acetate:hexane (1:5) as an eluent. At the end of the fourth hour, the reaction was confirmed to be completed and the resulting yellow precipitate was suction filtered, washed with acetic acid and methanol and dried to give compound **47** (0.48 g, 45.71%).

^{1}H-NMR (400.13 MHz, $CDCl_3$) δ: 8.11 (s, 2H, H-6, H-7), 7.87 (d, *J* = 3.6 Hz, 2H, H-5', H-5"), 7.75 (d, *J* = 8.4 Hz, 4H, H-2", H-6"), 7.53 (d, J = 1.2, 5.2 Hz, 2H, H-3'), 7.20 (dd, *J* = 4 Hz, 5Hz, 2H, H-4'), 6.93 (d, *J* = 8.8 Hz, 4H, H-3", H-5"), 1.34-1.54 (m, 12H), 0.93(t, *J* = 6.4 Hz, 6H). ^{13}C-NMR (100.6 MHz, $CDCl_3$) δ: 160.0 (C-4"), 151.3 (C-2, C-3), δ139.0 (C-9, C-10), 137.0 (C-2'), 131.9 (C-5, C-8), 131.0 (C-2"), 68.1, 31.9, 29.4, 29.3, 29.1, 22.7, and 14.2 (C-1'"-C-7"').

Compound 48

Compound **47** (0.48 g, 0.68 mmol) was dissolved in DMF (10 mL) and to it NBS (2.44 mL, 0.56M in DMF, 1.36 mmols) was added. The reaction mixture was then stirred at room temperature in the dark for 15 hours. At the end of the 15th hour, the resulting solution was treated with 1M HCl and the acidic solution was then extracted with dichloromethane, the organic layer was then dried, and the solvent was removed by rotary evaporator to give compound **48** (0.53 g, 89.8%). Mp: 103.3–105.1°C.

^{1}H-NMR (400.13 MHz, $CDCl_3$) δ: 7.85 (s, 2H, H-6, H-7), 7.63 (d, *J* = 8.8 Hz, 4H, H-2”’, H-6”’), 7.43 (d, *J* = 4.4 Hz, 2H, H-4’, H-4”), 7.06 (d, *J* = 4 Hz, 2H, H-3’, H-3”), δ4.20 (t, *J* = 6.4 Hz, 4H), 1.83 (p, *J* = 6.4 Hz, 4H), 1.25-1.53 (m, 12H), 0.92 (t, *J* = 7.2 Hz, 6H). ^{13}C-NMR (100.6 MHz, $CDCl_3$) δ: 160.2 (C-4”), 160.2 (C-5”), 151.7 (C-2, C-3), 139.7 (C-2’, C-2”), 136.2 (C-9, C-10), 132.4 (C-2’),131.9 (C-3’), 131.7 (C-5, C-8), δ130.2 (C-4’), 116.9 (C-1”), 114.7 (C-5’), 68.1, 31.9, 29.4, 29.3, 29.1, 22.7, and 14.2 (C-1”’-C-7”’).

Compound 49

Compound **48** (0.53 g, 0.62 mmol) was suspended in a two-necked round bottom flask and it was then dissolved by adding dry THF (30 mL) through a transfer needle. The mixture was then stirred at -78°C under nitrogen atmosphere and was treated with a 2.5 M solution of *n*-BuLi (0.54 mL, 0.68 mmol) after about 15 minutes, Bu_3SnCl (0.36 mL, 0.62 mmol) of was added to the reaction flask and stirring was continued for about three more hours allowing the reaction temperature to gradually rise to room temperature. At the end of the 3rd hour, a saturated solution NH_4Cl was added, the organic layer was separated and the aqueous layer was extracted with dichloromethane, dried and the solvent was removed by rotary evaporator. TLC analysis of the resulting brown sticky product using ethyl acetate: hexane (0.3:5) revealed the presence of impurities. Subsequently, an attempt was made to purify the compound by passing it through a column of silica gel using the same solvent system as the TLC analysis. Unfortunately, the product decomposed during the chromatographic separation.

Compound 50

The diamine was prepared from compound **45** (3 g, 10 mmol) following the same procedure as described above. To the resulting diamine solution in acetic

acid was added 2,3-butanedione (0.86 g, 10 mmol). The mixture was then stirred at 60°C for about three hours while checking the reaction progress by TLC using ethyl acetate: hexane (1:5) as a solvent system. At the end of the third hour, the reaction mixture was stopped and the resulting solid was filtered, washed with methanol, and dried to give compound **50** (2.13 g, 66.1%) as a lustrous yellow solid product.

^{1}H-NMR (400.13 MHz, $CDCl_3$) δ: 8.03 (s, 2H, H-6, H-7), δ7.86 (dd, *J* = 1.2 ,3.6 Hz, 2H, H-5', H-5"), 7.51 (dd, *J* = 0.8, 5.2 Hz, 2H, H-3', H-3"), 7.19 (dd, *J* = 3.6, 4.4 Hz, 2H, H-4', H-4"), 2.82 (s, 6H, H-1"'); ^{13}C-NMR (100.6 MHz, $CDCl_3$) δ: 155.2 (C-2, C-3), 139.2 (C-9, C-10), 137.6 (C-2'), 130.9 (C-5, C-8), 128.3 (C-6, C-7), 126.6 (C-4'), 126.4(C-3'), 126.1 (C-5'), 22.7 (C-1").

5,8-bis(5-bromothiophen-2-yl)-2,3-dimethylquinoxaline (51)

2,3-Dimethyl-5,8-di(thiophen-2-yl)quinoxaline (1.55 g, 4.81 mmol) was dissolved in DMF (40 mL) and to it was added NBS (17.2 mL, 0.56 M in DMF, 8.82 mmol). The reaction mixture was stirred at room temperature in the dark for about 15 hours. At the end of the 15th hour, yellow precipitate was collected by suction filtration, washed with MeOH and dried to afford compound **53** (1.79 g, 74.9%). Mp: 228-230°C;

^{1}H-NMR (400.13 MHz, $CDCl_3$)δ: 7.99 (s, 2H, H-6, H-7), 7.53 (d, *J* = 4 Hz, 2H, H-3', H-3"), 7.12 (d, *J* = 4 Hz, 2H, H-4', H-4"), 2.84 (s, 6H, H-1"').

Compound 52

Compound **51** (1.0 g, 2.08 mmol) was suspended in a two-necked round bottom flask and it was then dissolved by adding dry THF (30 mL) through a transfer needle. The mixture was then stirred at -78°C under nitrogen atmosphere and was treated with a 2.5 M solution of *n*-BuLi (0.54 mL, 4.16 mmol) after about 15 minutes, Bu_3SnCl (1.18 mL, 1.36 mmol) of was added to

the reaction flask and stirring was continued for about three more hours allowing the reaction temperature to gradually rise to room temperature. At the end of the 3rd hour, a saturated solution NH_4Cl was added, the organic layer was separated and the aqueous layer was extracted with dichloromethane, dried and the solvent was removed by rotary evaporator. TLC analysis of the resulting brown sticky product using ethyl acetate: hexane (0.5:5) revealed the presence of impurities. Subsequently, an attempt was made to purify the compound by passing it through an impregnated column of silica gel using the same solvent system as the TLC analysis, but the distannylated product could not be obtained in a reasonable purity.

Polymer 53

In a 25 mL round bottom flask, compound **51** (200 mg, 0.169 mmol), 2,2'-(9,9-dioctyl-9H-fluorene-2,7-diyl)bis(4,4,5,5-tetramethyl-1,3,2-dioxaborolane) (108.5 mg, 0.169mmol), and $Pd(PPh_3)_4$ (5.86 mg, 0.00169 mmol) were suspended in toluene (10 mL) and the mixture was then refluxed for about 15 minutes. A 20% solution of tetrabutylammonium hydroxide solution (0.51 mL) was added and the mixture was heated under reflux for two more hours. At the end of the second hour, bromobenzene (36.6 mg, 0.234 mmol) was added and refluxing continued for an hour. At this stage, phenylboric acid (28.49 mg) was added, and heating continued for one more hour. The mixture was then cooled to room temperature, and the polymer was precipitated out by slowly adding the mixture in to methanol. The resulting solid was then membrane-filtered, washed with methanol and dried. The resulting orange colored solid was dissolved in chloroform, washed with ammonia (2x) and distilled water (4x). The organic layer was then concentrated to a small volume and the polymer was precipitated once again from methanol, membrane filtered and dried. The resulting solid was Soxhlet extracted, first with diethyl ether to remove the low molecular weight polymer, and then with chloroform. The chloroform extract

was concentrated to small volume and the polymer was precipitated out from methanol, membrane filtered, and dried to give polymer **53** (165.78 g, 68.5%).

Polymer 54

Diethyl-2,5-di(thiophen-2-yl)terephthalate (200 mg, 0.417 mmol), 2,2'-(9,9-dioctyl-9H-fluorene-2,7-diyl)bis(4,4,5,5-tetramethyl-1,3,2-dioxaborolane) (267.5 mg, 0.417 mmol), and $Pd(PPh_3)_4$ (14.44 mg, 0.0125 mmol) were mixed with toluene (10 mL) in a 25 ml round bottom flask. The mixture was refluxed for 15 minutes and 20% solution tetrabutylammonium hydroxide (1.26 mL) was added. The mixture was then further refluxed for two and half hours. Bromobenzene (0.07 mL) was added and refluxing continued for an hour. At this stage, phenylboric acid (70.3 mg) was added, and heating continued for an hour. The mixture was cooled to room temperature, and the polymer was precipitated out from methanol by slowly adding the mixture in to methanol. The resulting solid was then membrane-filtered, washed with methanol and dried. The yellow colored solid was dissolved in chloroform, washed with ammonia (2x), and distilled water (4x). The organic layer was then concentrated to a small volume, precipitated once again from methanol, membrane filtered and dried. The resulting solid was Soxhlet-extracted, first with diethyl ether to remove the low molecular weight polymer, and then with chloroform. The chloroform extract was concentrated to a small volume, precipitated out from methanol, membrane filtered, and dried to give polymer **54** (185.63 g, 62.86%).

Synthesis of 9,9-dioctyl-9H-fluorene-2,3-dimethyl-5,8-di(thiophen-2-yl)quinoxaline copolymer (55)

In a 25 mL round bottom flask 2,3-dimethyl-5,8-di(thiophen-2-yl)quinoxaline (200 mg, 0.417 mmol), 2,2'-(9,9-dioctyl-9H-fluorene-2,7-diyl)bis(4,4,5,5-

tetramethyl-1,3,2-dioxaborolane) (267.5 mg, 0.417 mmol), and $Pd(PPh_3)_3$ (14.44 mg, 0.0125 mmol) were mixed with toluene (10 mL). The mixture was then refluxed for about 15 minutes and 20% solution of tetrabutylammonium hydroxide (1.26 mL) was added. The mixture was then further refluxed for one and half hours. Bromobenzene (0.07mL) was then added and refluxing continued for an hour. At this stage, phenylboric acid (70.3 mg) was added, and heating under reflux was continued for one more hour. The mixture was then cooled to room temperature, and the polymer was precipitated out by slowly adding the mixture in to methanol. The polymer was membrane-filtered, washed with methanol and dried. The yellow colored polymer was dissolved in chloroform, washed with ammonia (2x) and distilled water (4x). The organic layer was then concentrated to a small volume, precipitated once again from methanol, membrane filtered and dried. The resulting solid was Soxhlet extracted first with diethyl ether to remove the low molecular weight polymer and then with chloroform. The chloroform extract was concentrated, precipitated out from methanol, membrane filtered, and dried to give polymer **55** (0.161 g, 54.5 %).

7. REFERENCES

1. C. K. Chiang, C. R. J. Fincher, Jr., Y. W. Park, A. J. Heeger, H. Shirakawa, E. J. Louis, S. C. Gau, A. G. MacDiarmid, *Phys. Rev. Lett.*; **1977**, *39*, 1098.
2. H. Shirakawa, E. J. Louis, A. G. MacDiarmid, C. K. Chiang, A. J. Heeger, *Chem. Commun.*; **1977**, 578.
3. H. Shirakawa, *Angew. Chem. Int. Ed.*; **2001**, *40*, 2575.
4. A. J. Heeger, *Angew. Chem. Int. Ed.*; 2001, *40*, 2591.
5. A. G. MacDiarmid, *Angew. Chem. Int. Ed.*; **2001**, *40*, 2581.
6. H. Letheby, *J. Chem. Soc.*; **1862**, *15*, 161.
7. J. D. Rose, F. S. Statham, *Chem. Commun.*; **1950**, 69.
8. M. Hatano, K. Kambara, K. O. Kamoto, *J. Polym. Sci.*; **1961**, *51*, S26.
9. E. Menefee, Y. H. Pao, *J. Chem. Phys.*; **1962**, *36*, 3472.
10. V. V. J. Walatka, M. M. Labes, J. H. Perlstein, *Phys. Rev. Lett.*; **1973**, *31*, 1139.
11. R. L. Greene, G. B. Street, L. J. Suter, *Phys. Rev. Lett.*; **1975**, *34*, 577.
12. W. D. Gill, W. Bludau, R. H. Geiss, P. M. Grant, R. L. Greene, J. J. Mayerle, G. B. Street, *Phys. Rev. Lett.*; **1977**, *38*, 1305.
13. J.A.E.H. van Haare, L. Groenendaal, H.W.I. Peerlings, E.E. Havinga, J.A.J.M. Vekemans, R.A.J. Janssen, E.W.Meijer, *Chem. Mater.*; **1995**, 7, 1984.
14. C. K. Chiang, S. C. Gau, C. R. J. Fincher, Y. W. Park, A. *Chem. Rev.*; **1988**, *88*, 183.
15. M. Pope and C. E. Swenberg, *Electronic Processes in Organic Crystals and Polymers*, Second Edition, Oxford University Press, New York, **1999**.
16. A. J. Heeger, S. Kivelson, J. R. Schrieffer, and W.-P. Su, *Rev. Mod. Phys.*; **1988**, 60, 781.

17. Z. G. Soos, S. Ramasesha, and D. S. Galvao, *Phys. Rev. Lett.*; **1993**, 71, 1609; b. Z. G. Soos, S. Ramasesha, D. S. Galvao, R. G. Kepler, and S. Etemad, *Synth. Met.;* **1993**, 54, 35.
18. T.A. Skotheim, R.L. Elsenbaumer, J.R. Reynolds (Eds.), *Handbook of Conducting Polymers*, Marcel Dekker, New York, **1998**.
19. H.S. Nalwa, *Handbook of Organic Conductive Molecules and Polymers*, Wiley, Chichester, **1997**.
20. R.-S. Wang, L.-M. Wang, Z.-M. Su, Y.-J. Fu, *Synth. Met.*; **1995**, 69, 511.
21. S. –H Chan, C. –H. Chen, T. –C. Chao, C. Ting, C. –S. Lin, B.-H. Ko. *Macromolecules; **2008***, 41, 5519.
22. J.L. BreÂdas, R.H. Baughman, *J. Polym. Sci., Polym. Lett.*; **1983**, 21, 475.
23. J.L. Bredas, B. TheÂmans, J.M. AndreÂ, *J. Chem. Phys.;* **1983**, 78, 6137.
24. K. Mullen, U. Scherf, Makromol. *Chem., Macromol. Symp.;* **1993**, 69, 23.
25. U. Scherf, *J. Mater. Chem.*; **1999**, 9, 1853.
26. M. Kertesz, *Macromolecules*; **1995**, 28, 1475.
27. C.J. Ruud, C. Wang, G.L. Baker, *Synth. Met.;* **1997**, 84, 363.
28. A.K. Bakhshi, *Mater. Sci. Eng.*; **1995**, 3, 249.
29. Y. Yao, J.J.S. Lamba, J.M. Tour, *J. Am. Chem. Soc.;* **1998**, 120, 2805.
30. U. Scherf, K. MuÈllen, Makromol. *Chem., Rapid Commun.*; **1991**,12, 489.
31. U. Scherf, K. Mullen, *Synthesis;* **1992**, 23.
32. U. Scherf, K. MuÈllen, *Macromolecules;* **1992**, 25, 3546.
33. I. Osaka, G. Sauvé, R. Zhang, T. Kowalewski, R. D. McCullough, *Adv. Mater.;* **2007**, 19, 4160.
34. S. Ando, J. Nishida, Y. Inoue, S. Tokito, Y. Yamashita, *J. Mater. Chem.;* **2004**, 14, 1787.
35. S. Ando, J. Nishida, Y. Inoue, S. Tokito, Y. Yamashita, *J. Am. Chem. Soc.;* **2006**, 14, 1787.
36. E.E. Havinga, W. ten Hoeve, H. Wynberg, *Polym. Bull.*; **1992**, 29,119.
37. E.E. Havinga, W. ten Hoeve, H. Wynberg, *Synth. Met.*; **1993**, 55, 299.
38. G. Brocks, A. Tol, *J. Phys. Chem.*; **1996**, 100, 1838.

39. G. Brocks, A. Tol, *Synth. Met.;* **1996**, 76, 213.
40. G.A. Sotzing, C.A. Thomas, J.R. Reynolds, *Macromolecules*; **1998**, 31, 3750.
41. A. Berlin, A. Canavesi, G. Pagani, G. Schiavon, S. Zecchin, G. Zotti, *Synth. Met.*; **1997**, 84, 451.
42. G. Zotti, S. Zecchin, G. Schiavon, A. Berlin, G. Pagani, M. Borgonovo, R. Lazzaroni, *Chem. Mater.*; **1997**, 9, 2876.
43. S.-C. Lin, J.-A. Chen, M.-H. Liu, Y.O. Su, M.-K. Leung, *J. Org. Chem.*; **1998**, 63, 5059.
44. Q.T. Zhang, J.M. Tour, *J. Am. Chem. Soc.*; **1997**, 119, 5065.
45. Q.T. Zhang, J.M. Tour, *J. Am. Chem. Soc.*; **1998**, 120, 5355.
46. A. Devasagayaraj, J.M. Tour, *Macromolecules*; **1999**, 32, 6425.
47. M. Poster, K. O. Annan, U. Scherf, *Macromolecules;* **1999**, 32, 3159.
48. K. Pilgram, M. Zupan, R. Skiles, *J. Heterocycl. Chem.;* **1970,** 7, 629.
49. M. J. Edelman, J. –M. Raimundo, N. F. Uteseh, F. *Heliv, Chim. acta.;* **2002**, 85, 2195.
50. E. Perzon, *Polymer;* ***2006***, 47, 4261.

8. APPENDIX

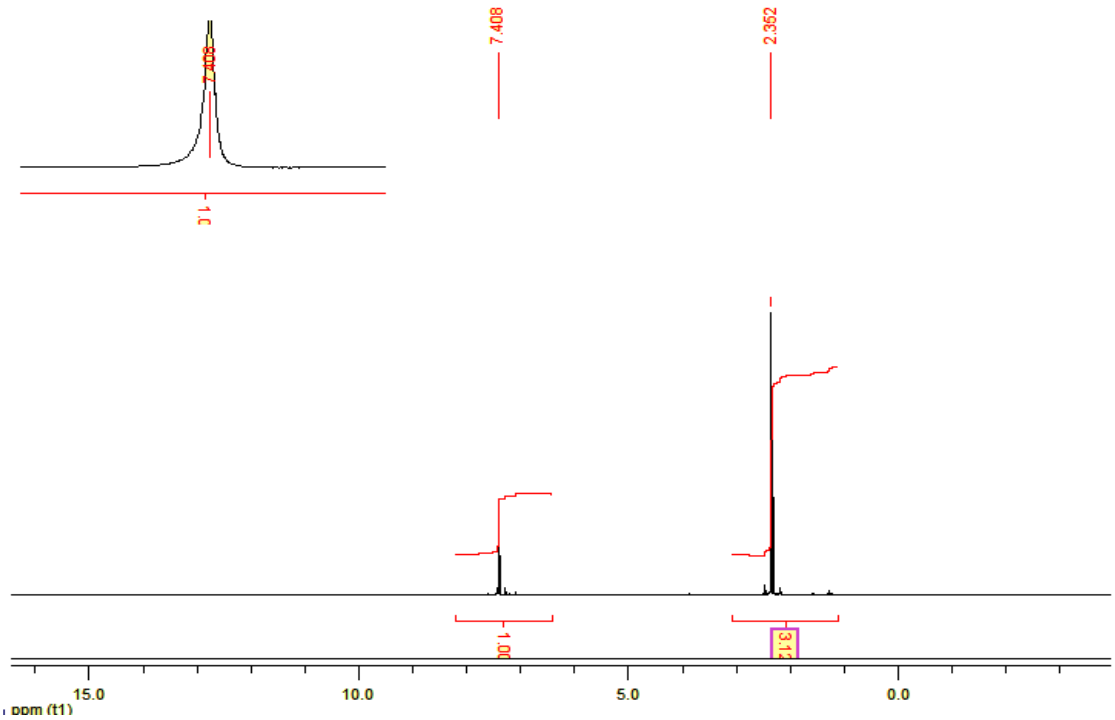

Appendix 1.[1]H NMR spectrum of 1,4-dibromo-2,5-dimethylbenzene (**36**).

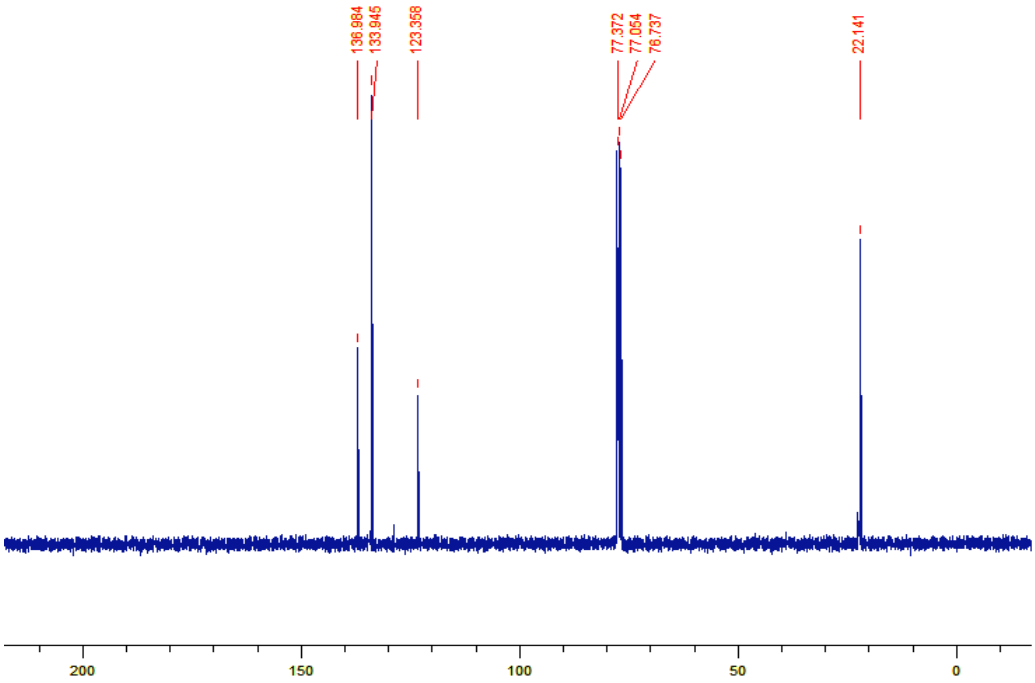

Appendix 2.[13]C NMR spectrum of 1,4-dibromo-2,5-dimethylbenzene (**36**).

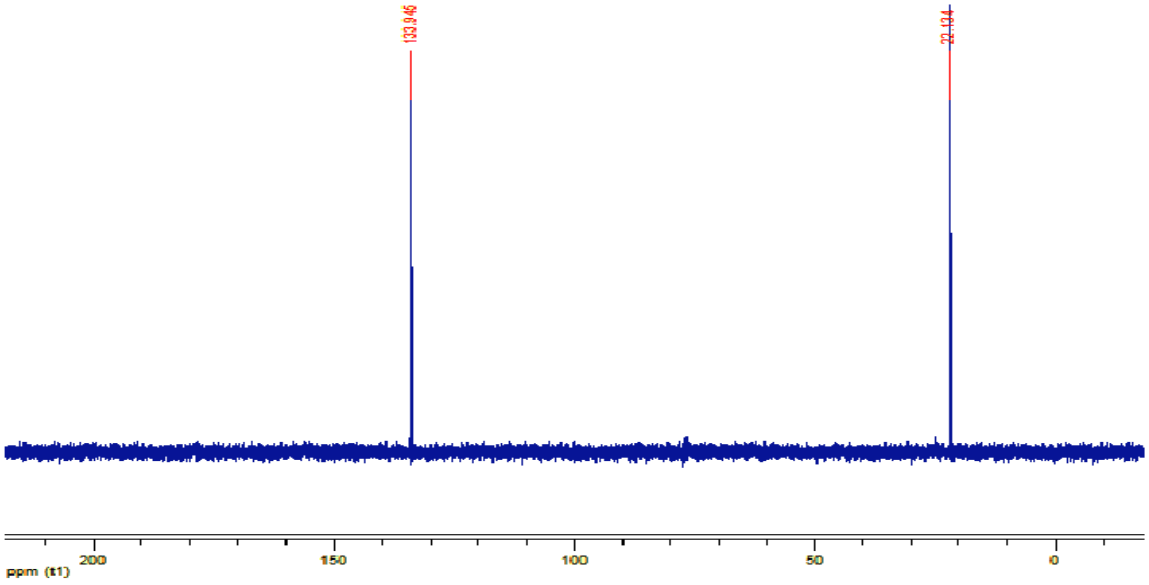

Appendix 3.DEPT-135 spectrum of 1,4-dibromo-2,5-dimethylbenzene (**36**).

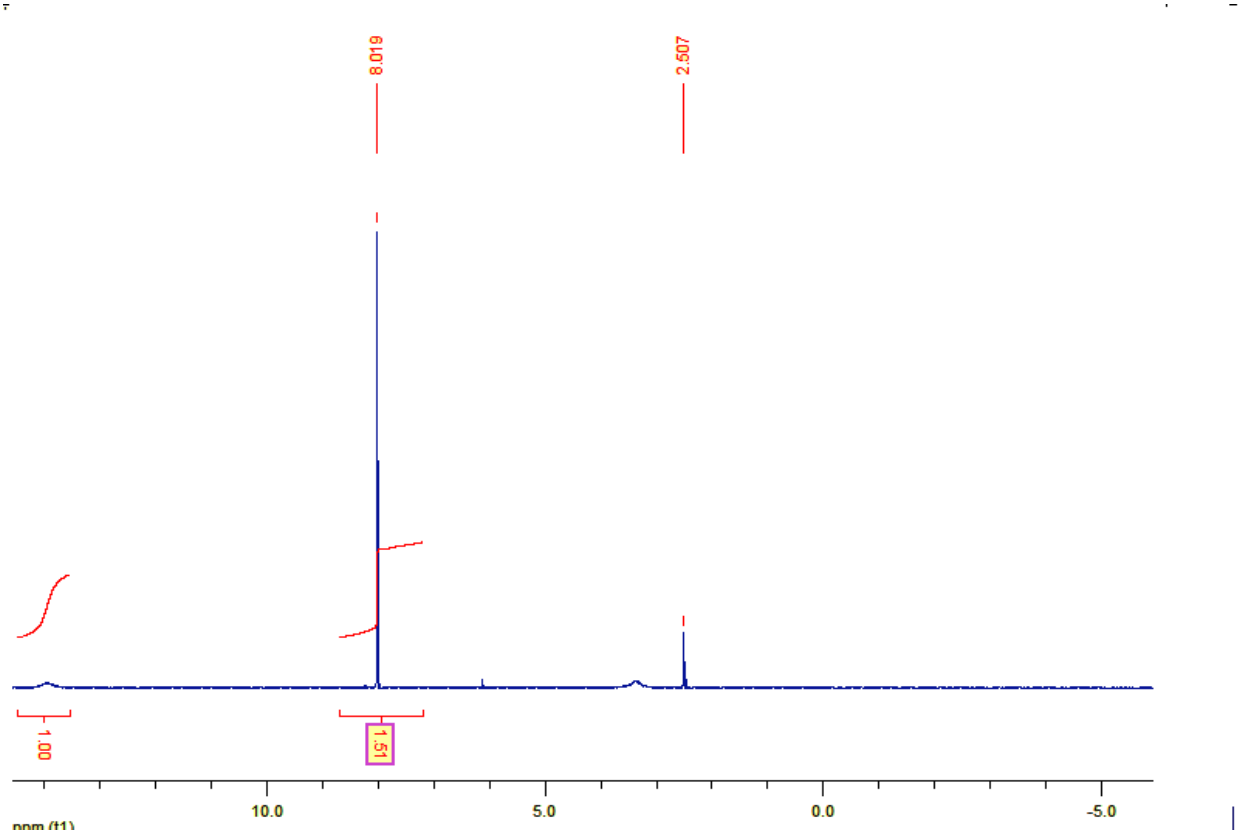

Appendix 4. ^{1}H NMR spectrum of 2,5-dibromoterephthalic acid (**37**).

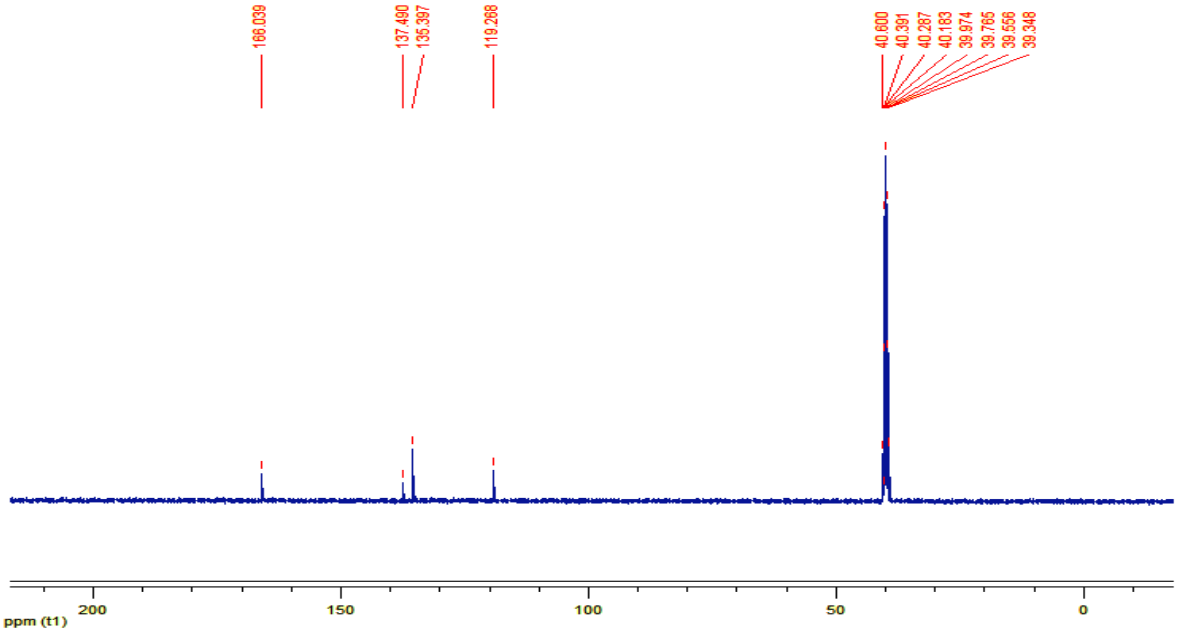

Appendix 5. ^{13}C NMR spectrum of 2,5-dibromoterephthalic acid (**37**).

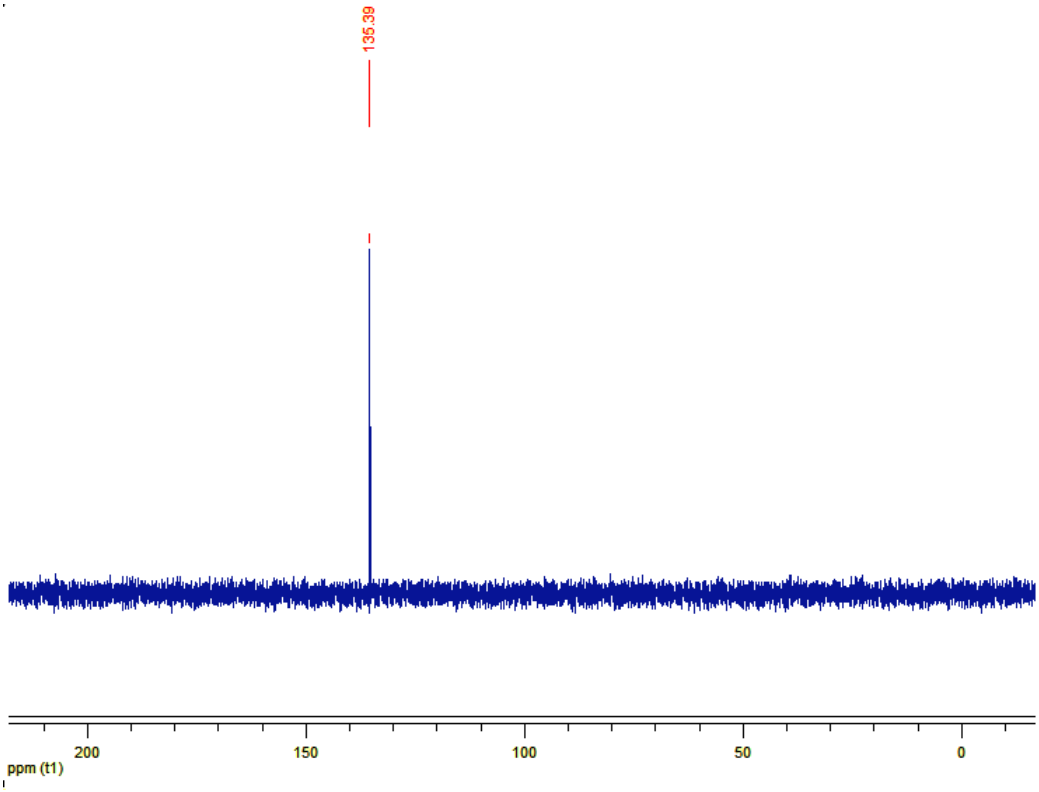

Appendix 6. DEPT-135 spectrum of 2,5-dibromoterephthalic acid (**37**).

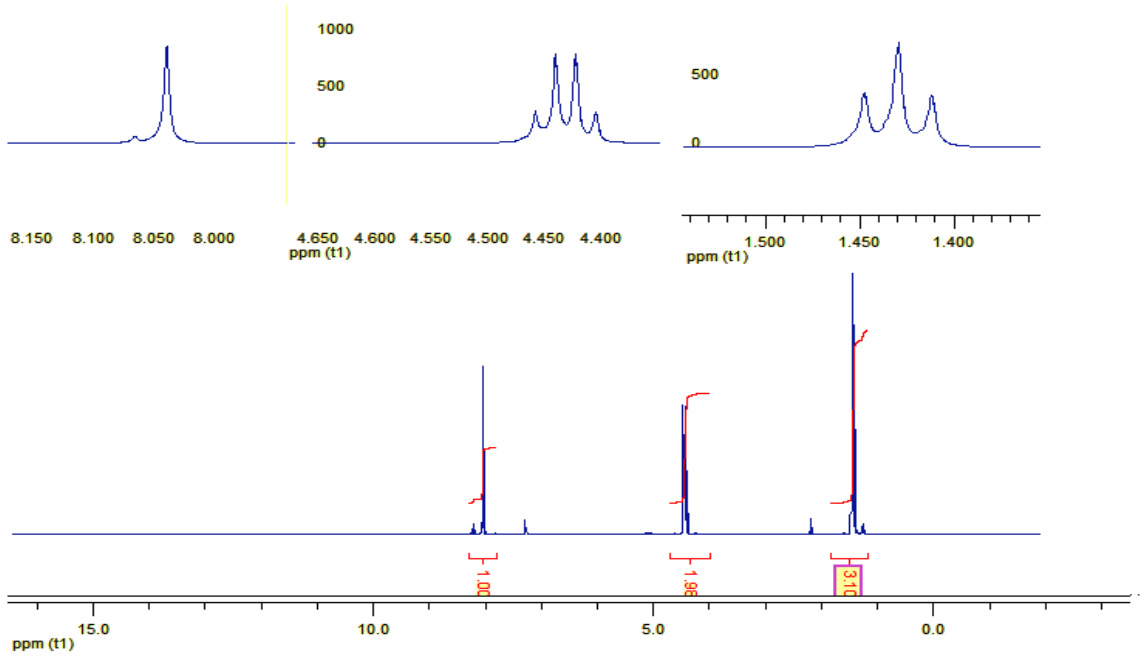

Appendix 7. ^{1}H NMR spectrum of diethyl-2,5-dibromoterephthalate (**38**).

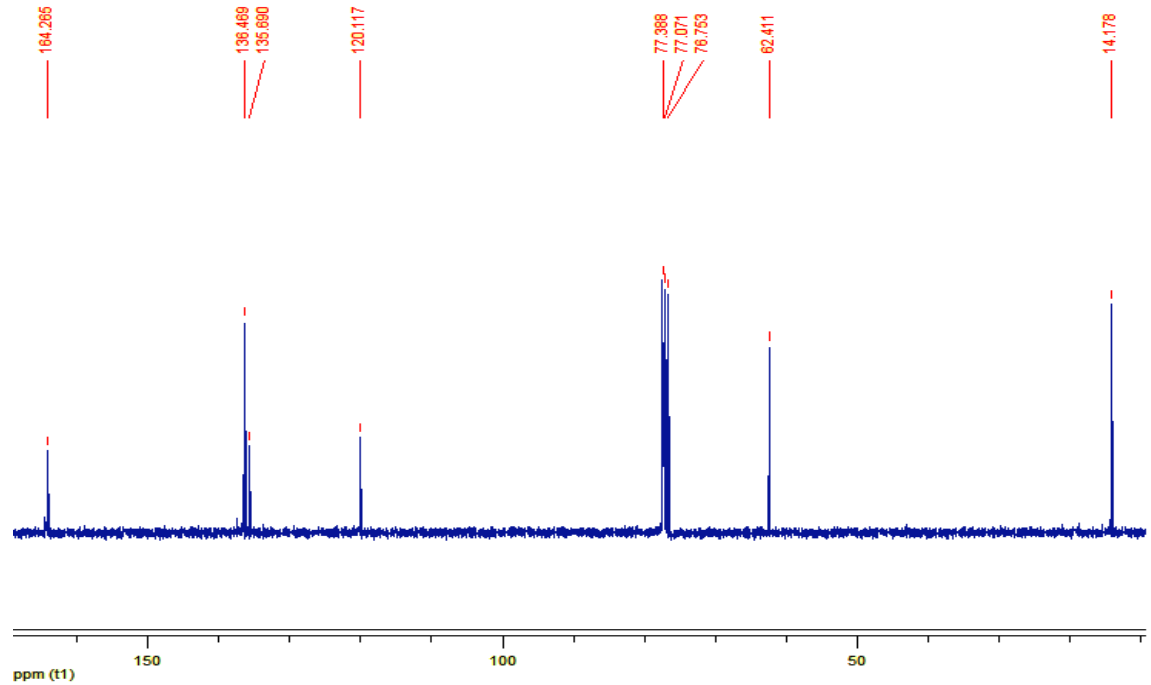

Appendix 8. ^{13}C NMR spectrum of diethyl-2,5-dibromoterephthalate (**38**).

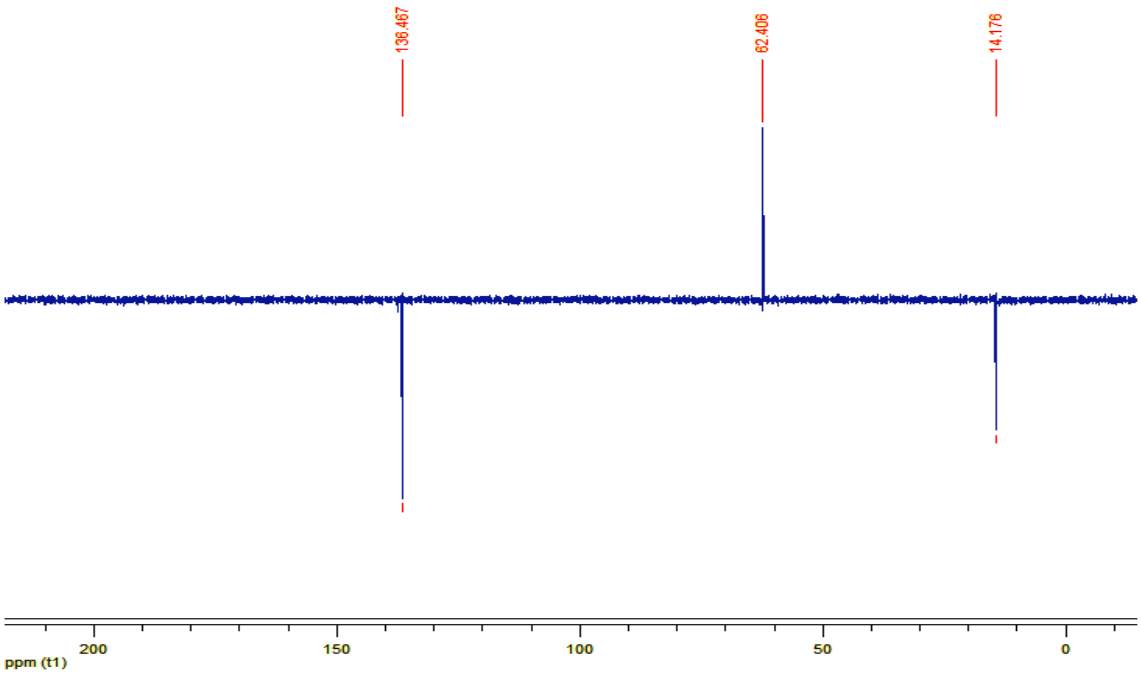

Appendix 9. DEPT-135 spectrum of diethyl-2,5-dibromoterephthalate (**38**).

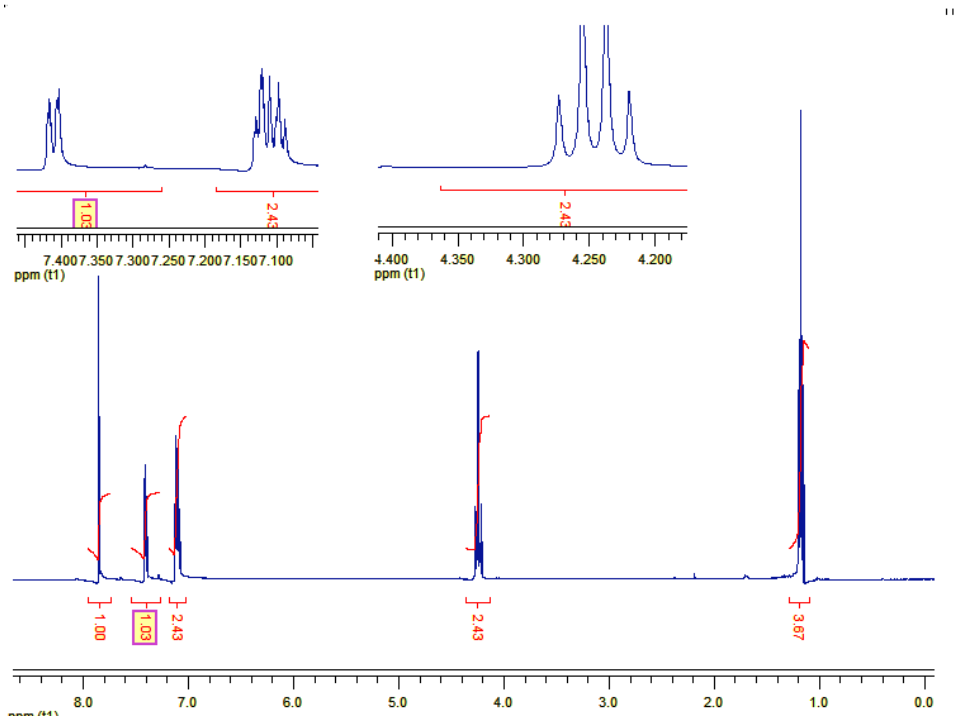

Appendix 10. ^{1}H NMR spectrum of diethyl-2,5-di(thiophen-2-yl)terephthalate (**39**).

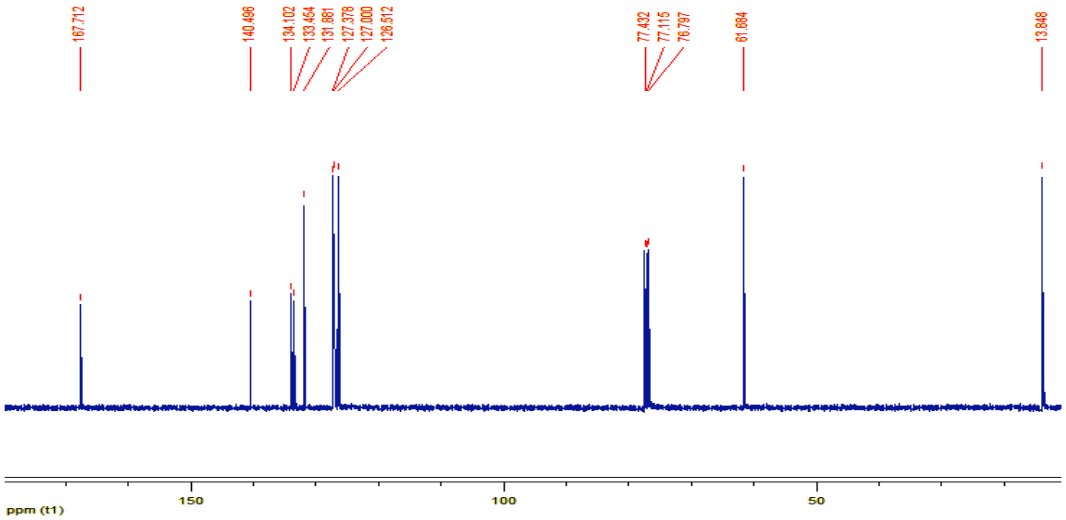

Appendix 11. ^{13}C NMR spectrum of diethyl-2,5-di(thiophen-2-yl)terephthalate (**39**).

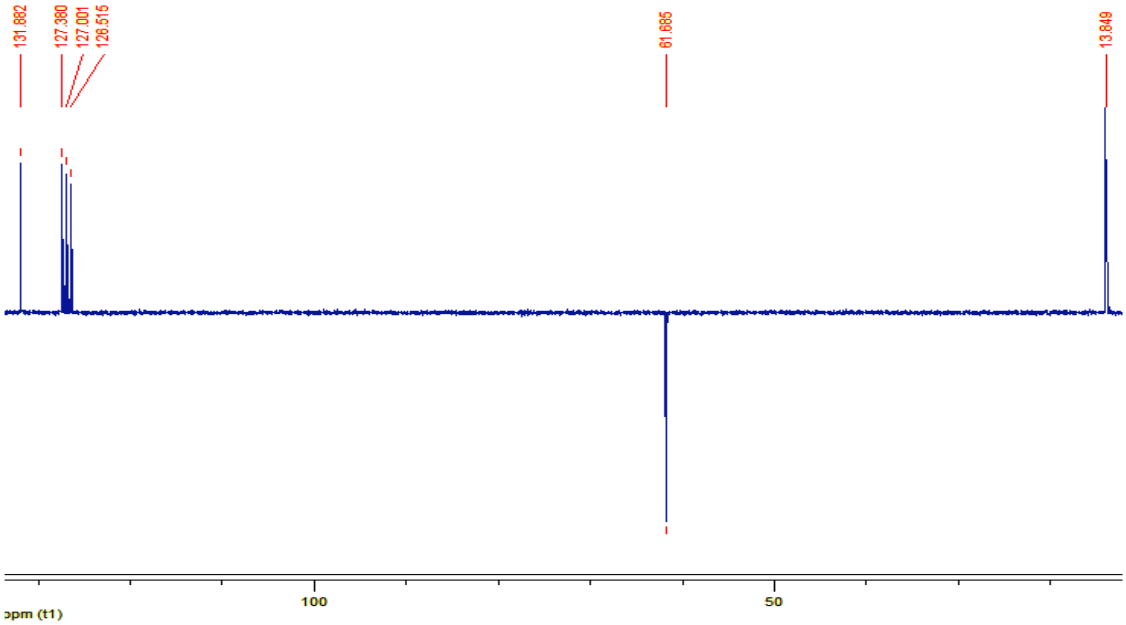

Appendix 12. DEPT-135 spectrum of diethyl-2,5-di(thiophen-2-yl)terephthalate (**39**).

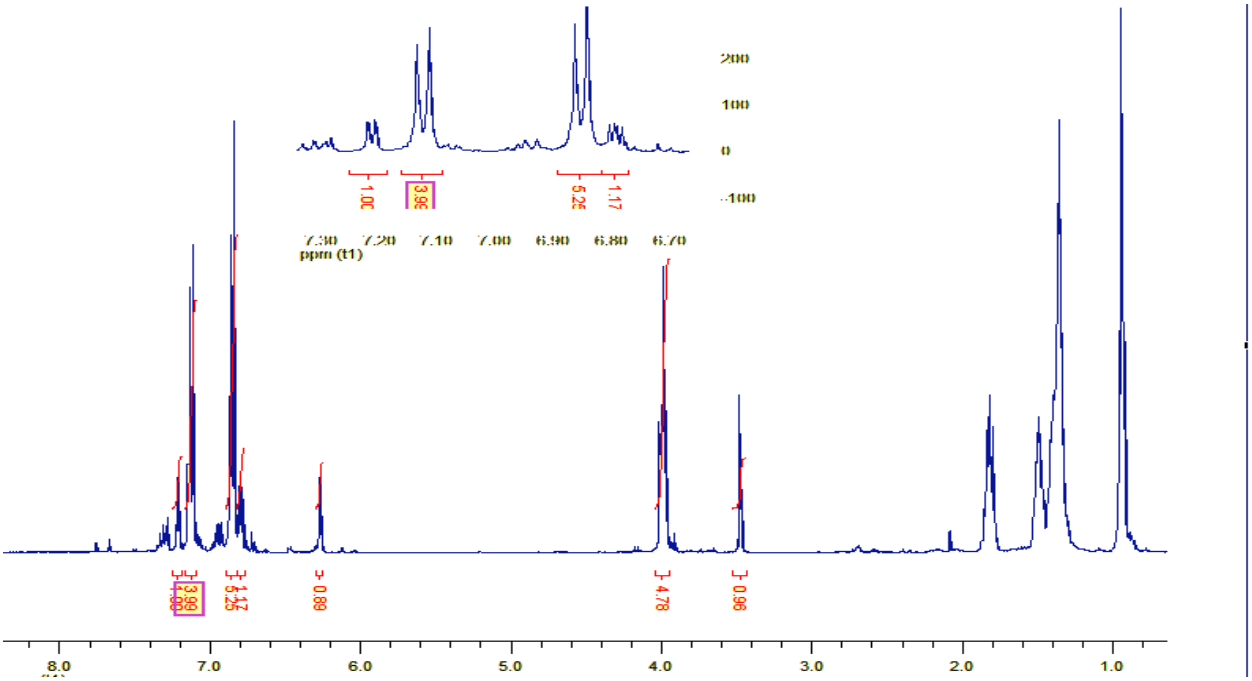

Appendix 13. ^{1}H NMR spectrum of diethyl-2,5-bis(bromothiophen-2-yl)terephthalate (**40**).

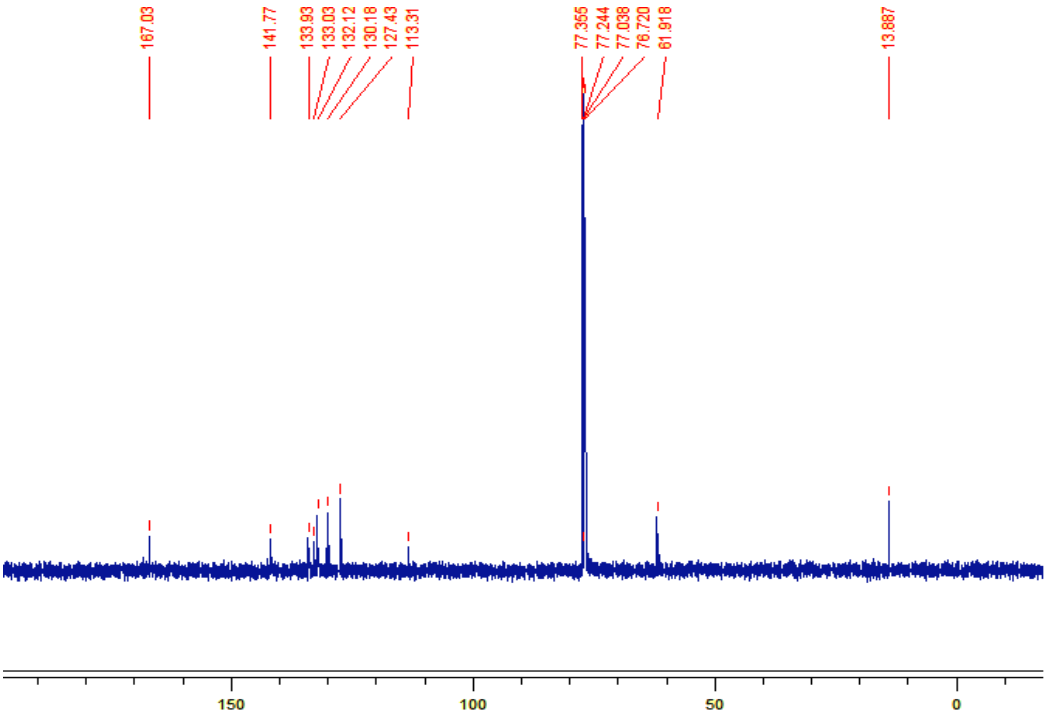

Appendix 14. ^{13}C NMR spectrum of diethyl-2,5-bis(bromothiophen-2-yl)terephthalate (**40**).

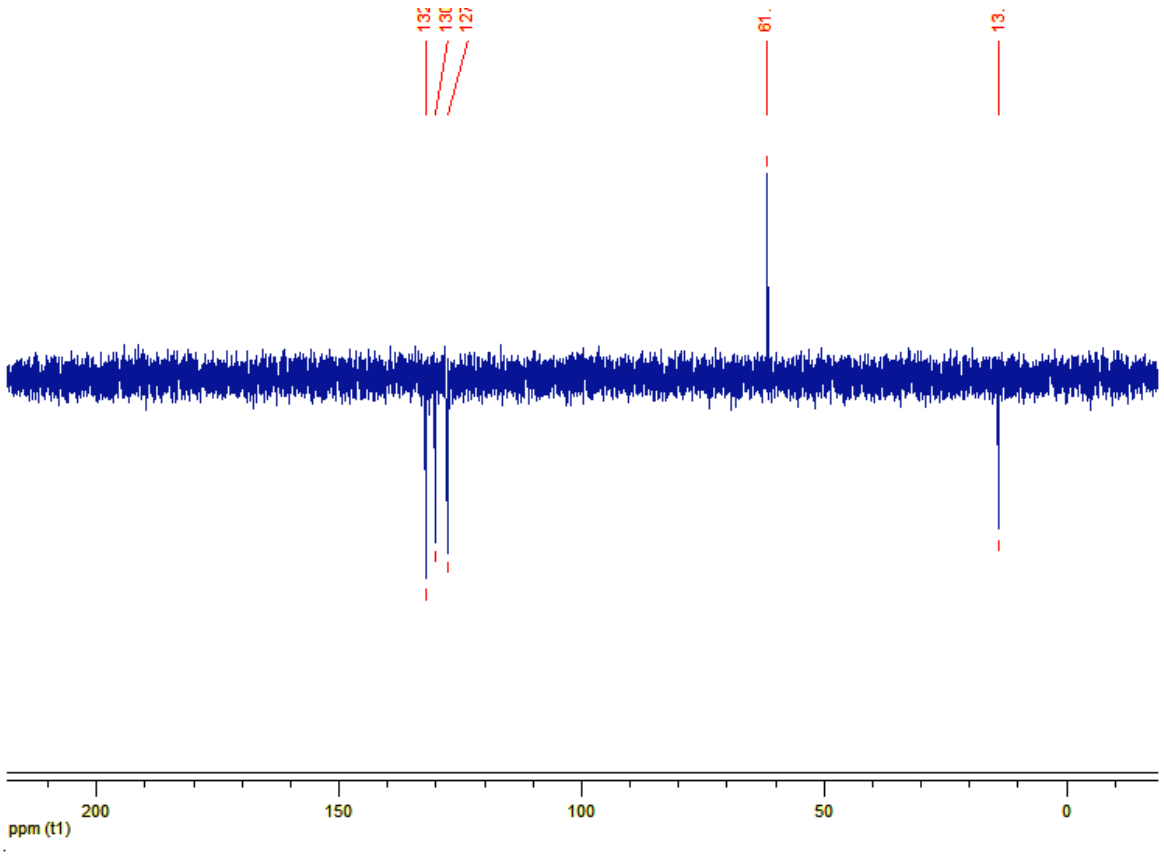

Appendix 15. DEPT-135 spectrum of Diethyl-2,5-bis(bromothiophen-2-yl)terephthalate (**40**).

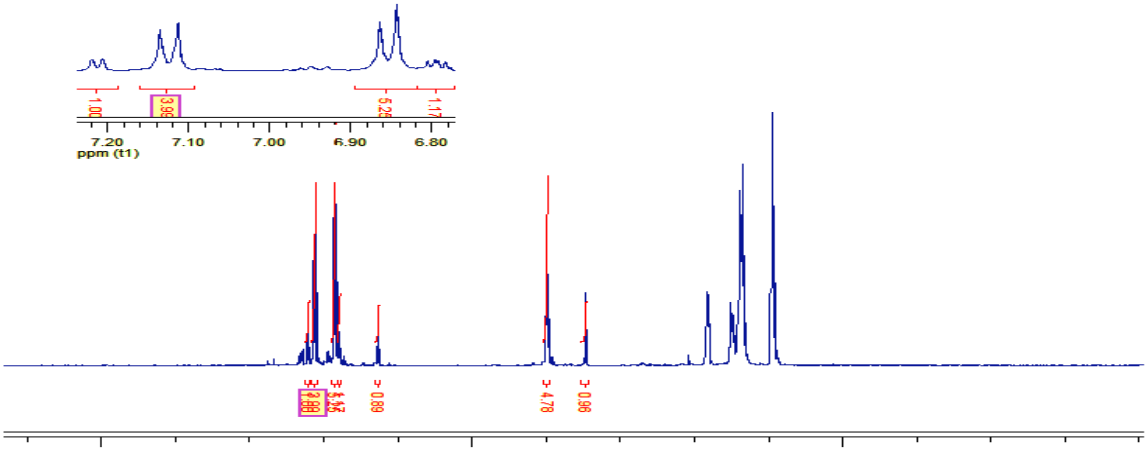

Appendix 16. ^{1}H NMR spectrum of compound **42**.

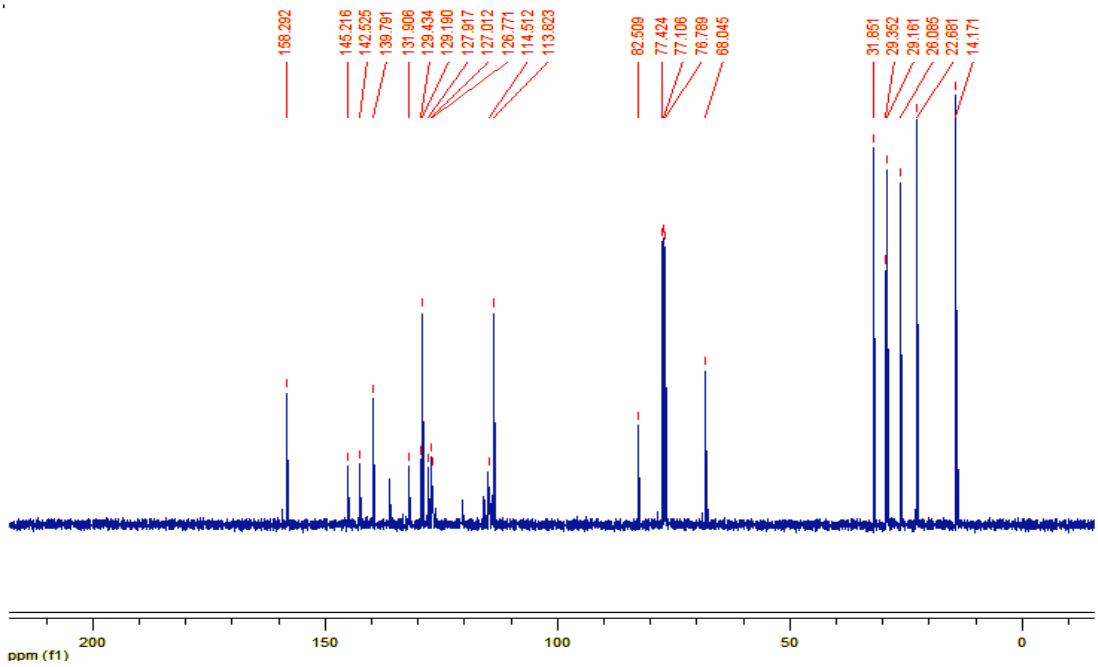

Appendix 17. ^{13}C NMR spectrum of compound **42**.

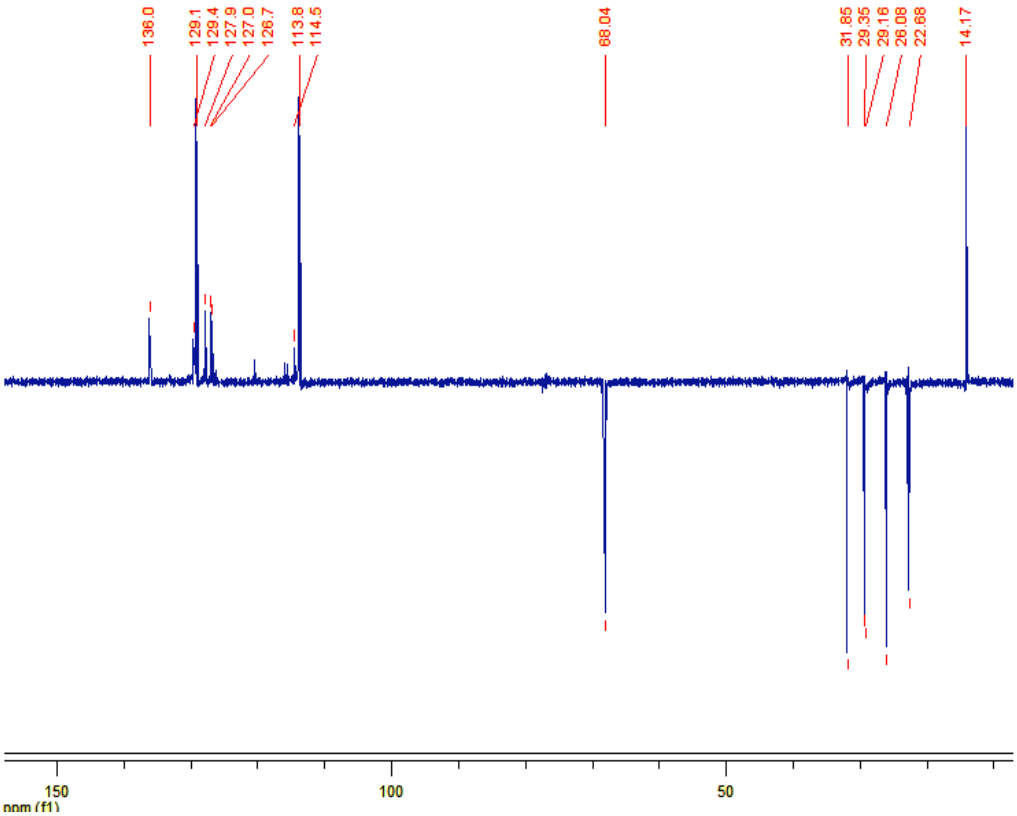

Appendix 18. DEPT-135 spectrum of compound **42**.

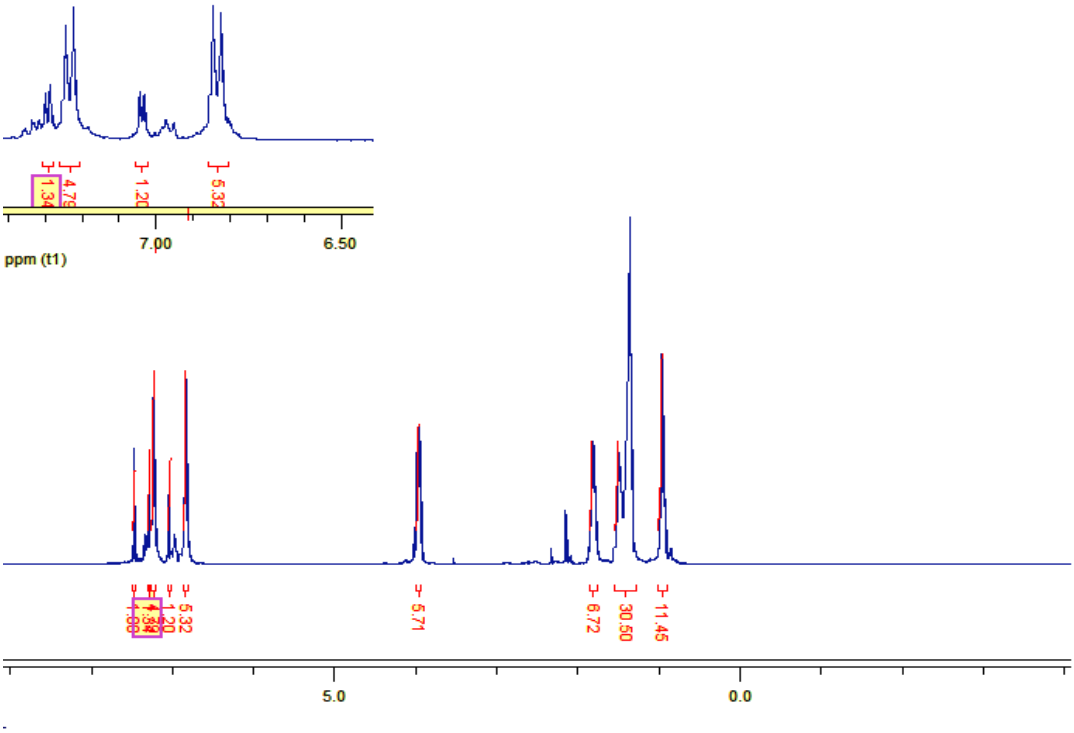

Appendix 19. ^{1}H NMR spectrum of compound **43**.

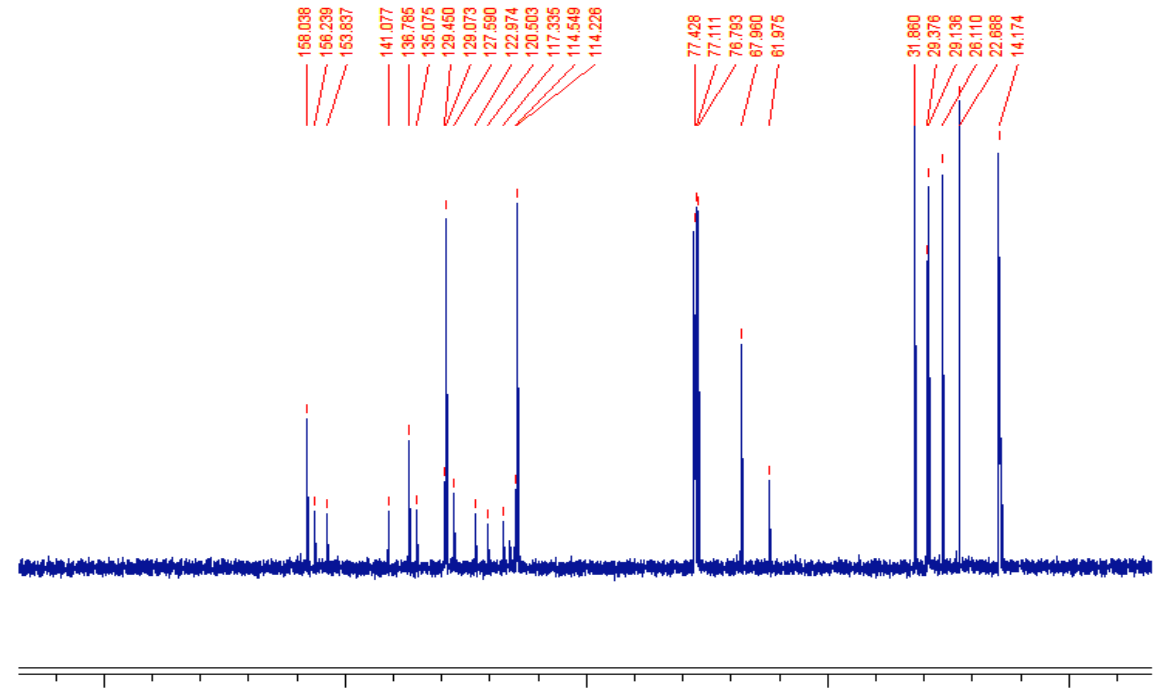

Appendix 20. ^{13}C NMR spectrum of compound **43**.

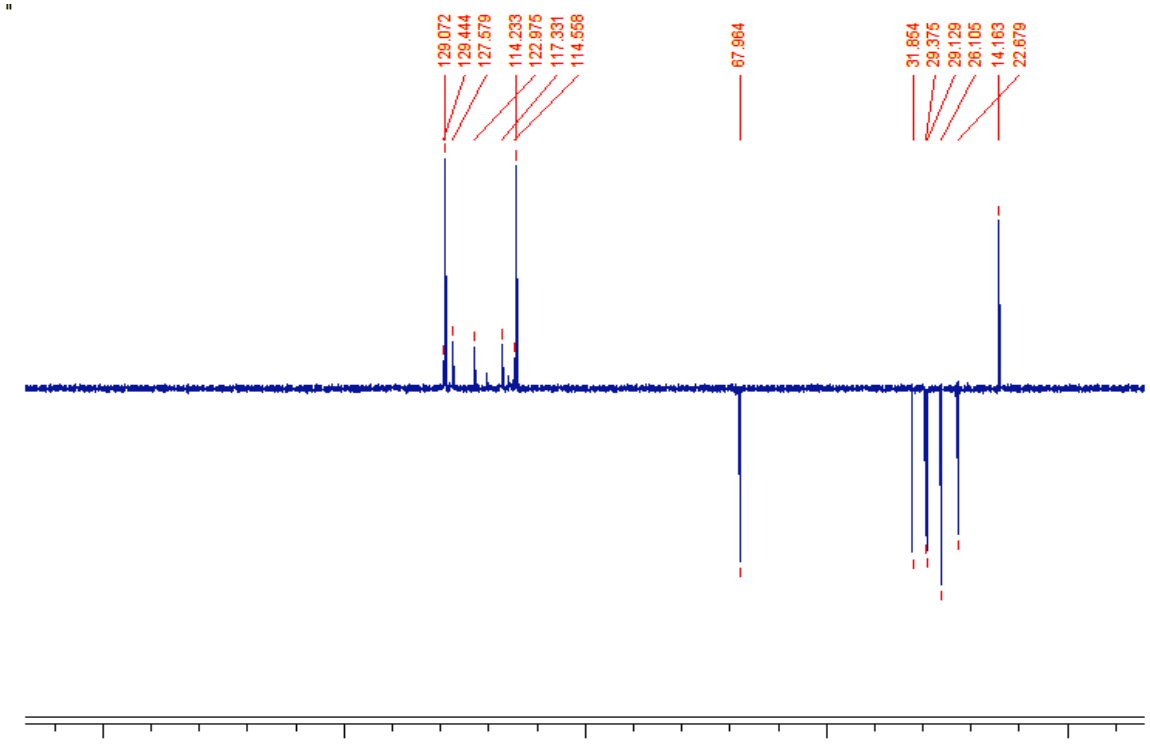

Appendix 21. DEPT-135 spectrum of compound **43**.

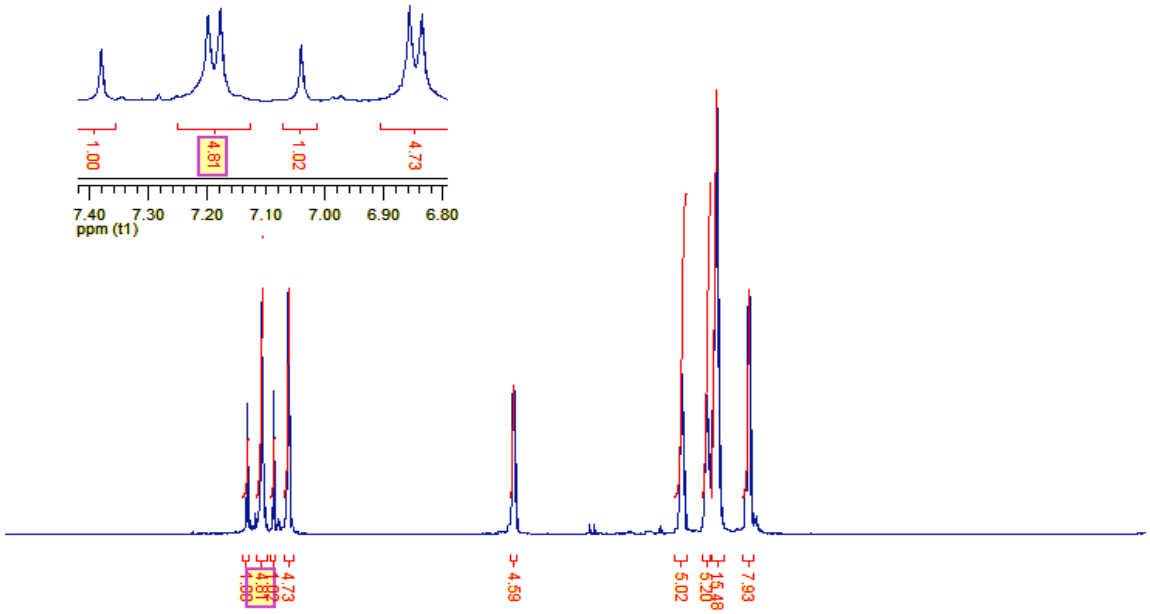

Appendix 22. ^{1}H NMR spectrum of compound **44**.

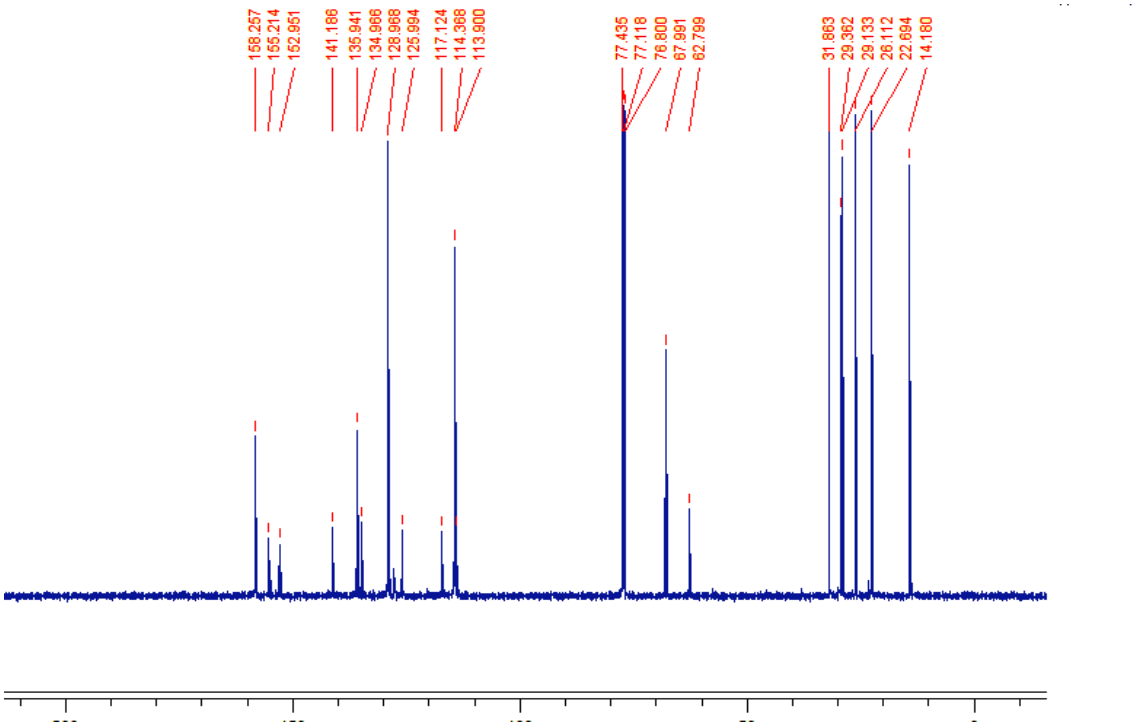

Appendix 23. ^{13}C NMR spectrum of compound **44**.

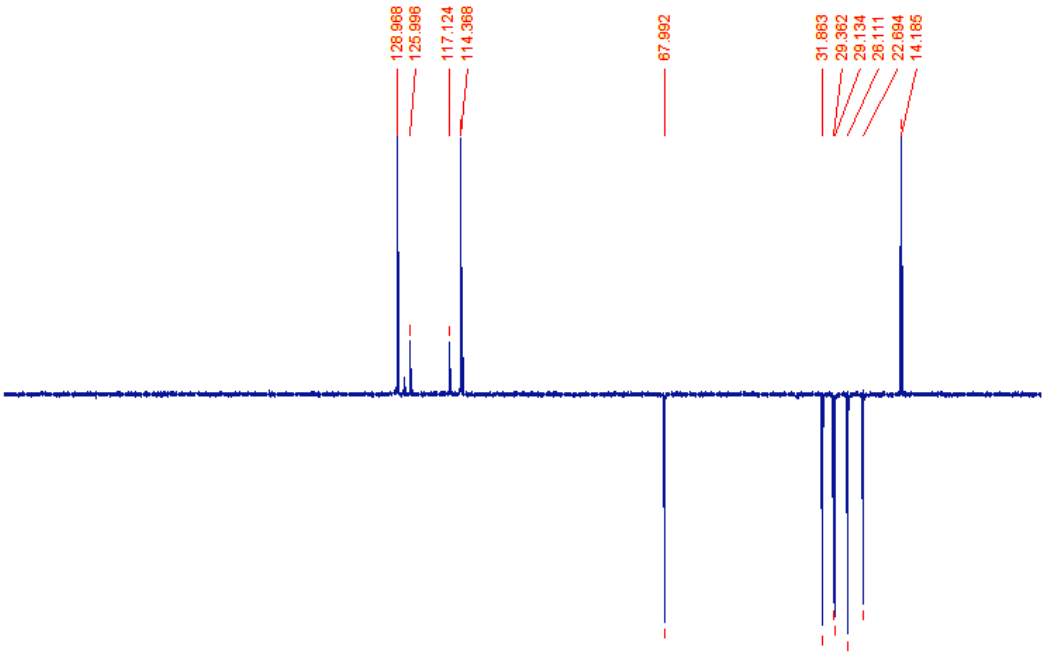

Appendix 24. DEPT-135 spectrum of compound **44**.

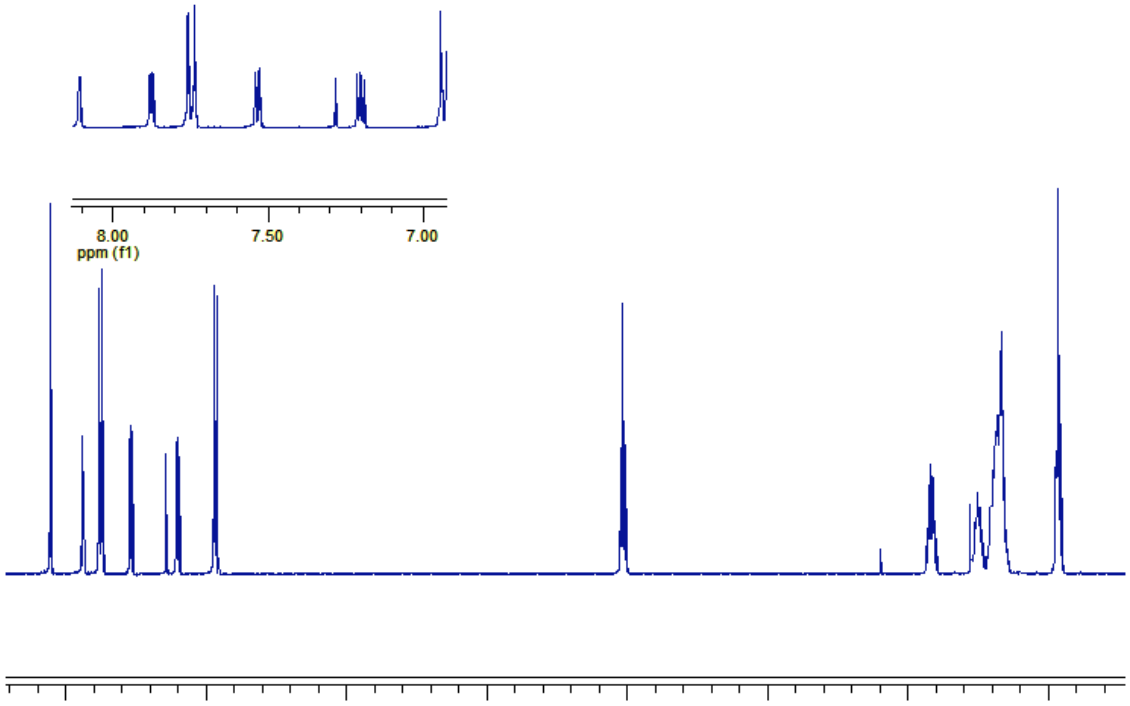

Appendix 25. ^{1}H NMR spectrum of compound **47**.

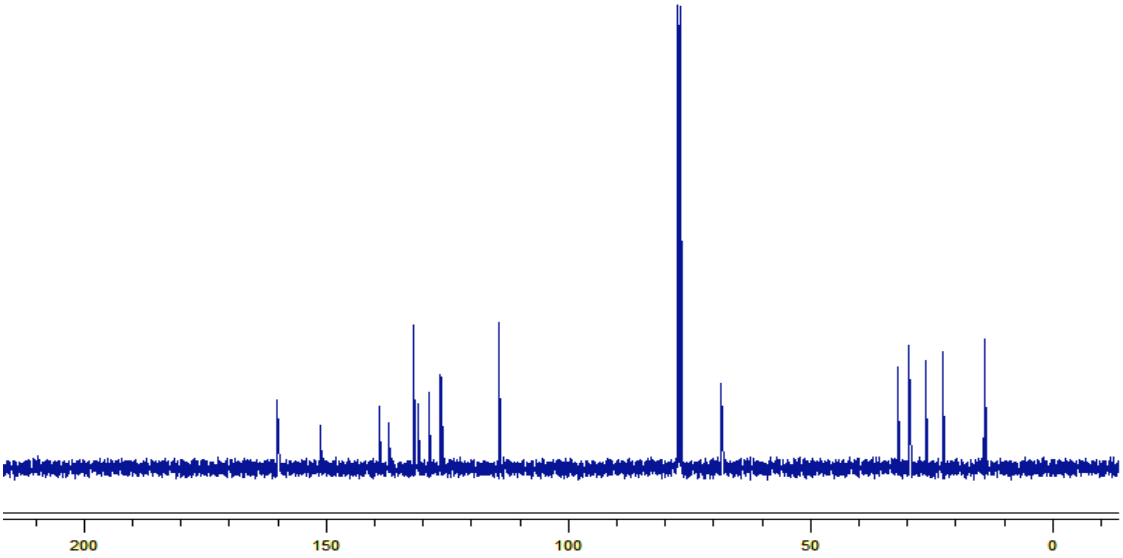

Appendix 26. ^{13}C NMR spectrum of compound **47**.

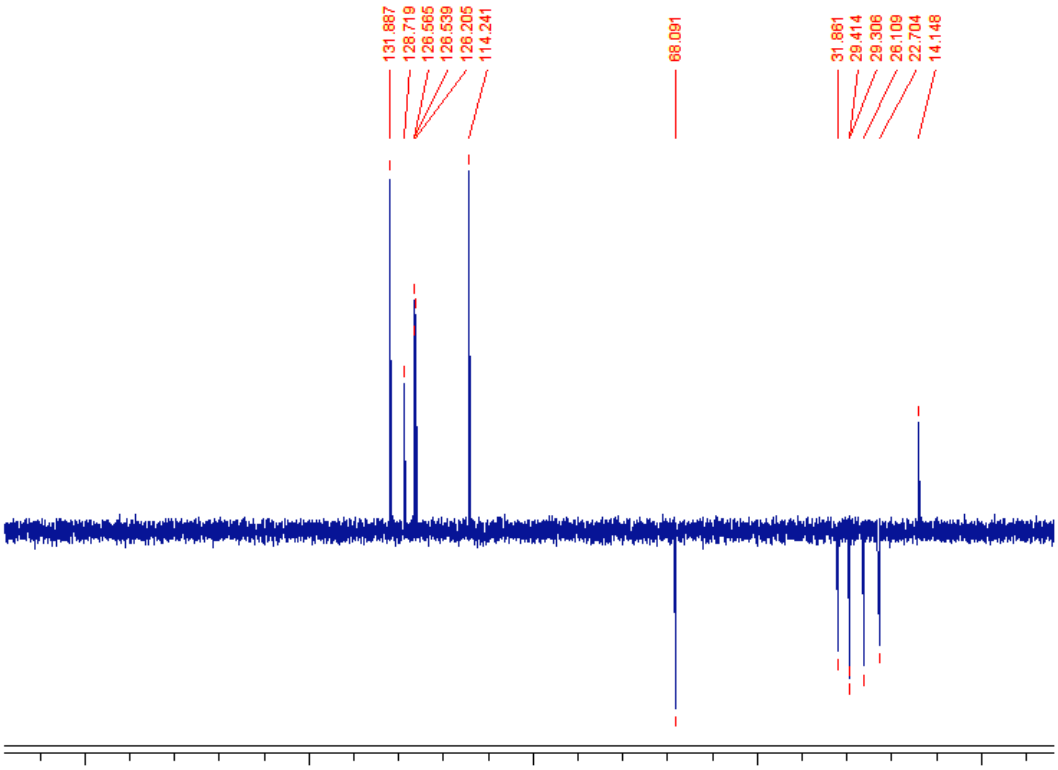

Appendix 27. DEPT-135 spectrum of compound **47**.

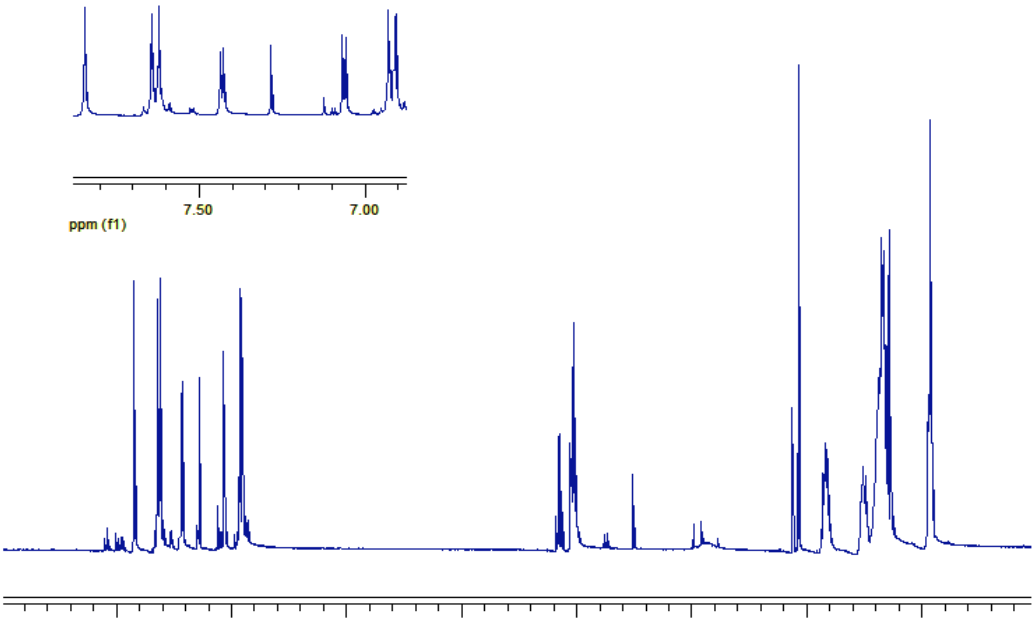

Appendix 28. ^{1}H NMR spectrum of compound **48**.

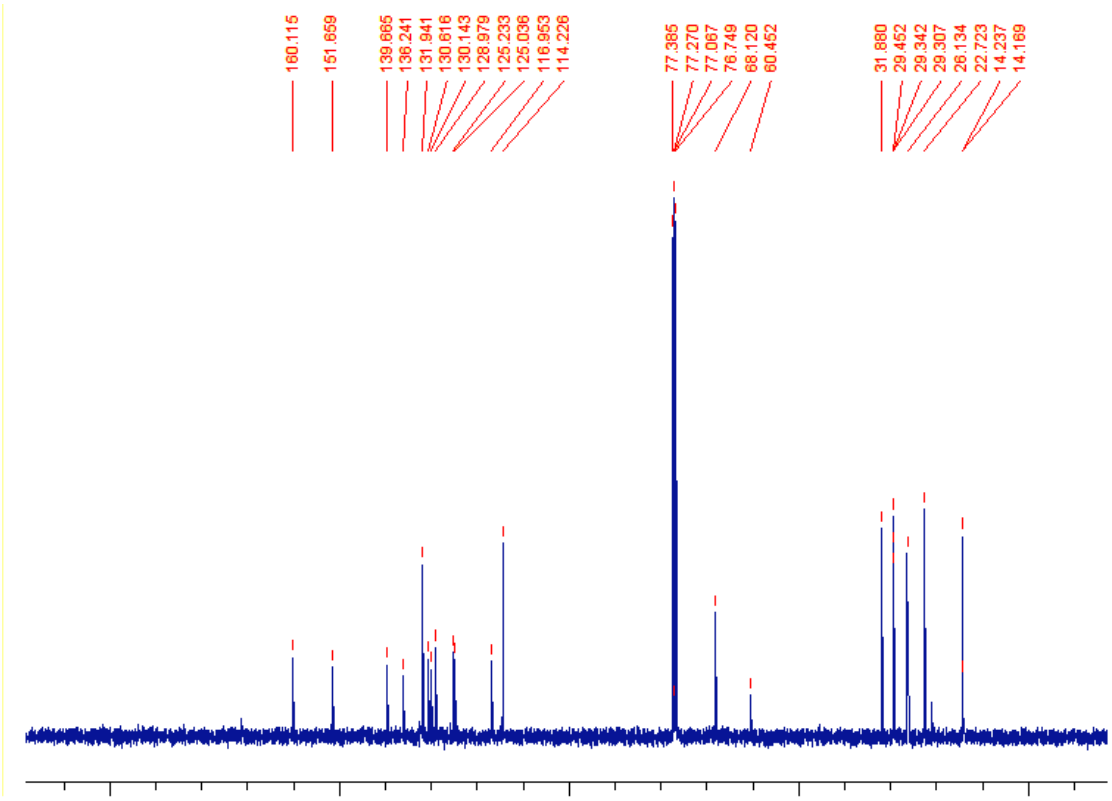

Appendix 29. ^{13}C NMR spectrum of compound **48**.

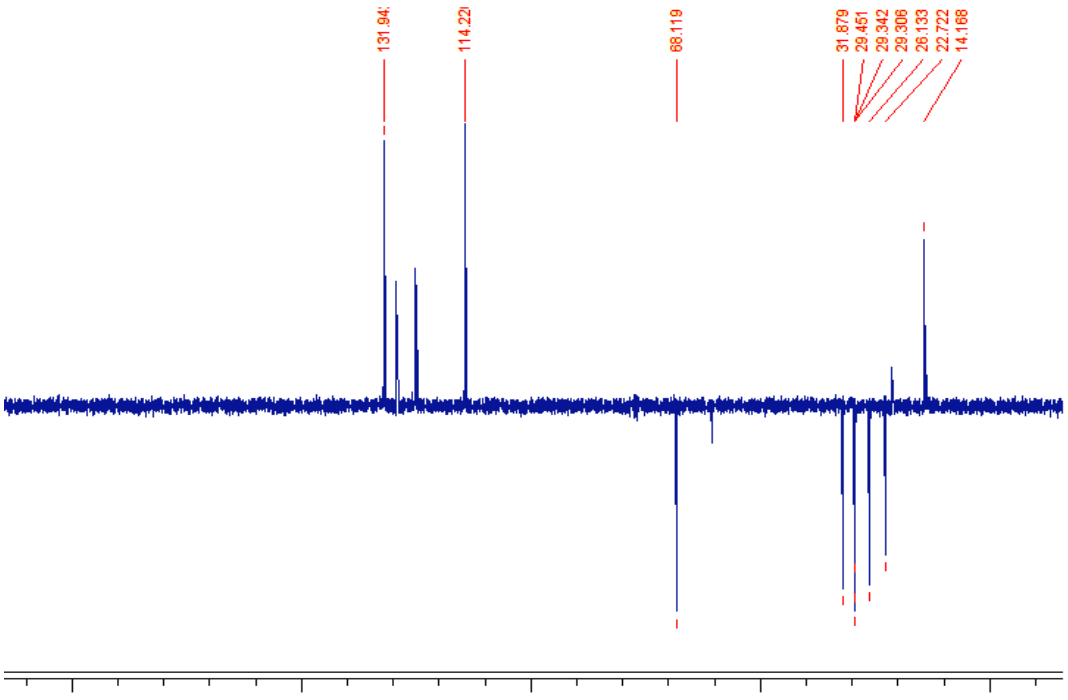

Appendix 30. DEPT-135 spectrum of compound **48**.

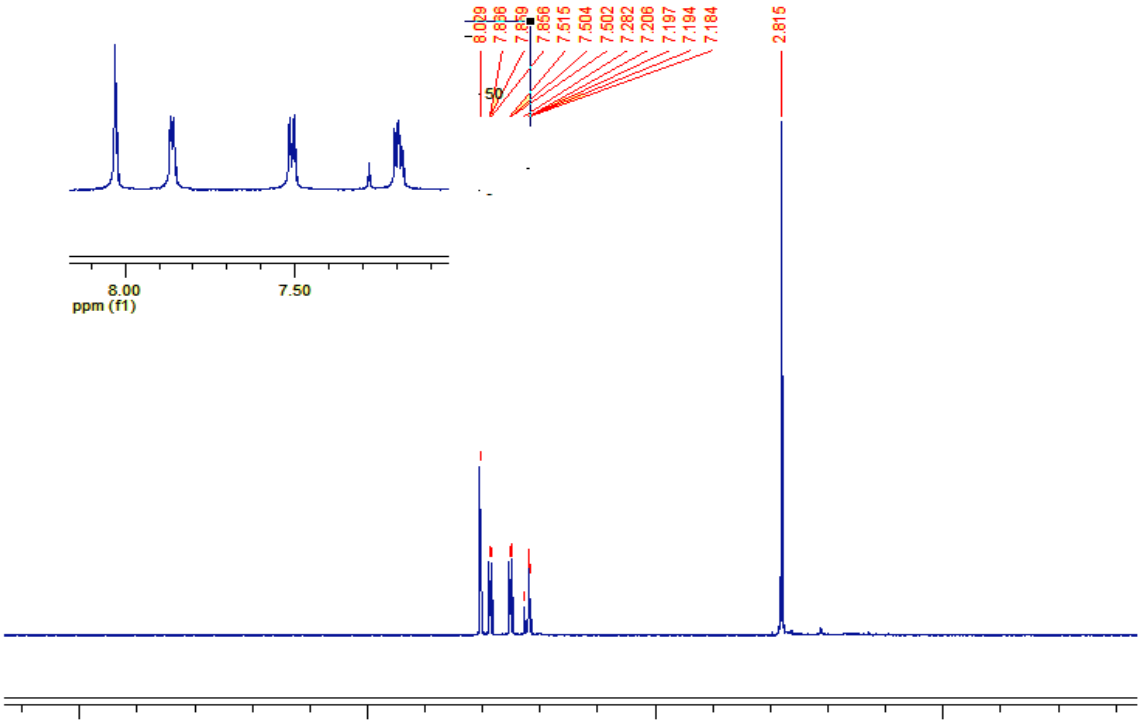

Appendix 31. ^{1}H NMR of compound **50**.

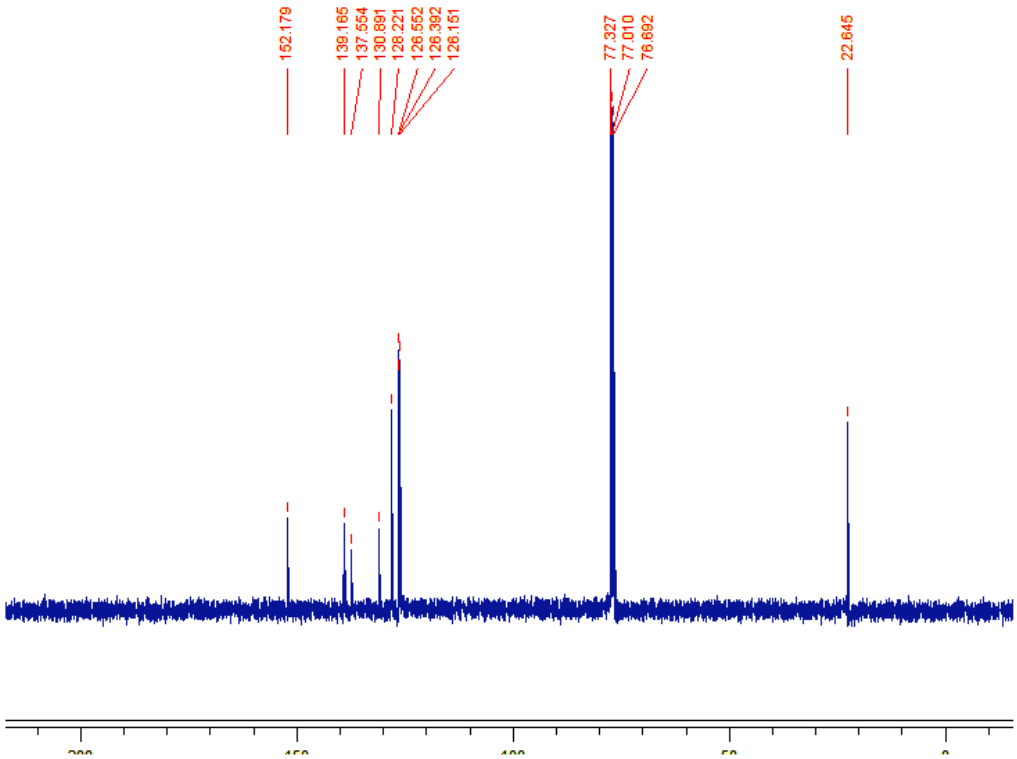

Appendix 32. ^{13}C NMR spectrum of compound **50**.

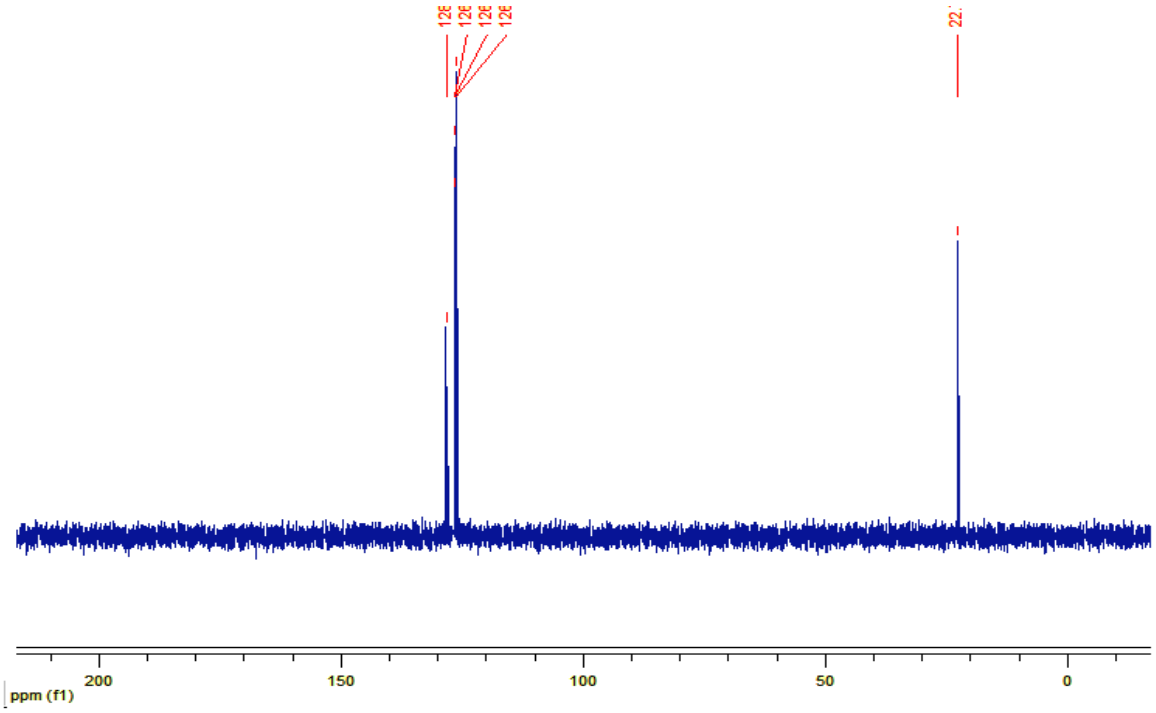

Appendix 33. DEPT-135 spectrum of compound **50**.

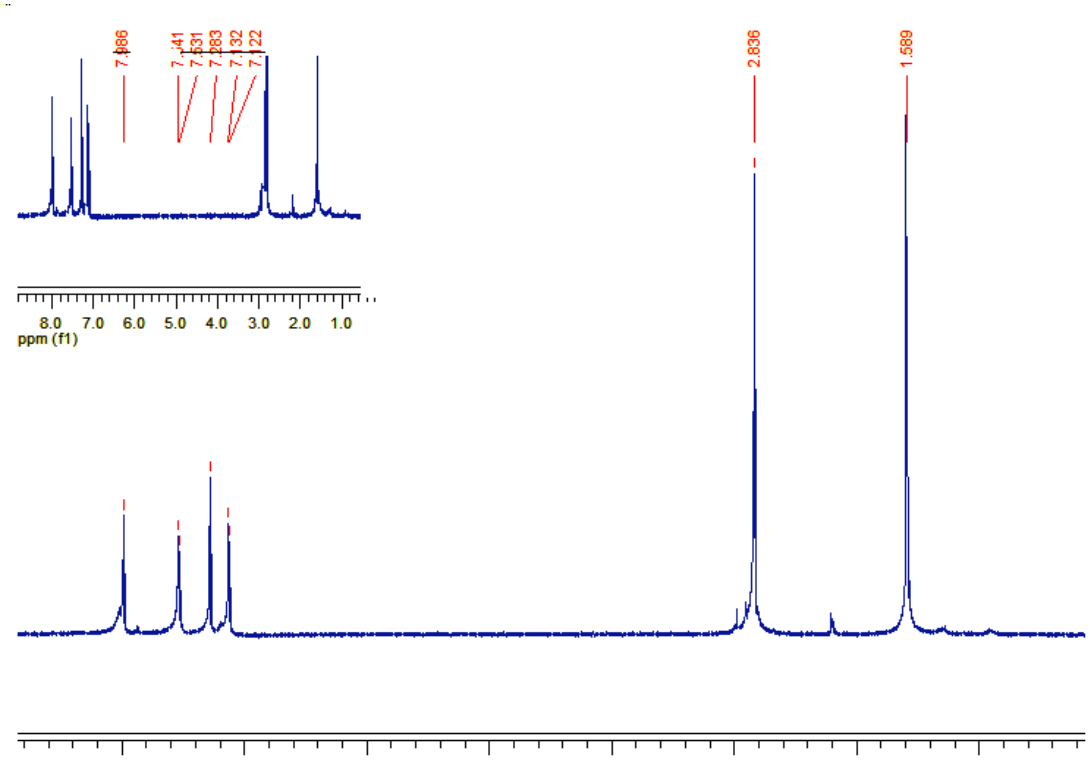

Appendix 34. ^{1}H NMR of compound **51**.